Synthesis and Characterization of Regioselective Cellulose Derivatives

Dissertation

for the obtainment of the academic degree doctor rerum naturalium
(Dr. rer. nat.)

submitted to the Council of the Faculty of Chemistry and Geoscience of the Friedrich-Schiller- Universität Jena

by M. Sc. Yunhui Wang

born on 11.07.1982 in Shashi, Hubei, China

Gutachter 1...

Gutachter 2...

Datum der Verteidung...

List of abbreviations

3PC, 3-mono-*O*-(n-propyl) cellulose;

3EC, 3-mono-*O*-ethyl cellulose;

3MC, 3-mono-*O*-methyl cellulose;

AGU, anhydroglucose unit;

COSY, proton-proton correlation spectroscopy;

Cryo-TEM, cryo-transmission electron microscopy;

DLS, dynamic light scattering;

DMSO, dimethylsulfoxide;

DMA, dimethylacetamide;

DMAP, 4-*N,N*-dimthylaminopyridine

DMF, dimethylformamide;

DMTA, dynamic mechanical thermal analysis;

DS, degree of substitution;

DS_{Et}, DS of ethyl groups;

DS_{Me}, DS of methyl groups;

DS_{Pr}, DS of n-propyl groups;

DSC, differential scanning calorimetry ;

DP_n, number average degree of polymerization;

ESI-IT-MS, electrospray ionization ion trap mass spectrometry;

GC-FID/MS, gas chromatography combinated with flame ionization detector mass spectrometry;

HSQC, heteronuclear singular quantum correlation;

LCST, lower critical solution temperature;

$\overline{M}_n$, number average molercule weight

MC, methyl cellulose;

n-BuLi, *n*-butyl lithium;

SEC, size exclusion chromatography;

THF, tetrahydrofuran;

TBAI, tetra-n-butylammonium iodide;

TBAF·3H$_2$O, tetra-nbutylammoniumfluoride trihydrate;

TBDMS, tetrabutyldimethylsilyl;

TBPA$^+$• SbCl$_6^-$, tris(4-bromophenyl)aminium hexachloroantimonate;

TDMS, thexyldimethylsilyl;

TMS, Trimethylsilyl;

Selectfluor, 1-Chloromethyl-4-fluoro-1,4-diazoniabicyclo[2.2.2]octane bis(tetrafluoroborate);

WAXRD, wide angle X-ray diffraction.

List of schemes and figures

(v/v), r. t., 29 h

List of Tables

Contents

different conditions

bearing two different ether groups (Me, Et, Pr)

spectrometry (GC-FID/MS) and electrospray ionization ion trap mass
spectrometry (ESI-IT-MS)

1. Introduction

Cellulose is the most abundant biopolymer found in the nature, and is a particularly important polysaccharides because of its wide variety of applications in industry, (e.g. paper, textiles etc). Cellulose is the main component of plants cell walls, and can be isolated from cottons, woods and bacteria. Cellulose exists in wood together with hemicelluloses and lignin, and must be therefore separated from these constituents prior to use in commercial applications. In contrast, cellulose from cotton linters and bacterial cellulose is very pure [1].

As shown in Scheme 1.1, cellulose consists of β-(1,4)-linked D-glucose repeating anhydroglucose unit (AGU), with a C4 hydroxyl at one end (the non reducing end) and a C1 hyrdroxyl at the other (the reducing end), which is in equilibrium with the aldehyde structure.
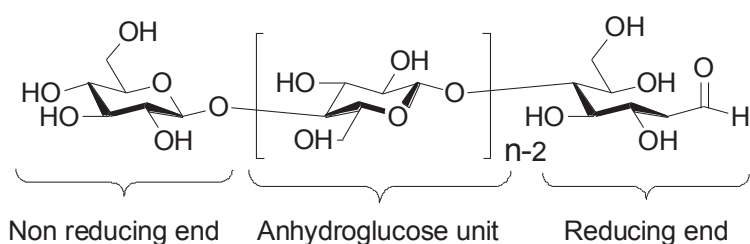
Scheme 1.1 Structure of cellulose chain

As an important raw material for the chemical industry as well as for laboratory research, cellulose functionalization chemistry has been developed to obtain a wide variety of different derivatives. Cellulose esters and cellulose ethers are the two most important derivatives of cellulose, while oxidized products play a relatively minor role [2].

It is well known that the properties of cellulose derivatives are not only influenced by the type of substituent and its degree of substitution (DS) of the respective functional groups, but also by the 8 possible substitution patterns (non-substituted, tri-substituted, 2-mono-*O*, 3-mono-*O*, 6-mono-*O*, 2,3-di-*O*, 3,6-di-*O*, 2,6-di-*O*) within AGU, in addition to the distribution of functional groups along the cellulose backbone [3]. Therefore, besides the comprehensive

structure characterization, an investigation of structure property relationships of well-defined functionalization patterns is required.

When considering the acidity and the steric accessibility of the three hydroxyls (2, 3, and 6) on AGU, the reactivity order of the hydroxyl groups is: 2-OH>6-OH>3-OH [4]. Due to this difference of reactivity, regioselective protection by bulky groups can be realized.

As a matter of fact, cellulose ethers with all 6 possible regioselective functionalization patterns have been already reported, and 3-*O*-alkyl cellulose is one of the most studied derivatives (detailed in section 2.2.2.2 and 2.3). This research presented herein concentrates on the synthesis of novel 3-*O*-alkyl cellulose bearing two different alkyl groups (two of methyl, ethyl, and propyl) at position 3 within the same polymer chain. The tuning of lower critical solution temperature (LCST) compared to that of 3-mono-*O*-ethyl cellulose (3EC) and 3-mono-*O*-propyl cellulose (3PC) is described first. The physico-chemical characterizations of the products by various analytical methods were also carried out, in order to elucidate the structure-property-relationship of the regioselective cellulose derivatives with well-defined structure.

In addition, since several regioselective cellulose esters have been also synthesized (e.g. 6-mono-*O*-acetyl cellulose, 2,3-di-*O*-acetyl-6-mono-*O*-propanoyl cellulose, 2,6-di-*O*-acetyl cellulose, detailed in section 2.4.1), the synthesis of 3-*O*-acetyl cellulose with a new functionalization pattern was also studied.

2. State of the art

As mentioned in chapter 1, cellulose has a wide variety of application in various industries. Cellulose derivatives play more important roles in both commercial products and scientific research as detailed in section 2.1.

There are 3 accessible hydroxyl groups on the anhydroglucose unit (AGU) of cellulose, which can be chemically functionalized in a selective way. When the supramolecular structure of cellulose is taken into account, the inter- and intramolecular hydrogen bonds, and Van der Waals interactions act in concert to form a 3-dimensional microfibrillar structure (Scheme 2.1), which leads to the extraordinary strength of cellulose fibres and their insolubility in water and other common organic solvents, in spite of their highly hydrophilicity nature [1, 5].
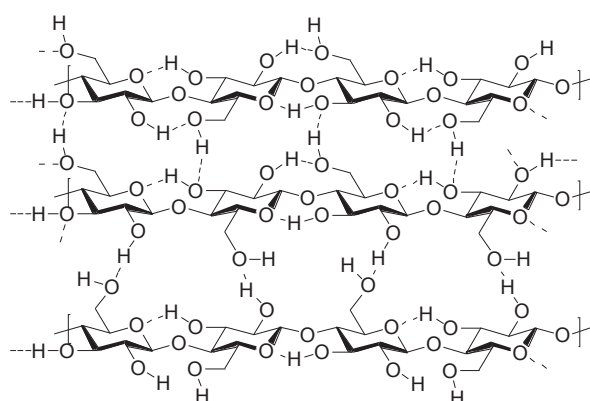
Scheme 2.1 Inter- and intrachain hydrogen bonds of cellulose

As a result, the hydroxyl groups of cellulose are poorly accessible, which reduces their reactivity. Therefore, activation by swelling or dissolution of the polymer is necessary and important, in order to increase the accessibility of the OH groups. A typical example is the activation of cellulose in NaOH aqueous solution (mecerization), which leads to a highly swollen and, hence reactive polymer [6].

Upon the development of versatile solvents for cellulose, functionalization in homogeneous

solution became possible, which is currently only a focus of laboratory research interest, and has not yet been applied on an industry scale. Homogeneous conditions can facilitate the cellulose functionalization and moreover, the design of cellulose derivatives with novel structures (detailed in section 2.2).

2.1 Cellulose derivatives

2.1.1 Cellulose esters

Cellulose esterification is the most important chemical functionalization of cellulose in an industrial scale. Cellulose esters are classified into inorganic esters (cellulose nitrate, sulphate, borate etc.) and organic esters (cellulose acetate, propionate) in accordance with the nature of attached ester group.

2.1.1.1 Typical inorganic cellulose ester: cellulose nitrate

Cellulose can form esters with inorganic acids such as nitric acid, etc. Only cellulose nitrate is of commercial interest: nitric ester of cellulose was prepared already in 19th century, by reaction of nitric acid (HNO_3) with cellulose in the presence of sulfuric acid (H_2SO_4) and water, as a means of synthesizing of explosives [7]. Thereafter, the synthesis of the first thermoplastic polymer material named "celluloid" was carried out in industry scale by the Hyatt Manufacturing Company in 1870 [8].

2.1.1.2 Typical organic cellulose ester: cellulose acetate

Organic cellulose esters are obtained by the esterification of cellulose with organic acid, including cellulose acetate, cellulose propionate, cellulose butyrate and cellulose mixed esters which are of great industrial interest. The industrial production of cellulose acetate was conducted by its conversion with a mixture of acetic acid and acetic anhydride, in the

presence of sulphuric acid as a catalyst which can form acetyl sulphuric acid during the acetylation reaction (Scheme 2.2) [9, 10].
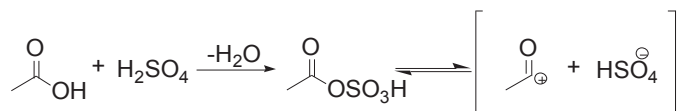
Scheme 2.2 Formation of reactive intermediate acetyl sulphuric acid during the acetylation of cellulose

Fully acetylated cellulose can be partially deacetylated to give cellulose acetate of DS_{Ac} 2.4-2.6 which is soluble in acetone [11]. This synthesis "detour" is necessary because the cellulose acetates with comparable DS synthesized directly from cellulose are insoluble in acetone, but the acetone solubility of cellulose acetate is indispensable for industrially important processes such as fibre spinning [12].

Besides this method using acetic anhydride in the presence of sulphuric acid, other alternative methods for the synthesis of cellulose are shown by Scheme 2.3.

Esterification of cellulose with mixtures of carboxylic acids and trifluoroacetic anhydride (TFAA) decreased chain degradation [13, 14]. For research interest, *in situ* activation of carboxylic acid by *p*-toluensulfonic acid chloride (TosCl) [15, 16], as well as carbonyldiimidazole (CDI) [17] efficiently initiated and facilitated the esterification of cellulose.

Considering the simplicity of the synthesis, diminished use of toxic reagents, and the reaction efficiency, cellulose acetate synthesis via acetylation of cellulose by acetic anhydride in the presence of 4-*N,N*-dimethylaminopyridine (DMAP) as a catalyst is particularly attractive [18]. The mechanism of stabilization of the acylpyridinium ion is involved during the catalysis (Scheme 2.4). Cellulose acetate (DS 2.5) is used in the textile industry for the production of fibres or filaments; cellulose triacetate (DS 2.8-3.0) is applied in photographic films

fabrication.

R= -CH₃, -CH₂CH₃, -CH₂CH₂CH₃ → R= -CH$_3$, -CH$_2$CH$_3$, -CH$_2$CH$_2$CH$_3$

R'= R or H

p-toluensulfonic acid chloride (TosCl)

4-N,N-dimethylaminopyridine (DMAP)

carbonyldiimidazole (CDI)
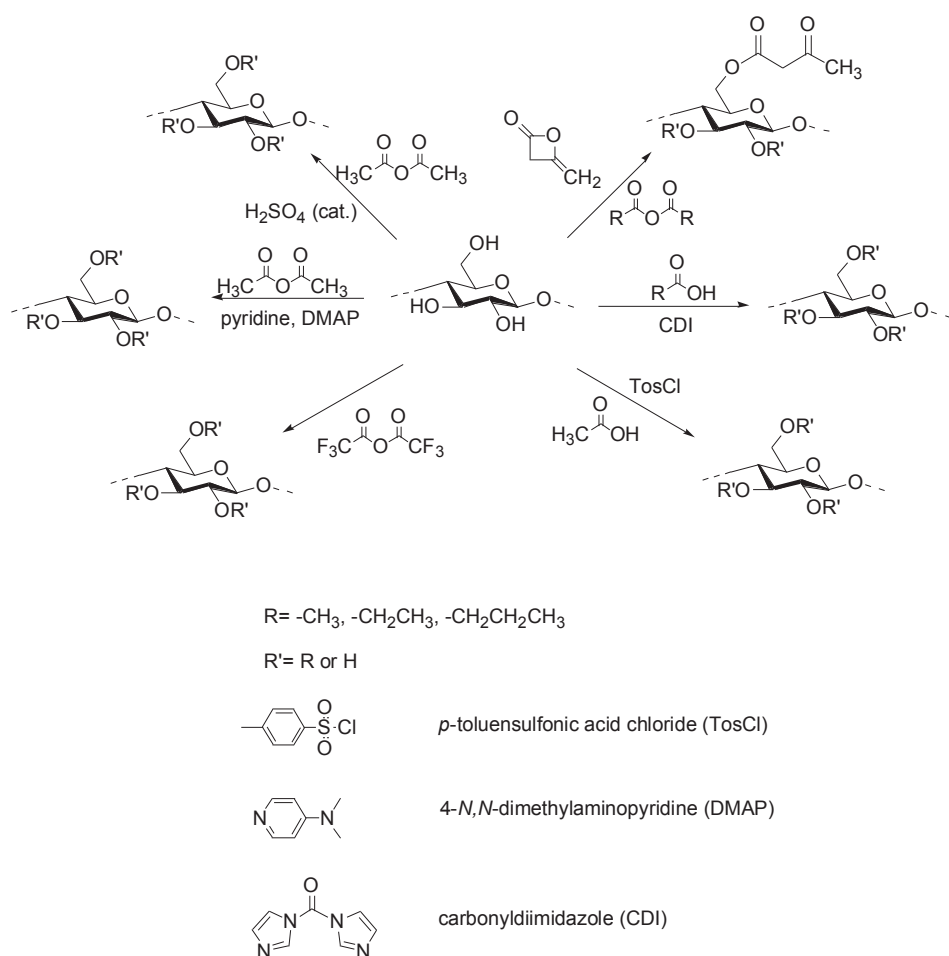
Scheme 2.3 Divers synthesis ways of cellulose esters

Another classical application of cellulose acetate is plastic materials, such as acetopropionate and acetobutyrate which find a wide application as thermoplastic raw materials for coating and insulation, etc [11].
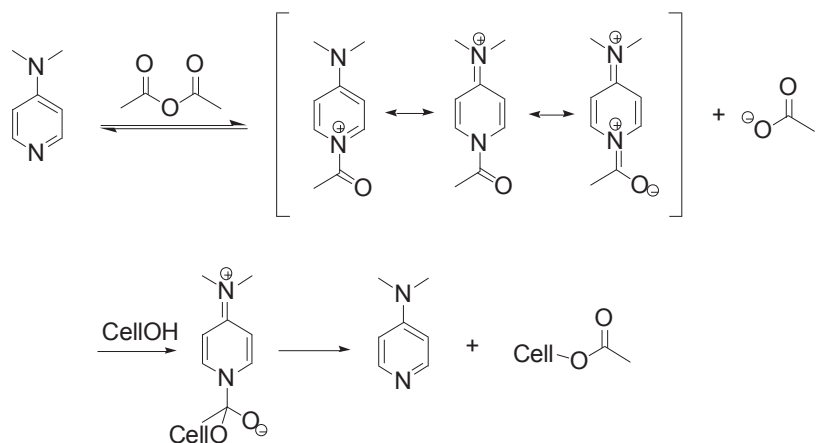
Scheme 2.4 Mechanism of cellulose acetylation by acetic anhydride and DMAP

In the past decade, cellulose esters have also demonstrated promise in areas such as coatings, controlled release of drugs, composites and membranes [19].

2.1.2 Cellulose ethers

Cellulose etherification was firstly reported in 1905, via the reaction of dimethyl sulphate with cellulose yield methylcellulose [20]. Afterwards, methyl cellulose, ethyl cellulose and benzyl cellulose became commercially available around 1935 [21][22]. Nowadays, carboxylmethyl cellulose (CMC, anionic cellulose ether), hydroxylethyl cellulose (HEC, non ionic cellulose ether), methyl cellulose (MC, non ionic cellulose ether) and hydroxyethylmethyl cellulose (HEMC, mixed cellulose ether) are all important commercially available cellulose ethers [23].

1) Cell-OH + R—I $\xrightarrow{\text{NaOH}_{aq}}$ Cell-OR + NaI

2)

3) Cell-OH+ H$_2$C=CH-M $\xrightarrow{\text{NaOH}_{aq}}$ Cell-OCH$_2$CH$_2$-M
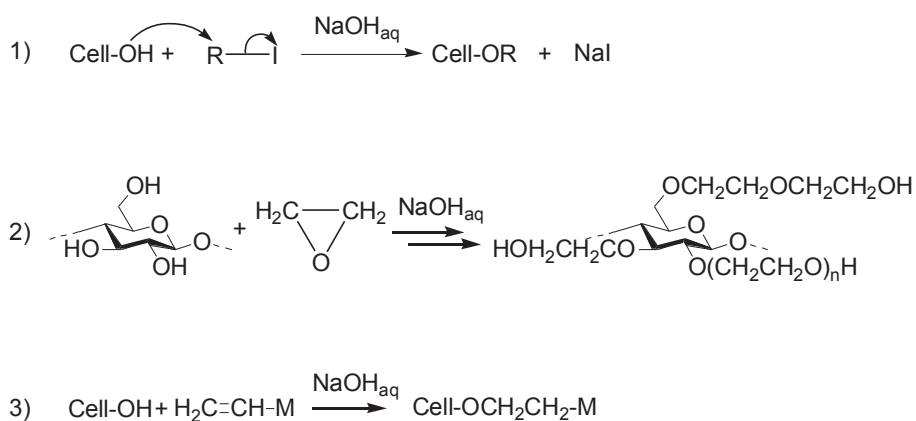
Scheme 2.5 Three different ways of synthesis of cellulose ethers

The commercial production of alkyl cellulose was realized in three ways (Scheme 2.5): 1) Williamson reaction of cellulose activated by an aqueous solution of NaOH with alkyl or aryl halides (MC, benzyl cellulose, etc); 2) ring-opening reaction with epoxides (HEC, HPC); 3) Michael reaction with activated double bonds, M stands for an electron withdrawing group [24].

2.1.2.1 Alkyl cellulose

As mentioned in section 2.1.2, alkyl cellulose like methyl cellulose and ethyl cellulose are important commercially available cellulose ethers. The industrial production of methyl or ethyl cellulose applying NaOH (aq.) activated cellulose requires large quantities of alkylation reagents and produces large quantities of the by product (NaCl). In the research presented herein, the methods which are of academic interest are discussed. In the lab research, alternative methods exist for the synthesis of alkyl celluloses, such as methylation with dimethyl sulphate, diazomethane, or methyl triflate [25-27].

Moreover, sodium hydride (NaH) with methyl iodide has been reported to be a quite efficient method for the permethylation of cellulose derivatives, for example, 6-*O*-thexyldimethylsilyl cellulose [28, 29]. The mechanism is shown in Scheme 2.6:
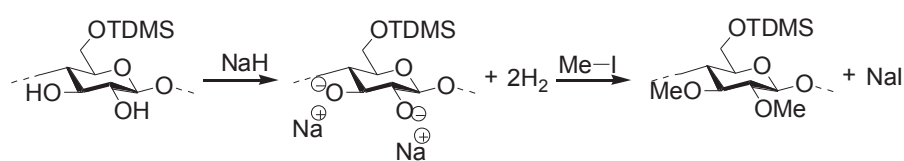
Scheme 2.6 Peralkylation of 6-*O*-thexyldimethylsilyl cellulose by NaH and methyl iodide

Alkyl cellulose is soluble in water or organic solvents depending on their DS (Table 2.1) [30]. The thermoreversible gelation of the aqueous solution of MC was firstly reported by Heymann in 1935 [31]; thereafter, the influence of the substituent, DS, as well as the substitution pattern along the backbone were intensively studied during the past decades as described in section 2.3.2.

Table 2.1 Solubility of alkyl cellulose depending on their DS

Product	Degree of substitution	Solubility
	0.4-0.6	4% aqueous NaOH
Methyl cellulose	1.3-2.6	cold water
	2.5-3.0	organic solvents
	0.5-0.7	4% aqueous NaOH
Ethyl cellulose	0.8-1.7	cold water
	2.3-2.6	organic solvents

Alkyl celluloses have a wide variety of applications. For example, ethyl cellulose is used in lacquer, adhesives and tablet binders [32], moreover, it can form Langmuir-Blodgett films [33]. Alkyl cellulose are not only used as end products, but also are of great interests on academic research in a lab scale, such as cellulose silyl ether or triphenylmethyl ether which are important intermediates for the synthesis of regioselectively funcionalized cellulose derivatives (see section 2.2).

2.2 Regioselectively functionalized cellulose derivatives

As mentioned in the introduction, cellulose is insoluble in both water and organic solvents, because of the inter- and intrachain hydrogen bond interactions. Consequently, swelling or dissolution is a prerequisite for its functionalization. In many cases mentioned in section 2.1, cellulose was swollen by aqueous alkali solution and then functionalized under heterogeneous conditions, yielding products with "statistical" functionalization patterns of AGU. With the development of solvent for celluloses, DMA/LiCl [34], TBAF/DMSO [35], Urea/NaOH [36], ionic liquids [37], functionalization under homogenous condition became possible. Under homogenous conditions, the polymer chains are liberated from intra- and intermolecular hydrogen bonds, and the hydroxyl groups are more accessible for functionalization, yet the resulting functionalized products showed random substitution patterns along the polymer backbone.

It is well known that the properties of these derivatives are not only affected by the degree of substitution, but also by the distribution of the functional groups along the backbone of the polymer [3]. A good example is the different flocculation temperature of conventionally prepared ethyl cellulose and regioselective 3-mono-*O*-ethyl cellulose [38].

In order to establish an unambiguous structure-property relationship, it is of great importance to impart regioselectivity into functionalized cellulose, namely, to prepare cellulose

derivatives with well-defined functionalization patterns within AGU.

As to cellulose, the regioselectivity means the exclusivity or significant preference of the reaction on one or two of the accessible hydroxyl groups at position 2, 3 and 6. Taking methyl cellulose as an example, except cellulose itself and 2,3,6-tri-*O*-methyl cellulose, there are 6 different regioselective functionalization patterns (Scheme 2.7).
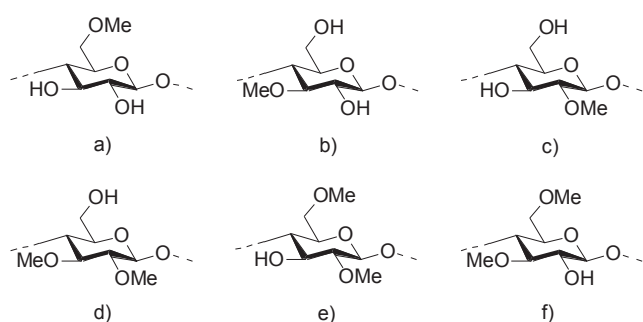
Scheme 2.7 Regioselective substitution patterns for methyl cellulose: a) 6-mono-*O*-methyl cellulose; b) 3-mono-*O*-methyl cellulose; c) 2-mono-*O*-methyl cellulose; d) 2,3-di-*O*-methyl cellulose; e) 2,6-di-*O*-methyl cellulose; f) 3,6-di-*O*-methyl cellulose

One should note that the 7 possible regioselective functionalization patterns including 2,3,6-tri-*O*-methyl cellulose are already synthesized by cationic ring-opening polymerization [4, 39]. In this PhD thesis, it is the polymer analogous functionalization that will be discussed.

There are several ways to synthesize regioselectively functionalized cellulose derivatives (Scheme 2.8). First is the selective cleavage, a typical example of which is selective deacetylation under aqueous acidic or alkaline condition with the presence of amines [40]. Another way is to introduce activating groups, for example, *p*-toluensulfonyl (tosyl) [41, 42], yet tosyl chloride doesn't reacts in a strictly regioselective way with primary hydroxyl group, it reacts also with secondary OH groups when applying an excess of the reagent. Moreover, the following nucleophilic substitution cannot take place easily with the secondary hydroxyl group [43].

As a result, selective cleavage and activating group methods only cover a minority area of

regioselective functionalization. The most studied method is the advanced protecting group technique. The protecting group must be introduced selectively, be stable during the subsequent reactions and removable without losing other functional groups. Two types of widely used bulky protecting groups in organic synthesis, tripheylmethyl ether and trialkylsilyl ether are of special importance.
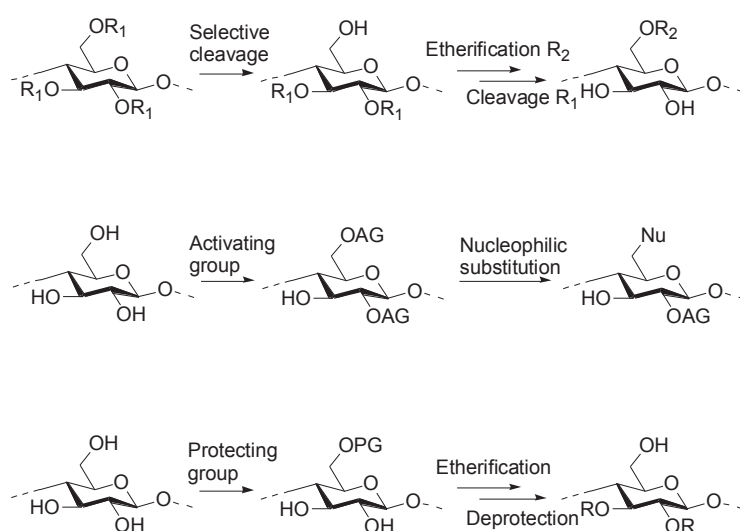
Scheme 2.8 Three synthesis ways of regioselective cellulose derivative

2.2.1 Triphenylmethyl ether moiety as protecting group in the synthesis of 2,3-di-O-methyl cellulose

Triphenylmethyl ether, also known as trityl ether, is one of the earliest protecting groups used in polysaccharide chemistry. It has the preference to react with primary hydroxyl groups on position 6 [44]. The tritylation of cellulose was firstly carried out under heterogeneous starting conditions [45, 46], and in order to exclude some of the problems of solubility of the polymers and accessibility of the hydroxyl groups, the well investigated cellulose solvent DMA/LiCl [47] was used instead.

Starting from 6-mono-O-trityl cellulose, regioselective 2,3-di-O-methyl celluose was synthesized (Scheme 2.9) [48]. 6-mono-O-trityl cellulose was dissolved in dimethylsulfoxide

(DMSO) and reacted with methyl iodide and sodium hydroxide to give the permethylation product. 2,3-di-*O*-methyl cellulose was obtained after detritylation with HCl gas.

In the past few decades, synthesis with substituted triphenylmethyl ether groups were also investigated, especially the (4-methoxy)triphenylmethylchloride which can largely accelerate both the protection and the deprotection reactions [49].
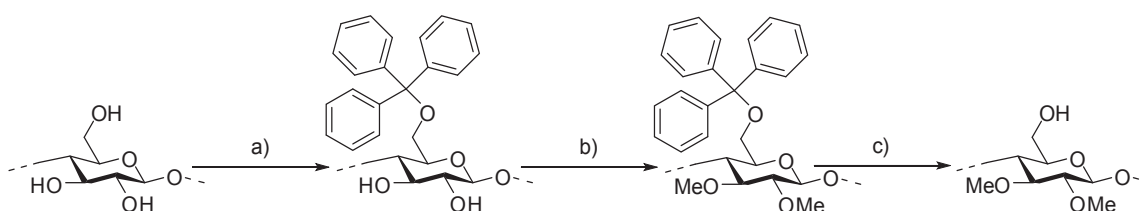
Scheme 2.9 Synthesis of 2,3-di-*O*-methyl cellulose by trityl: a) trityl chloride, pyridine, DMA/LiCl, 70 ºC, 3 d; b) methyl iodide, NaOH, DMSO, 70 ºC, 24 h; c) HCl (gas), dichloromethane, 0 ºC, 3 min

2.2.2 Alkylsilyl ether moiety as protecting group

Another useful protecting group is trialkylsilyl ether. Trimethylsilyl ether (TMS) is widely used for the protection of alcohols, albeit without significant regioselectivity. Nearly fully functionalized trimethylsilyl cellulose can be prepared in liquid ammonia (DS 1.5-1.6) or DMA/LiCl [50]. The regioselectivity was observed to be markedly improved by replacing TMS into thexyldimethylsilyl ether (TDMS) [51] or *t*-butyldimethylsilyl ether (TBDMS) [52]. In the case of silylation by TDMS ether, the functionalization pattern was also controlled by reaction conditions, which will be discussed in detail in the following two sections.

2.2.2.1 Protection of the hydroxyl group on position 6 in the synthesis of 2,3-*O*-methyl cellulose

The cellulose was activated heterogeneously in *N*-methyl pyrrolidone (NMP) and ammonia at -15 to -25 °C, and then the silylation by TDMSCl was carried out at the higher temperature of 80 °C [29, 51]. The 6-mono-*O*-TDMS cellulose obtained permits a similar way to synthesize the

2,3-O-methyl cellulose (Scheme 2.10).

However, unlike the products prepared from 6-mono-O-trityl cellulose, the products of 2,3-di-O-methyl celluloses with the same substitution pattern are water insoluble, as the former contains some structure irregularity of 2-O-trityl groups [53] which imparts water solubility. The application of TDMS ethers forms a more uniform 2,3-di-O-alkyl substitution pattern and it is therefore water insoluble.
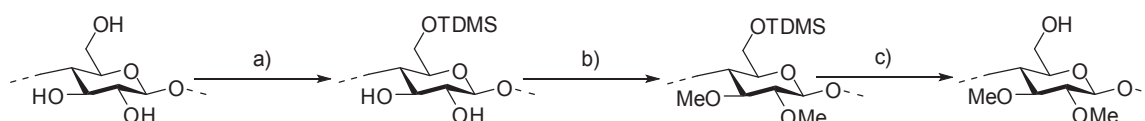
Scheme 2.10 Synthesis of 2,3-di-O-methyl cellulose by TDMS: a) thexyldimethylsilyl chloride, N-methylpyrrolidone/ammonia, 80 ºC, overnight; b) methyl iodide, NaH, THF, 50 ºC, 3 d; c) tetra-butylammonium fluoride trihydrate, THF, 50 ºC, 24 h

2.2.2.2 Protection of hydroxyl groups on position 2 and 6 in the synthesis of 3-mono-O-methyl cellulose

Under homogenous conditions using DMA/LiCl as cellulose solvent, the treatment of cellulose with thexyldimethylsilylchloride, with the presence of imidazole as base, affords 2,6-di-O-TDMS cellulose with a DS of TDMS up to 2 (Scheme 2.11) [51].
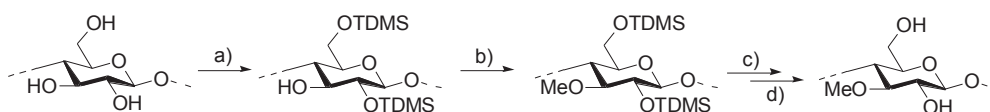
Scheme 2.11 Synthesis of 3-mono-O-methyl cellulose: a) thexyldimethylsilyl chloride, imidazole, DMA/LiCl, 100 ºC, 24 h; b) methyl iodide, NaH, THF, 50 °C, 4 d; c) tetra-butylammonium fluoride trihydrate, THF, 50 ºC, 24 h; d) tetra-butylammonium fluoride trihydrate, DMSO, 50 ºC, 24 h

The subsequent alkylation of hydroxyl group at position 3 with methyl iodide in the presence of NaH yield 3-mono-O-methyl-2,6-di-O-TDMS cellulose. After desilylation in TBAF trihydrate, 3-mono-O-methyl cellulose was obtained [54].

13

According to the published methods, the alkylation of 2,6-O-TDMS cellulose **2** was conducted at 50 °C for 4 d. It was demonstrated that the addition of TBAI as phase transfer catalyst enables the peralkylation at room temperature within the same reaction time [55-58]. Thus, it is of interest to conduct 3-O alkylation of 2,6-di-O-TDMS cellulose under this mild condition to verify whether it could lead to any reduction of polymer degradation.

One should also notice that the similar reaction of 2,6-di-O-TDMS cellulose and methoxypoly(ethylene glycol) iodide with various chain length (DS 0.5) on position 3 yields a special product that is able to form films with a "honey comb" structure [58].

The protection of position 2 and 6 *tert*-butyldimethylsilyl (TBDMS) under homogenous condition was also studied [59]. The silylation of cellulose with TBDMS in DMA/LiCl at room temperature shows the same regioselectivity as the functionalization with TDMS, yet lower levels of regioselectivity (2,3,6-tri-O-silyl units) were found at high reaction temperatures (e.g. 100 °C). Regarding the simplicity of silylation-desilylation and the cost of reagent compared to TDMS ether, 2,6-di-O-TBDMS is an alternative intermediate for synthesizing 3-O functionalized cellulose derivatives.

2.2.3 Orthogonal protecting groups

2.2.3.1 Synthesis of 6-mono-O-methyl cellulose

Besides the utilization of these two bulky groups, the combined use of orthogonal protecting group chemistry is also necessary for the synthesis of regioselectively functionalized cellulose which cannot be prepared directly using bulky protecting groups. Allyl groups were frequently used because it is stable under harsh reaction conditions that are able to cleave silyl ether groups (TBAF) and triphenylmethyl ether group (HCl).

6-mono-O-alkyl cellulose was efficiently synthesized, which was reported by Tetsuo Kondo (Scheme 2.12) [60]: After protecting position 6 with trityl groups in DMA/LiCl in the presence

of pyridine, it was allowed to react with allyl chloride in DMSO with the presence of NaOH, in order to yield 2,3-di-*O*-allyl-6-mono-*O*-trityl cellulose. Then the allyl group was isomerized into the 1-propenyl group. After detritylation by HCl gas in dichloromethane, position 6 was methylated. The last step is to cleave the 1-propenyl on 2 and 3 (isomerization-detritylation-permethylation) in HCl acid. An alternative route of detritylation-permethylation-isomerisation was proven to be inefficient because of the poor solubility of product after permethylation.
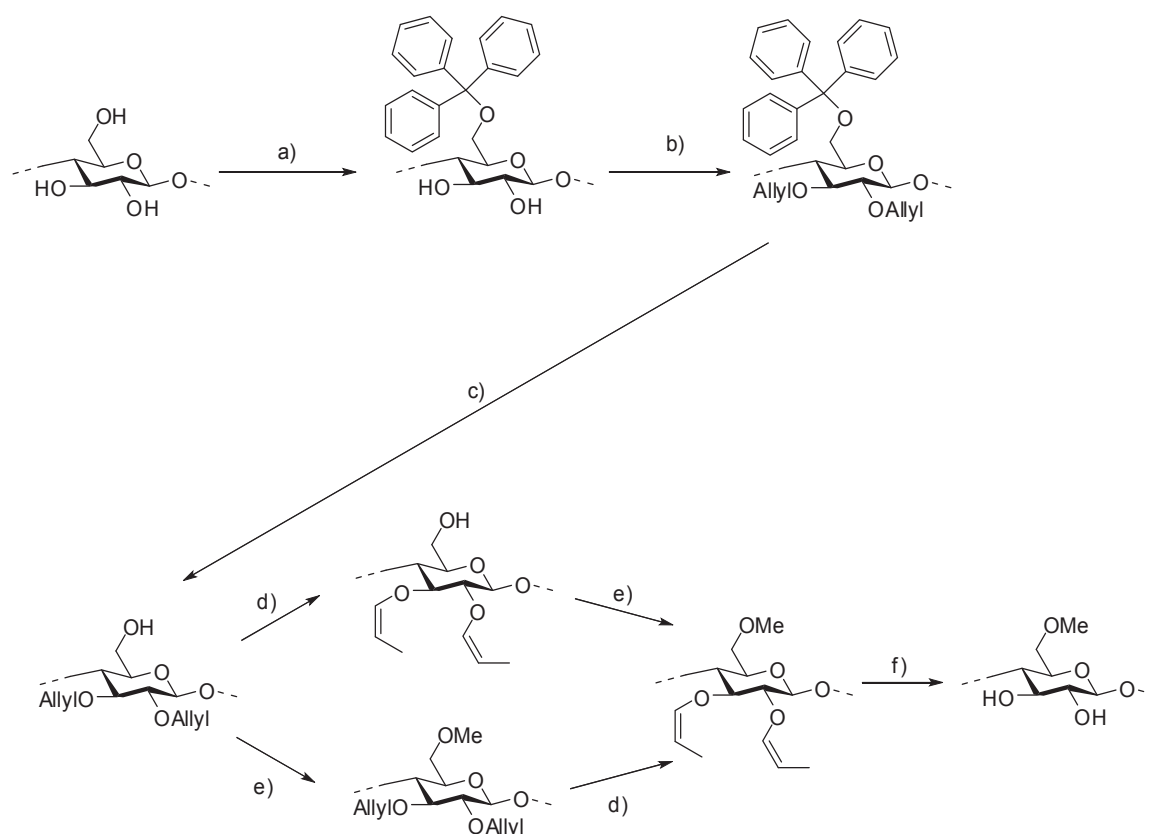
Scheme 2.12 Synthesis of 6-mono-*O*-methyl cellulose: a) trityl chloride, pyridine, DMA/LiCl, 70 ℃, 3 d; b) allyl chloride, NaOH, DMSO, 70 ℃, 24 h; c) HCl (gas), dichloromethane, 0 ℃, 3 min; d) *t*-BuOK, DMSO, 50 ℃, 4 h; e) methyl iodide, NaOH, DMSO (trace of water), 70 ℃, 24 h; f) HCl (0.1 M), MeOH (90 % aq. solution), r. t., 3 h

2.2.3.2 Synthesis of 2,6-di-*O*-methyl cellulose

The synthesis was started with 3-mono-*O*-allyl cellulose (Scheme 2.13) [61]. After permethylation with methyl iodide and deallylation by palladium catalyst,

3-mono-*O*-acetyl-2,6-di-*O*-methyl cellulose was obtained. The 2,6-di-*O*-methyl cellulose was finally obtained after hydrolysis of the acetyl in MeONa/MeOH.
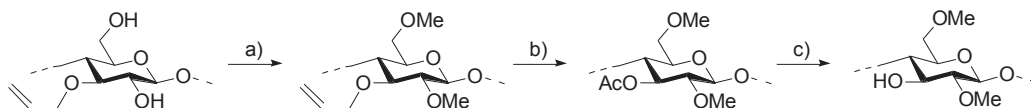
Scheme 2.13 Synthesis of 2,6-di-*O*-methyl cellulose: a) methyl iodide, NaH, THF, 50 ℃, 3 d; b) palladium chloride (PdCl$_2$), MeOH/chloroform (1.5 d), acetic anhydride, DMAP (1.5 d); c) MeONa/MeOH, MeOH/chloroform=1/4 (v/v), r. t., 29 h

Moreover, compared with the 2,6-di-*O*-methyl cellulose synthesized by ring-opening cationic polymerization, the polymer analogous 2,6-di-*O*-methyl cellulose shows identical FT-IR and NMR spectra [61].

2.2.3.3 Synthesis of 3,6-di-*O*-methyl cellulose and 2-mono-*O*-methyl cellulose

Very recently, Nakagawa *et al.* reported the synthesis of 3,6-di-*O*-methyl cellulose and 2-mono-*O*-methyl cellulose (Scheme 2.14 and Scheme 2.15) [62]. The starting material for these two syntheses are 3-mono-*O*-methyl cellulose (for 3,6-di-*O*-methyl cellulose) and 3-mono-*O*-allyl cellulose (for 2-mono-*O*-methyl cellulose) respectively.
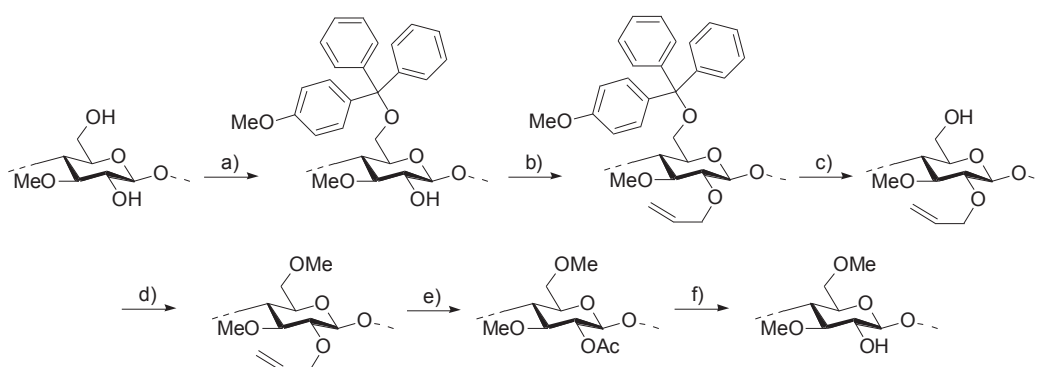
Scheme 2.14 Synthesis of 3,6-di-*O*-methyl cellulose: a) 4-methoxytrityl chloride, pyridine, DMA/LiCl, 4 h, 70 ℃; b) allyl bromide, NaH, DMF, r. t., 1 d/50 ℃, 3 d; c) FeCl$_3$ 6H$_2$O, CH$_2$Cl$_2$, r. t., 1 h; d) methyl iodide, NaH, DMF, r. t., 1 d/50 ℃, 3 d; e) PdCl$_2$, MeOH/CHCl$_3$, r. t., 24 h; acetic anhydride, pyridine, DMAP, 80 °C, 24 h; f) MeONa/MeOH, MeOH/THF, r. t., 6 h

So far, all 6 possible regioselective cellulose ethers are prepared by polymer analogous synthesis applying advanced protecting group techniques; therefore, specific structure property relationships could be established for each substitution pattern.
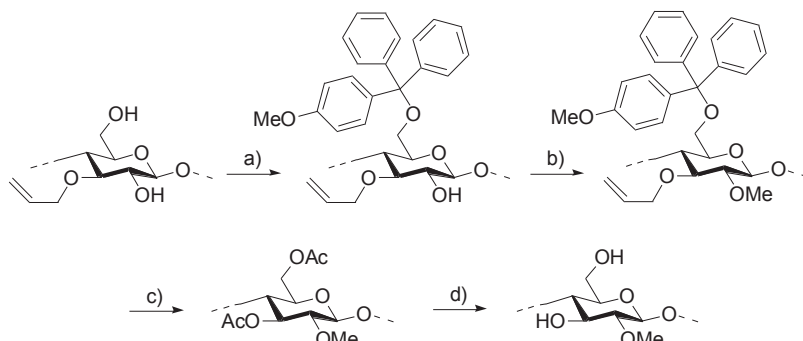
Scheme 2.15 Synthesis of 2-mono-O-methyl cellulose: a) 4-methoxytrityl chloride, pyridine, DMA/LiCl, 4 h, 70 ºC; b) methyl iodide, NaH, DMF, r. t., 1 d/50 ºC, 3 d; c) PdCl$_2$, MeOH/CHCl$_3$, r. t., 24 h; acetic anhydride, pyridine, DMAP, 80 °C, 24 h; d) MeONa/MeOH, MeOH/THF, r. t., 24 h

2.3 Properties of regioselectively functionalized cellulose ethers

2.3.1 Water solubility of regioselectively functionalized cellulose ethers

One important property of regioselective cellulose ethers is their water solubility as summarized in Table 2.2:

Table 2.2 Water solubility of regioselective cellulose: "+" soluble, "-" insoluble

Cellulose ether	DS	Water solubility
2-mono-O-methyl cellulose	0.82-0.77	+ [62]
3-mono-O-methyl cellulose	1.00	- [51]
6-mono-O-methyl cellulose	0.77-1.00	- [60]
2,3-O-methyl cellulose	From 6-O-trityl cellulose 0.87-1.12	+ [48]
	From 6-O-TDMS cellulose 0.89	- [63]
2,6-di-O-methyl cellulose	n.a.	- [61]
3,6-di-O-methyl cellulose	2.11	+ [62]

It can be concluded that the water solubility of regioselectively functionalized methyl cellulose depends on the substitution pattern within the AGU.

Studies on the solubility of 3-mono-O-alkyl cellulose revealed a distinct influence of the alkyl chain length on the solubility of the polymer (Table 2.3).

Table 2.3 3-mono-*O*-functionalized celluloses and their solubility: "+" soluble, "-" insoluble

Substituent at position 3	Solubility				
	water	Ethanol	DMA	DMSO	THF
Methyl [54]	-	-	-	-	-
Ethyl [38]	+	-	+	+	-
n-Propyl [64, 65]	+	-	+	+	-
n-Butyl [64]	-	-	+	+	-
n-Pentyl [66]	-	+	+	+	+
i-Pentyl [66]	-	+	+	+	+
Dodecyl [66]	-	-	-	-	+
Allyl [54]	-	-	+	+	-

2.3.2 Thermal behaviour of regioselectively functionalized cellulose in aqueous solution

In order to understand the thermal behaviour of the aqueous solution of cellulose ethers, thermoreversible gelation of MC aqueous solution was intensively studied and the parameters such as the onset temperature were influenced by the nature of the substituents, degree of substitution and substitution pattern along the cellulose chain [67-72]. Substituted fragments causes the chains to dispersed in bundles in the solution; when heating is applied, the bundles gradually open first, and then after further heating, the disruption of the hydrogen bonding around the polymer will dehydrate the backbone, which encourages the hydrophobic associations [67, 73-77].

Some other researchers focus on the concurrent phase separation [78-80]. Nevertheless, the proposed mechanisms all involve interaction between the hydrophobic moieties on the cellulose backbones [81].

One unique property of regioselective cellulose ethers with well defined structure is that the lower critical solution temperature (LCST) of its aqueous solution is distinct from the LCST of the solution of randomly substituted cellulose ethers: the LCST of the aqueous solution of 3EC is about 60 °C, whereas randomly substituted ethyl cellulose (EC) flocculates at about 30 °C [38].

Thus, the well defined structure of regioselective cellulose ethers make themselves ideal "model compounds" for understanding the mechanism of the solution behaviour of cellulose

ethers. In addition, the unique thermoreversible gelation and/or phase separation property of regioselectively functionlaized cellulose ethers also make them very promising regarding their great potential of application in the medical or pharmaceutical fields.

2.4 Regioselectively functionalized cellulose esters

2.4.1 Previously reported syntheses of regioselectively functionalized cellulose esters

The challenge in the synthesis of regioselectively functionalized cellulose esters are the unstable ester bond under aqueous alkaline or acid conditions. Regioselective cellulose esterification was comprehensively reviewed by Edgar *et al.* recently [4].

Deriatives like 2,3-di-*O*-propionyl-6-mono-*O*-acetyl and 2,3-di-*O*-acetyl-6-mono-*O*-propionyl cellulose were synthesized via 6-*O*-triphenylmethyl cellulose ether, which show specific properties in crystallinity [82]. As shown in Scheme 2.16, triphenylmethyl was used for the protection of position 6. Then propanoyl or acetyl groups were introduced in positions 2 and 3 by using corresponding anhydrides (propanoic anhydride or acetic anhydride respectively) in the presence of 4-*N,N*-dimethylaminopyridine (DMAP). Detritylation in hydrobromic acid was carried out in order to liberate the hydroxyl on position 6.
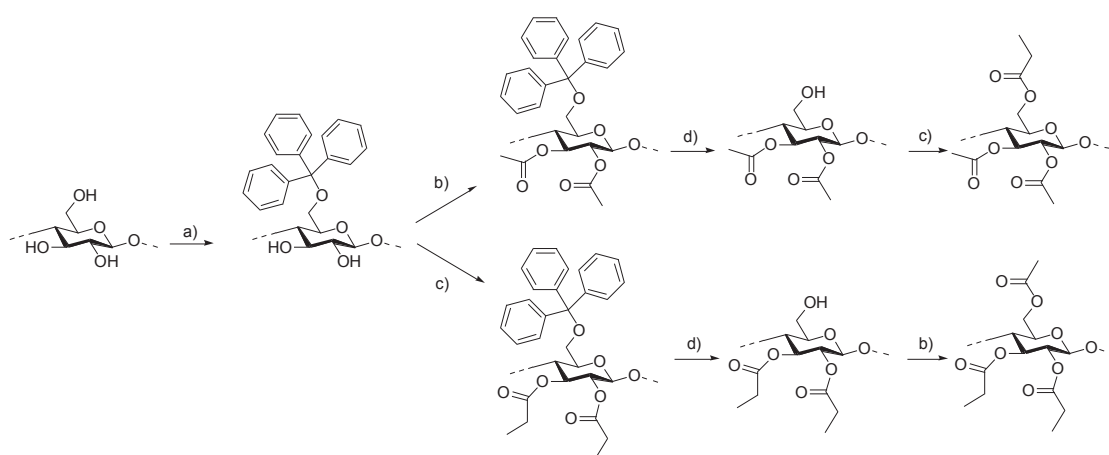
Scheme 2.16 Synthesis of 2,3-di-*O*-acetyl-6-mono-*O*-propionyl cellulose and 2,3-di-*O*-propionyl-6-mono-*O*-acetyl cellulose: a) trityl chloride, pyridine, DMA/LiCl, 100 ºC, 48 h; b) acetic anhydride, pyridine, DMAP, 80 ºC, 24 h; c) propanoic anhydride, pyridine, DMAP, 80 ºC, 24 h d) HBr (25% in HAc), HAc/chloroform, r. t., 5 min

Finally, the regioselectively functionalized product was yielded after detritylation and corresponding propanoylation (2,3-di-O-acetyl-6-mono-O-propionyl cellulose) or acetylation (2,3-di-O-propionyl-6-mono-O-acetyl cellulose).

Recently, Xu and Edgar also reported that cellulose triacetate was selectively deacetylated at positions 2 and 3 by treatment of TBAF in THF at 50 °C to obtain 6-mono-O-acetyl cellulose (Scheme 2.17) [83].
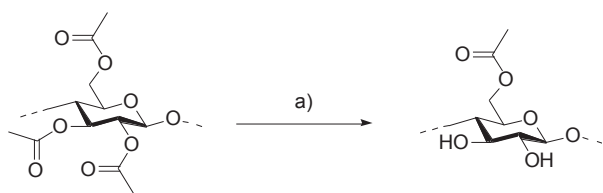
Scheme 2.17 Selective cleavage of triacetate: a) tetra-butylammoniumfluoride trihydrate (TBAF·3H$_2$O), tetrahydrofuran (THF), 50 °C, 24 h

This method provides an alternative way to prepared 2,3-di-O-acetyl-6-mono-O-propanoyl of cellulose. Compared to the method applying triphenylmethyl ether protecting group, the synthesis was simplified and the steps are reduced.

More recently, another 2,6-di-O-acetyl cellulose was prepared by Xu and Edgar [84]. The synthesis was demonstrated in Scheme 2.18. Starting from the key intermediate 3-mono-O-allyl cellulose, hydroxyls on position 2 and 6 were peracetylated or perpropionated. After deallylation by palladium chloride in chloroform/methanol which is a mild condition for deprotection, 2,6-di-O-acetyl cellulose was obtained.
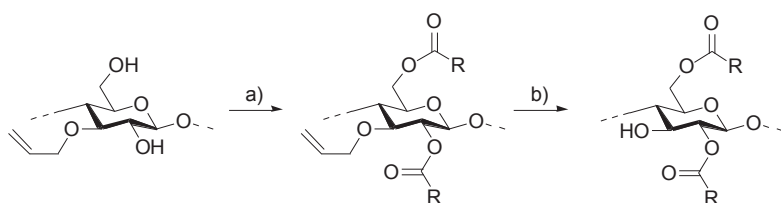
Scheme 2.18 Synthesis of 2,6-di-O-acetyl and 2,6-di-O-propionyl cellulose (R=acetyl or propionyl): a) (RCO)$_2$O, pyridine, DMAP, 80 °C, 24 h ; b) chloroform/MeOH=8/5 (v/v), PdCl$_2$, room temperature, 24 h, R=-CH$_3$ or -CH$_2$CH$_3$

The obtained 2,6-di-*O*-acetyl and 2,6-di-*O*-propionyl cellulose could also be applied for the synthesis of 3-mono-*O*-propionyl-2,6-di-*O*-acetyl and 3-mono-*O*-acety-2,6-di-*O*-propanoyl cellulose.

2.4.2 A new challenge—the synthesis of 3-mono-*O* cellulose esters

Alkylation of position 3 of the AGU of cellulose applying advanced protecting group techniques has been extensively investigated during the past years. The challenge is the synthesis of regioselectively functionalized cellulose esters with other functionalization patterns. As a widely applied and efficient method, the advanced protecting group technique was considered, but the key step is the deprotection. The most applied desilylation method is the use of tetra-butylammonium fluoride (TBAF), but the main drawback is that the strong base reaction condition causes also the cleavage of the ester groups. Typical example is the selective deacetylation in TBAF reported by Edgar *et al.* [83]. However, as plenty of methods of desilylation of smaller molecules under mild conditions by catalyst were reported ($FeCl_3$ in MeOH [85]; $InCl_3$ in CH_3CN [86]; Cs_2CO_3 in DMF [87]; $NaIO_4$ in $THF/H_2O=4/1$ [88]), it is also of great interest to carry out desilylation of cellulose silyl ethers under mild conditions without cleavage of the ester groups.

Another alternative method is desilylation by fluorides in mild conditions, in this presented work, desilylation by three fluorides are involved: HF/Pyridine [89, 90], CsF [91], and 1-Chloromethyl-4-fluoro-1,4-diazoniabicyclo[2.2.2]octane bis(tetrafluoroborate), also known as Selectfluor® [92] (see section 3.6.2).

2.5 Characterization of regioselective cellulose ethers

Conventional analytical methods such as NMR and FT-IR are very usual for the strucuture characterization of molecules: NMR for the clarification of the chemical structure of cellulose

derivatives, and FT-IR for the identification of the functional groups.

Besides, considering the unique properties of regioselectively functionalized cellulose ethers, especially the thermal behaviour of the molecules in solution, supplementary analyses like differential scanning calorimetry (DSC) and rheology measurements are also frequently involved in the property characterization of cellulose derivatives.

2.5.1 Differential Scanning Calorimetry (DSC)

DSC is a useful technique for determination of glass transition temperatures, melting or recrystallisation temperatures and enthalpies, and measurements on reacting systems [93]. As discussed in section 2.3.2, the thermal reversible gelation and the concurrent flocculation of alkyl cellulose in aqueous solution are due to dehydration and consequent hydrophobic interactions of the polymer chains. Energy is required for the dehydration, and the enthalpy changes during the heating or cooling process of alkyl cellulose aqueous solution could be evaluated by DSC in order to understand the thermal behaviour of alkyl cellulose molecules in aqueous solution.

2.5.2 Rheological measurements

Dehydration and consequent hydrophobic interactions of alkyl cellulose in aqueous solution can form network of polymer chains. For conventional polymers, the chemical cross-linkages of the chains are mainly covalent and therefore thermostable. However, the network formed by ionic forces or hydrogen bonds are thermally reversible [94]. In this case, thermally induced structure changes of alkyl cellulose in water can be assessed by small deformation dynamic viscoelastic measurements, which is a supplement to DSC measurements regarding the thermal behaviour investigation.

2.5.3 Analysis of the distribution of substituents along cellulose backbone by mass spectroscopy

Besides the functionalization pattern, the distribution of substituents along the polysaccharide chain also influences the properties such as thickening, gelation, and film forming [95]. Mischnick *et al.* also have developed an advance method to investigate the substitution pattern of cellulose derivatives [95, 96]: a) Complete degradation products of cellulose derivatives are analyzed by gas chromatography combined with flame ionization detector mass spectrometry (GC-FID/MS), and the monomer composition with different substitution patterns were calculated; b) Then cellulose derivatives were partially depolymerized by mild methanolysis or mild reductive cleavage, and the obtained oligomeric mixture was submitted to mass spectrometry in order to identify the substitution patterns within the oligomers; c) The experimental results of substitution pattern of oligomers are compared with theoretical statistical arrangement of the monomers which are calculated from the monomer composition. Finally, information of "statistical" (random) distributions and "block like" (regular) distributions of substituents can be obtained by this comparison.

3. Results and discussions

3-mono-*O*-propyl cellulose (3PC) has a LCST of 20 °C [65]. Compared to 3-mono-*O*-ethyl cellulose, there is only one carbon difference in alkyl chain length, which leads to 40 °C difference of LCST. Thus, it is of great interest to tune the LCST of the 3-*O*-alkyl ethers, for instance, to body temperature. To achieve this goal, two different methods are suggested. First is to synthesis 3-*O*-alkyl ether bearing two different alkyl moieties within the same chain; second is to physically mix the solution of two different 3-*O*-alkyl ethers, 3EC and 3PC for example.

3.1 Synthesis and structure characterization

3.1.1 Synthesis of 3-mono-*O*-alkyl cellulose bearing one single ether group

Firstly, starting from microcrystalline cellulose (Avicel PH-101), 2,6-di-*O*-TDMS cellulose **2** was prepared homogeneously in *N,N*-dimethylacetamide (DMA)/LiCl with TDMSCl in the presence of imidazole (Scheme 3.1) [54].
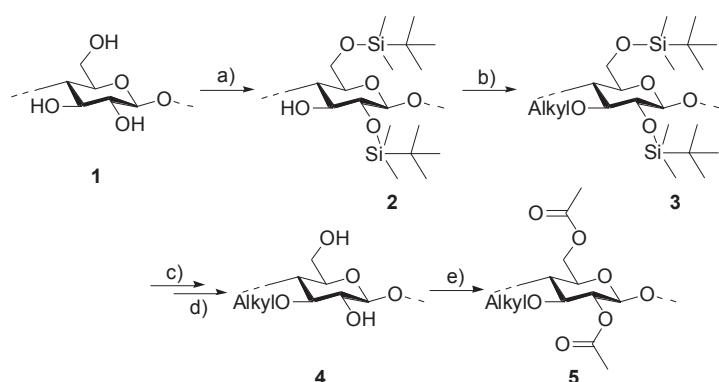
Scheme 3.1 Typical synthesis route for 3-mono-*O*-alkyl cellulose and 2,6-di-*O*-acetyl-3-mono-*O*-alkyl cellulose: a) thexyldimethylsilyl chloride, imidazole, DMA/LiCl, 100 ºC, 24 h; b) alkyl iodide, NaH, THF, 50 ºC/r. t. with tetra-*n*-butylammonium iodide, 4 d; c) tetra-*n*-butylammonium fluoride trihydrate, THF, 50 ºC, 24 h; d) tetra-*n*-butylammonium fluoride trihydrate, DMSO, 50 ºC, 24 h; e) acetic anhydride, pyridine, DMAP, 80 ºC, 20 h

2,6-di-*O*-TDMS cellulose **2** has a DS 2.06 as calculated from the silicon content of the

product determined gravimetrically by combustion with sulphuric acid. With this 2,6-di-O-TDMS cellulose, 3MC (sample **4i**, DS 1.05) [54], 3EC (sample **4j**, DS 1.07) [38] and 3PC (sample **4k**, DS 1.13) [65] were prepared according to the published procedures.

3.1.2 Synthesis of 3-O-alkyl cellulose bearing two ether groups by simultaneous alkylation

2,6-di-O-TDMS cellulose was allowed to react simultaneously with two different alkyl iodides (MeI, EtI, PrI) in the presence of sodium hydride followed by desilylation. The ratio between the two alkyl moieties bound at position 3 of the repeating unit was adjusted by changing the ratio of the alkylating agents while maintaining the molar ratio of hydroxyl group to alkylating agent of 1:10 as summarized in Table 3.1. The conversion of 2,6-di-O-TDMS cellulose with an equimolar mixture of EtI and PrI and subsequent desilylation afforded sample **4a** with DS_{Et} of 0.95 and DS_{Pr} 0.15. Obviously, PrI possesses a significantly lower reactivity compared with EtI. Changing the molar ratio EtI:PrI from 5:5 to 3:7 yielded sample **4b** with DS_{Et} 0.77 and DS_{Pr} 0.27. Further increase of the ratio EtI:PrI to 2:8 led to increase of DS_{Pr} while maintaining the total DS constant (sample **4c**, DS_{Et} 0.54, DS_{Pr} 0.42). Applying 1 mol EtI and 9 mol PrI per mol of modified repeating unit afforded sample **4d** with DS_{Et} 0.27 and DS_{Pr} 0.56.

In a further set of experiments, the conversion of the 2,6-di-O-TDMS cellulose with MeI/EtI and MeI/PrI was studied (Table 3.1). The reaction of 5 mol MeI and EtI per mole modified AGU yielded sample **4e** with DS_{Me} 0.99, DS_{Et} 0.08. Similar to the conversion of 2,6-di-O-TDMS cellulose with EtI and PrI, the difference in partial DS results from the more reactive MeI compared with EtI. A ratio of MeI:EtI=1:9 afforded sample **4f** with DS_{Me} 0.19 and DS_{Et} 0.91. Comparable results were observed for conversion of 2,6-di-O-TDMS cellulose with MeI and PrI. Thus, a reaction with equimolar amounts of MeI and PrI gave sample **4g** with DS_{Me} 0.97 and DS_{Pr} 0.12. Applying a ratio of MeI:PrI=1:9 afforded sample **4h** with

DS_{Me} 0.46 and DS_{Pr} 0.58. The total DS of the 3-*O*-alkyl cellulose is about 1 and in accordance with the general reaction scheme of 2,6-di-*O*-protection, 3-mono-*O*-alkylation, and 2,6-di-*O*-deprotection. Deviations might be caused by different methods used for DS determination and their inherent errors, namely elemental analysis of 2,6-di-*O*-TDMS cellulose **2** and ^{1}H-NMR spectroscopy after peracetylation for samples **4a-h**.

Table 3.1 Conditions for and results of the conversion of 2,6-di-O-thexyldimethylsilyl (TDMS) cellulose **2** simultaneously with two different alkylating agents in the presence of sodium hydride (NaH, 10 mol/mol modified AGU) for 4 d in tetrahydrofuran and subsequent desilylation

Conditions					Results										
Molar ratio[a]				Temp.[b] °C	2,6-di-O-TDMS-3-O-alkyl cellulose			3-O-alkyl cellulose							
					Sample	$\overline{M}_n$[d] g/mol	DP_n[e]	Sample	DS^b Me	Et	Pr	Σ DS	$\overline{M}_n$[d] g/mol	DP_n[e]	LCST[f] °C
2	MeI	EtI	PrI												
1	-	5	5	50	**3a**	-[b]	-	**4a**	-	0.95	0.15	1.10	45917	235	58
1	-	3	7	50	**3b**	18833	40	**4b**	-	0.77	0.27	1.04	49276	252	44
1	-	2	8	50	**3c**	21453	49	**4c**	-	0.54	0.42	0.96	41477	212	38
1	-	2	8	rt[g]	**3c'**	15911	33	**4c'**	-	0.59	0.43	1.02	4028	20	38
1	-	1	9	50	**3d**	-[h]	-	**4d**	-	0.27	0.56	0.83	33308	172	33
1	5	5	-	rt[g]	**3e**	-[h]	-	**4e**	0.99	0.08	-	1.07	6778	38	-[h]
1	1	9	-	rt[g]	**3f**	25488	53	**4f**	0.19	0.91	-	1.10	6569	34	71
1	5	-	5	rt[g]	**3g**	-[h]	-	**4g**	0.97	-	0.12	1.09	6419	35	-[h]
1	1	-	9	rt[g]	**3h**	22512	46	**4h**	0.46	-	0.58	1.04	9287	48	38
1	10	-	-	50	**3i**	-[h]	-	**4i**	1.05	-	-	1.05	33506	190	-[h]
1	10	-	-	rt[g]	**3i'**	-[h]	-	**4i'**	-[h]	-	-	-	-[h]	-	-[h]
1	-	10	-	50	**3j**	-[h]	-	**4j**	-	1.07	-	1.07	24698	130	60
1	-	-	10	50	**3k**	9342	19	**4k**	-	-	1.13	1.13	-[h]	-	18

[a]Molar ratio of 2,6-di-O-TDMS cellulose **2**:alkyl iodide (methyl iodide, MeI; ethyl iodide, EtI, n-propyl iodide, PrI):sodium hydride.

[b]Temperature, room temperature (r.t.)

^cDegree of substitution of methyl (Me)-, ethyl (Et)-, and propyl (Pr) groups determined by ^{1}H-NMR spectroscopy after peracetylation of the samples.

^dNumber average molar mass measured by SEC in tetrahydrofuran (samples **3b**, **3c**, **3f**, **3h**) and *N,N*-dimethyl acetamide/LiCl (samples **4a-4h**).

^eNumber average degree of polymerization calculated from SEC data.

^fLower critical solution temperature of 1% (w/w) solutions of the samples in water.

^gAddition of tetra-*n*-butylammonium iodide as phase transfer catalyst.

^hNot measured.

3.1.3 Fourier transform infrared (FT-IR) spectroscopic characterization of 3-*O*-alkyl celluloses

Fourier transform infrared spectroscopy (FT-IR) was applied to confirm the total alkylation of position 3 during the synthesis of the alkyl celluloses. After the alkylation, all three accessible hydroxyl groups of cellulose are substituted, therefore, the absorbance of OH groups is absent in the spectra. Figure 3.1 showed the FT-IR spectrum of 2,6-di-*O*-TDMS-3-mono-*O*-ethyl cellulose.
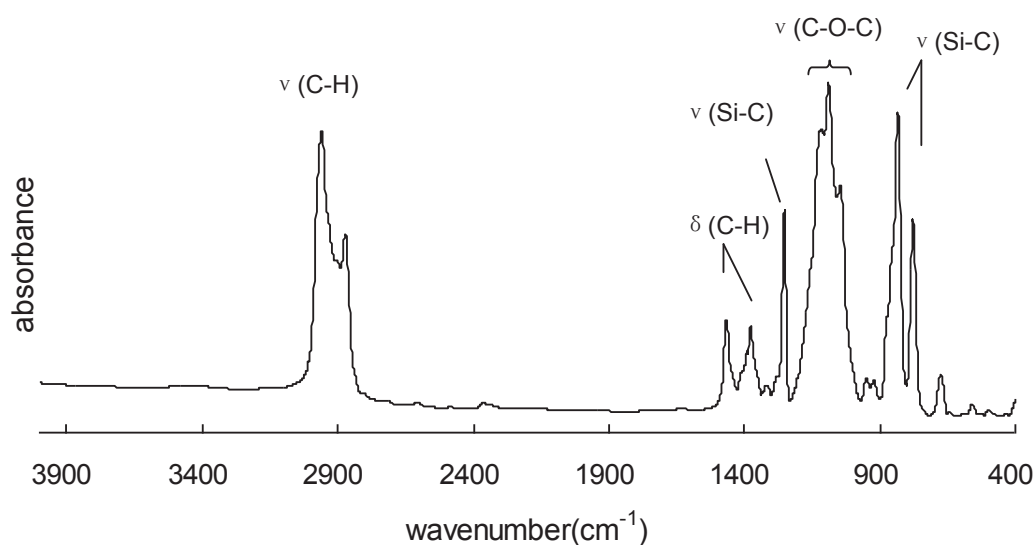
Figure 3.1 FT-IR spectrum of 2,6-di-*O*-TDMS-3-mono-*O*-ethyl cellulose (**3j)**

Firstly, no absorbance was observed around 3500 and 1640 cm^{-1}, which indicated the complete alkylation of hydroxyl groups on position 3. Other typical signals of the 2,6-di-*O*-TDMS-3-mono-*O*-ethyl cellulose were also assigned: peaks at 2963, 2873 cm^{-1} were due to the C-H stretching, while peaks at 1468 and 1379 cm^{-1} are caused by C-H bending; Si-C stretching peaks were found at 832, 777 and 1255 cm^{-1}; C-O-C stretching of the glucose unit was characterized by the absorbance at 1089 cm^{-1}.

As discussed in section 2.2.2.2, peralkylation under milder condition (room temperature with the presence of phase transfer catalyst TBAI) was carried out in order to reduce the polymer

degradation. The FT-IR spectra of sample **3i** (3MC synthesized without catalyst at 50ºC) and sample **3i'** (3MC synthesized at room temperature in presence of TBAI) was shown in Figure 3.2: Both **3i** and **3i'** gave similar FT-IR spectra as that of **3j**: typical absorbance for C-H stretching, C-H bonding, Si-C stretching, C-O-C stretching are well assigned. Moreover, these two alkylation products (**3i** and **3i'**) under different conditions show almost identical FT-IR spectra.
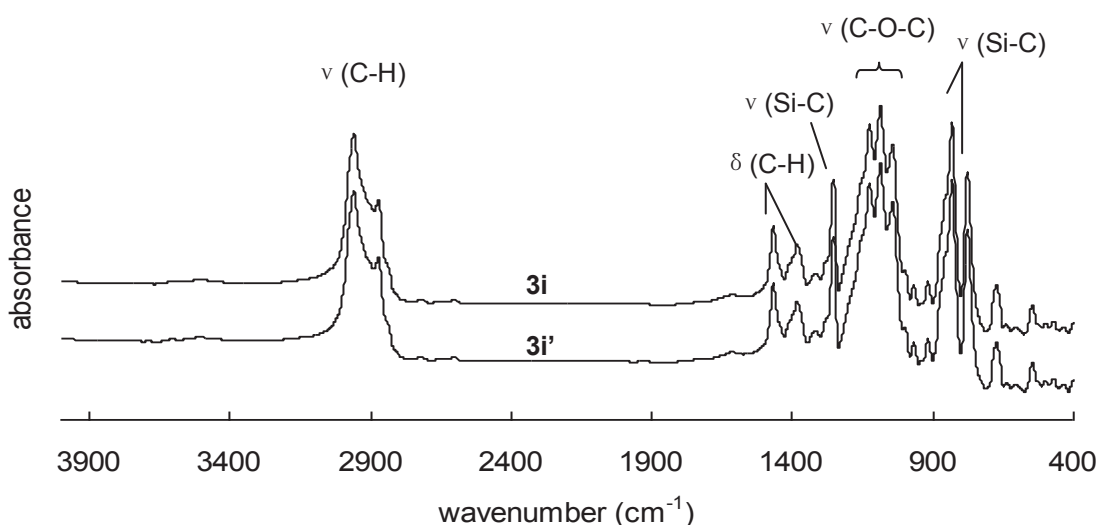
Figure 3.2 FT-IR spectra of 2,6-di-*O*-TDMS-3-mono-*O*-methyl cellulose synthesized via alkylation at 50 °C (**3i**) and with catalyst TBAI at room temperature (**3i'**)

Therefore, it can be concluded that the use of catalyst has no influence on the efficiency of alkylation, according to the comparison of sample **3i** and **3i'**.

3.1.4 Nuclear magnetic resonance (NMR) spectroscopic characterization of 2,6-di-*O*-acetyl-3-*O*-alkyl celluloses

NMR spectra were acquired after peracetylation of the samples in order to prevent the formation of hydrogen bonds, i.e. to reduce polymer-polymer interactions. Thus, the resolution of the NMR spectra is therefore improved (Figure 3.3). The ^{1}H NMR spectra of

2,6-di-O-acetyl-3-O-Et/Pr cellulose (**5a, 5d**), 2,6-di-O-acetyl-3-O-Me/Et cellulose (**5e, 5f**), and 2,6-di-O-acetyl-3-O-Me/Pr cellulose (**5g, 5h**) are shown in Figure 3.3. For **5a** and **5d** (numbering 1-8, 1'-9'), the signals in the high field from 0.50 to 2.25 ppm correspond clearly to the alkyl protons on 8, 8', 9' as well as the methyl protons of the acetyl group. Protons at 7 and 7' from -CH$_2$- next to the oxygen of the ether bond were found at 3.74 and 3.48 ppm respectively. The signals in the range from 2.90 to 5.20 ppm result from glucose unit protons: 3.41 H-3, 3.43 H-5, 3.63 H-4, 4.44 H-1, and 4.78 H-2 as well as the protons on position 6: 4.16 (α) and 4.36 (β) ppm.

Sample **5e** and **5f** (numbering 1-7, 1'-8') as well as **5g** and **5h** (numbering 1-7, 1'-9') gave similar spectra. The difference is a sharp peak at about 3.45 ppm that corresponds to the methyl protons on position 7. In addition, for samples with higher content of Et- or Pr moieties (**5g**, **5h**), the signals for glucose unit protons at position 5 were always overlapped by the alkyl protons on 7'. However, due to the lower content of Et- or Pr groups in **5e**, **5f**, it is impossible to assign the peaks of protons of attached on position 7' clearly.

Figure 3.4 shows the ^{13}C NMR spectra of 2,6-di-O-acetyl-3-O-ethyl/propyl cellulose. At high field, the carbons from alkyl groups were found: 10.2 ppm C9' (Pr), 15.2 ppm C8 (Et), 23.1 ppm C8' (Pr). Carbon signal at 20.5 ppm was assigned as methyl of acetyl group. The peak at 62.6 ppm is attributed to C6, while signals at 67.5 ppm stands for C7 (Et) and C7' (Pr). C2 and C5 were found at 73.9 ppm. The signal for C4, which is very close to the solvent peak, is situated at 77.5 ppm. C1 and C3 were clearly identified at 100.8 and 80.6 ppm, respectively.

At low field, there are two peaks for carbonyl group at 170 and 169 ppm, which indicates that only OH groups at position 2 and 6 were acetylated [97]. This fact reveals the selective alkylation of position 3.

The 2D NMR spectra of ^{1}H-^{1}H COSY and HSQC revealed the correlation of proton-proton and proton-carbon signals (Figure 3.5). Moreover, peaks of low intensity around 3.15 and

5.10 ppm (marked in dotted circle) were attributed to substructures due to deviation from the ideal structure to a small extent (3,6-*O*-acetyl-2-*O*-alkyl cellulose), which is already known from the literature [38, 65].
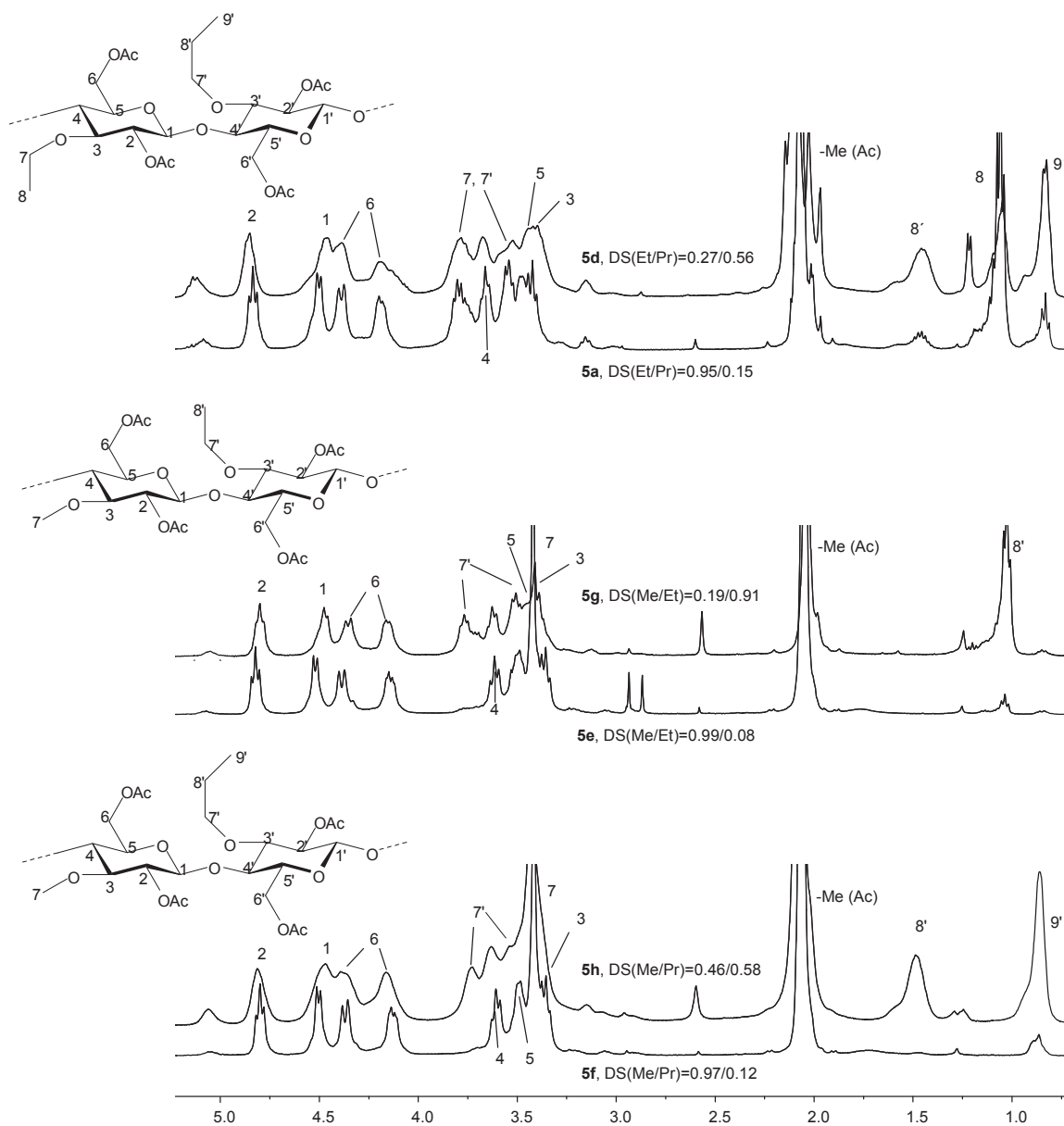
Figure 3.3 ^{1}H NMR spectra of different 2,6-di-*O*-acetyl-3-*O*-functionalized cellulose ethers bearing two alkyl moieties obtained by simultaneous conversion of 2,6-di-*O*-thexyldimethylsilyl cellulose with two alkylating agents in the presence of sodium hydride followed by desilylation and peracetylation (degree of substitution: DS; methyl: Me; ethyl: Et; *n*-propyl: Pr; recorded in CDCl$_3$)
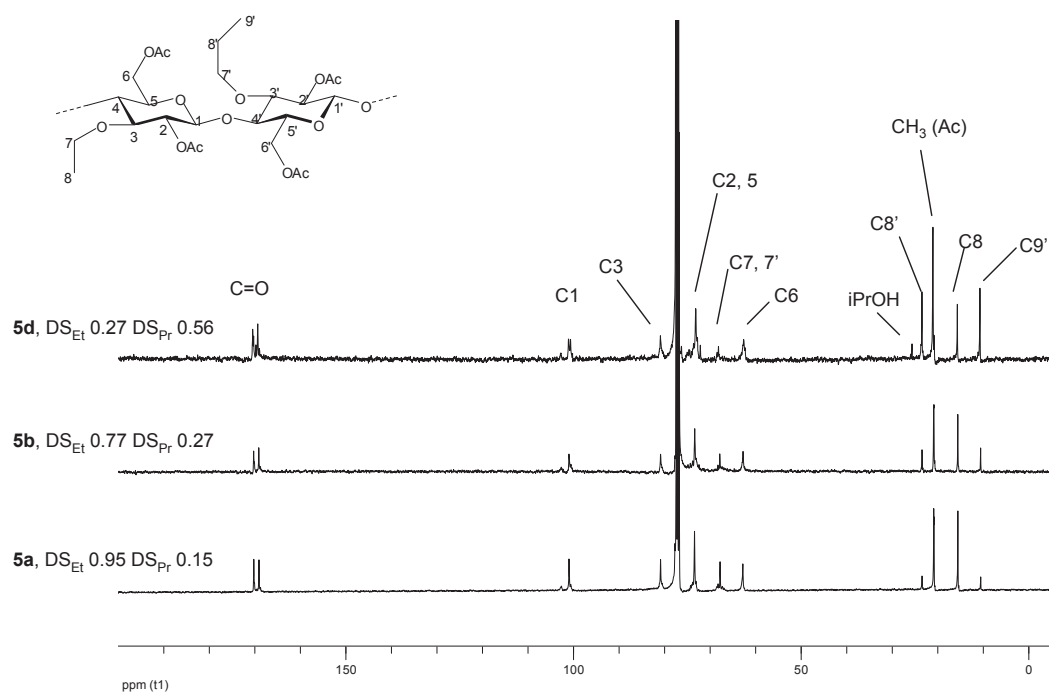
Figure 3.4 ^{13}C NMR spectra of different 2,6-di-*O*-acetyl-3-*O*-functionalized cellulose ethers bearing two alkyl moieties after peracetylation, with different DS of ethyl and propyl groups (**5d**, **5b** and **5a**, recorded in CDCl$_3$)

3.2 Determination of degree of polymerization (DP) of 3-*O*-alkyl cellulose

3.2.1 Size exclusion chromatography (SEC) of 3-*O*-alkyl celluloses in DMA/LiCl

Due to the fact that three synthesis steps are needed to get these sophisticated cellulose derivatives, a certain extent polymer degradation may occur. Thus, all intermediate compounds were anaylzed by size exclusion chromatography. The DP$_n$ were calculated from the results of SEC. The silylation of cellulose in DMA/LiCl with TDMS-Cl in the presence of imidazole causes a slight degradation from DP$_n$ 117 (starting material **1**, carbanilate method) to 94 (2,6-di-*O*-TDMS cellulose **2**, SEC in THF). Compared to the literature precedent of Schumann *et al.*, the Avicel as starting material with DP 222 increased to around 1500 after protection of TDMS on position 2 and 6 [98]. Considering the high reproducibility of the molar mass values of 2,6-di-*O*-TDMS cellulose **2** obtained by SEC within this presented work, it is suggested there might be an error in the work of Schumann *et al.*
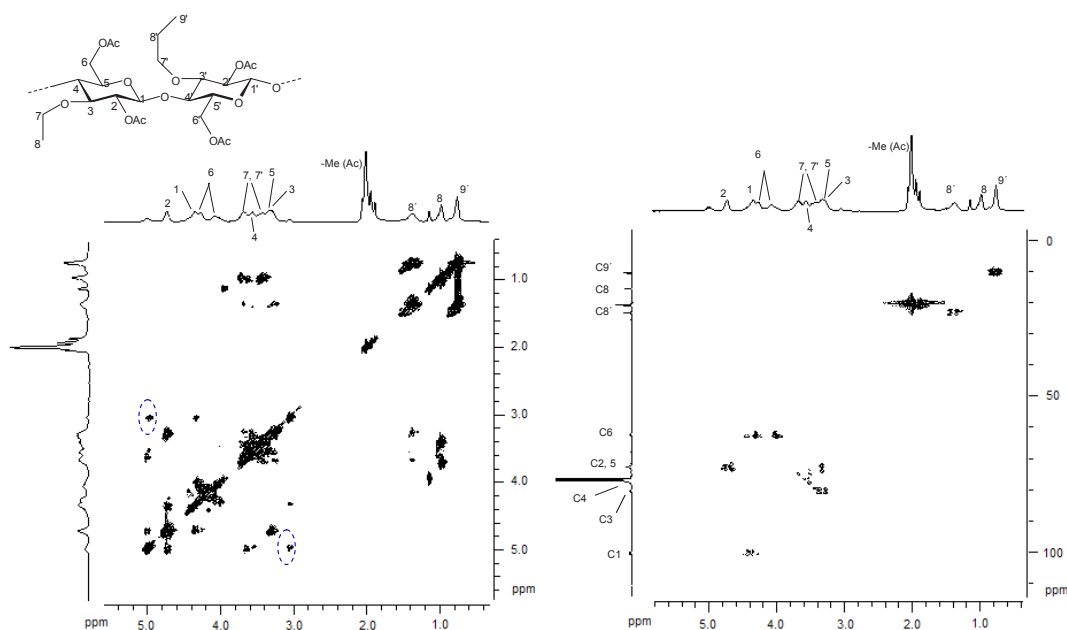
Figure 3.5 ^{1}H-^{1}H COSY and HSQC NMR spectra of 2,6-di-*O*-acetyl-3-*O*-functionalized cellulose after peracetylation (**5d**, DS_{Et}/DS_{Pr}=0.27/0.56, recorded in CDCl$_3$)

The 2,6-di-*O*-TDMS-3-*O*-alkyl celluloses possess DP_n values in the range from 40 to 53 (Table 1). Obviously, the DP_n values of 3-*O*-alkyl celluloses (**4a-f**) depend on the reaction conditions of the alkylation step. Thus, products synthesized at room temperature in the presence of TBAI possess DP_n values in the range from 34 to 48 (samples **4e-h**). On the contrary, alkylation of 2,6-di-*O*-TDMS cellulose at 50 °C afforded samples with significantly higher apparent DP_n values ranging from 172 to 252 (**4a-4d**), which are about 10 times higher compared with the DP_n of products synthesized at room temperature in the presence of TBAI. Considering the DP_n of the starting material microcrystalline cellulose **1** (DP_n 117), a different aggregation behaviour of the 3-*O*-alkyl celluloses must be taken into account.

In order to confirm that the different DP_n values result from different reaction conditions, two 3-*O*-Et/Pr celluloses were prepared by applying the same molar ratio of reagents to modified AGU but different alkylation conditions (50 °C without TBAI; room temperature with TBAI). Both DS_{Et} and DS_{Pr} of samples **4c** and **4c'** are comparable, but the DP_n values calculated from

$\overline{M}_n$ measured by SEC in DMA/LiCl differ by one order of magnitude (Table 1). In order to exclude the potential influence of TBAI, "blind tests" were made in order to evaluate the influence of the solvent and the catalyst: the 2,6-di-*O*-TDMS cellulose was dissolved in THF, treated without TBAI (**2b**) at 50 °C and with TBAI (**2c**) while stirring at room temperature and applying same reaction time of alkylation. As shown in Figure 3.6, the DP_n values of the precipitated products (**2b**, DP_n 113; **2c**, DP_n 112) exhibits no magnitude difference as that of the original 2,6-di-*O*-TDMS cellulose **2** (DP_n 94). The slight increase in DP may be due to the removal of the impurities with smaller molar mass through dissolving and reprecipitation (standard purification procedure).
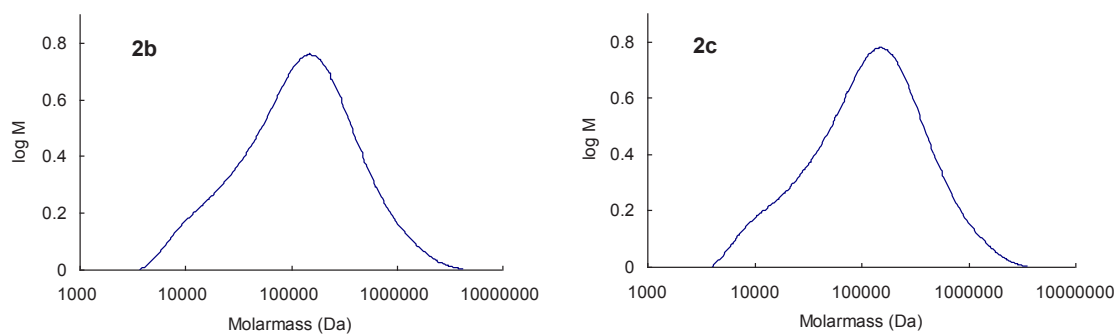
Figure 3.6 SEC trace of 2,6-di-*O*-TDMS cellulose treated under different conditions in THF **2b** and **2c** for 4 days

The DP_n values of other products of alkylation prepared under different conditions are also comparable (**3c**-49 at 50 °C; **3c'**-33 at r. t. with TBAI), so the possibility of the influence from catalyst and solvent can be excluded. Thus, it is assumed that in DMA/LiCl, samples prepared at 50 °C tend to form aggregates (DP_n 212, sample **4c**), while samples synthesized at room temperature did not form aggregates (DP_n 20, sample **4c'**).

In order to exclude the influence of possible aggregation, the SEC measurements of peracetylated products **5c** and **5c'** were also carried out in THF. **5c** has a DP_n 272, and **5c'** DP_n 138. These DP_n values are both higher than that of the sample products before peracetylation (**4c** 212, **4c'** 20) respectively. It was reported that the DP value of peracetylated products

depend on the DS of ether groups at position 3 [65], i.e., DP values between 148-191 are observed for samples with DS around 1 compared with a lower DP 45-63 for samples with DS <1, but a clear explanation was unavailable. It appears that the peracetylation cannot dissociate the aggregation of the polymer chains. Therefore, with the current results, the mechanism of this possible aggregation is as yet unclear.

In order to clarify the reason for this difference in magnitude of the DP_n values and to exclude any possible calculation error during the calibration, the elution diagram (elution volume against signal intensity) of the SEC measurements was also investigated. As shown in Figure 3.7, the elution volume of sample **4c** (around 16 mL) is smaller than sample **4c'** (18 mL). It is obvious that sample **4c** possesses a larger "apparent" weight average molar mass than that of sample **4c'**. Considering the mechanism of SEC, this difference implies that the molecules of **4c** went through the column faster than that of **4c'**.
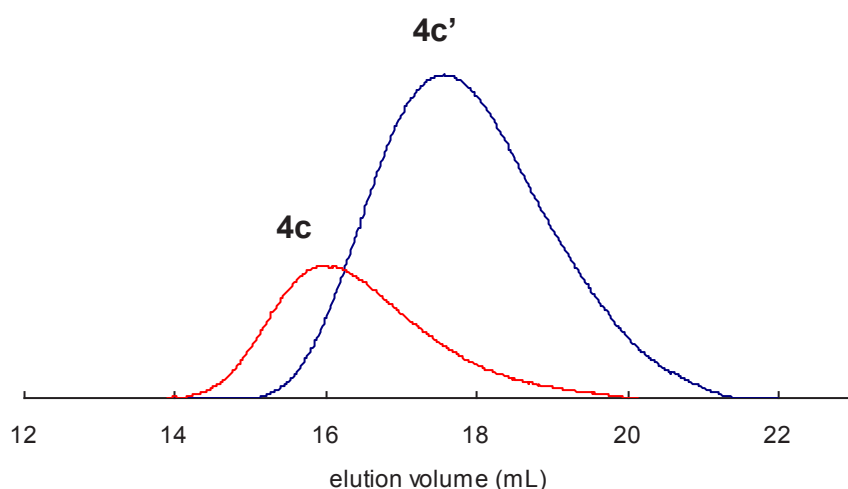
Figure 3.7 Elution curves of SEC measurements of **4c** (alkylation at 50 °C without catalyst) and **4c'** (alkylation at r. t. with catalyst) indicating the higher molar mass of **4c**

Therefore, two hypotheses were made: first one is that the difference in the size of the polymers or aggregates; and the second is the difference in polymer chain conformation. Firstly, the aggregation behaviour was considered. As reported previously [99], the benzylation

of cellulose at 50 °C without any catalyst at room temperature in the presence of TBAI leads to products with different structures: a block-wise functionalization was detected in products synthesized at 50 °C, while a random functionalization pattern was found after reaction at room temperature. A similar behaviour might be possible in the case of alkylation of 2,6-di-*O*-TDMS cellulose with two different alkylating agents, i.e., a block-like distribution of the different alkyl moieties may appear when the alkylation is carried out at 50 °C without catalyst, and this structure favours the hydrophobic interactions of polymer chains; the alternative alkylation reaction carried out at room temperature with the presence of catalyst leads to a random distribution of two ether groups, which somehow disables the interchain hydrophobic interactions (Scheme 3.2). In other words, it is likely that the sequence of repeating units being differently alkylated at position 3 depends on the alkylation conditions. Enzymatic hydrolysis of cellulose derivatives can be applied to investigate its "block-like" structures [100]. However, one should note that this method is based on the selective hydrolysis which takes place at the "border" between the "block" of substituted glucose units and the "block" of non-substituted AGUs. As the glucose units along the backbone of 3-*O*-ethyl/propyl cellulose are fully substituted, this analytical method of enzymatic hydrolysis is inappropriate.

Secondly, the influence of conformation must be taken into account, namely whether the polymer in solution is sphere, rigid rod or random coil like. This could be evaluated by measuring the intrinsic viscosity (section 3.4.5). Consequently, further studies on functionalization pattern along the polymer chain are required.

3.2.2 SEC measurement of sample **4c** and **4c'** in water

In order to compare with the SEC results in DMA/LiCl, the solvent was changed to water. Sample **4c** and **4c'** synthesized by alkylation under different conditions were measured in

aqueous solution at concentration of 1mg/mL.

a)   Hydrophobic interaction

b)

● Pr subsitituted AGU

○ Et subsitituted AGU
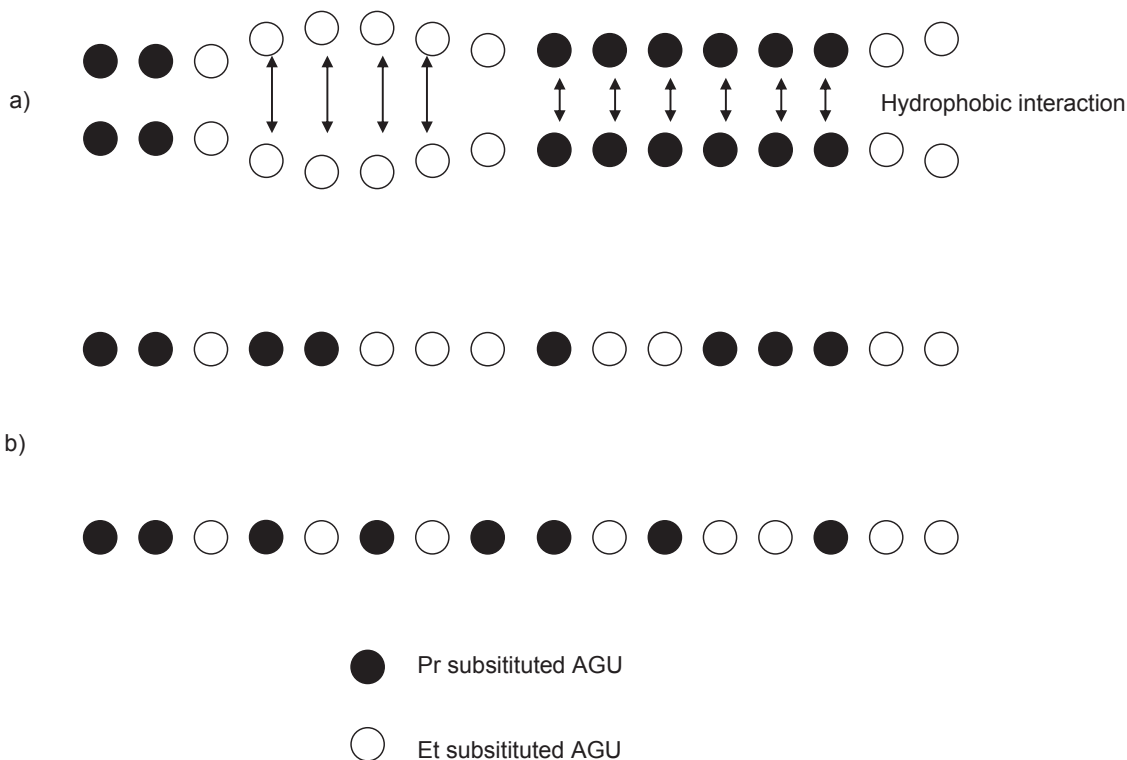
Scheme 3.2 Schematic representation of hypothetical distributions of two ether groups along the polymer backbone: a) block like distribution of Et and Pr; b) randomly distribution of Et and Pr

Due to the restriction of equipment, the working temperature of the column must be set no lower than 30 °C. As the cloud point of **4c** and **4c'** is around 38 °C, the multimodal distribution curves were obtained, which do not reflect the real structure of the macromolecules in solution (Figure 3.8).
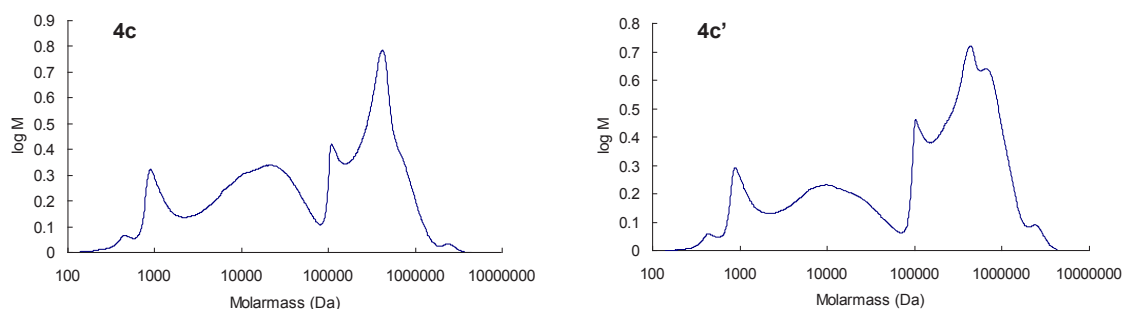
Figure 3.8 Size exclusion chromatography traces of **4c** and **4c'** in water at 30 °C

3.3 Synthesis of 3-*O*-alkyl ether by alkylation in the presence of *n*-BuLi

Regarding the "block like" hypothesis mentioned in section 3.2.1, an "induced phase separation" was believed to be responsible for the different "distributions" of two alkyl moieties along the backbone. Induced phase separation before chemical conversion was studied by Heinze *et al.* [101, 103]: The solid NaOH was added into the dissolved cellulose in DMA/LiCl and formed gel particles. This activated cellulose was then allowed to react with monochloroacetic acid to obtain carboxylmethyl cellulose with a non statistical distribution of substituents within the polymer chains, i.e. significantly higher content of tricarboxymethylated units and unsubsitituted units than that of the carboxymethyl cellulose synthesized under heterogeneous conditions in iPrOH/NaOH (aq.).

By adding NaH into the dissolved 2,6-di-*O*-TDMS cellulose in THF, a similar "induced phase separation" was also observed (section 4.2.2), which is supposed to be the reason for the "block like" distribution of two different ether groups along the polymer backbone.

In order to clarify this speculation, a conversion under fully homogenous conditions is necessary. Regarding the reactivity, the strong base *n*-BuLi was considered. *n*-BuLi was added to a solution of 2,6-di-*O*-TDMS cellulose (**2**) in THF at -78 °C, followed by the addition of two alkylation reagents in equimolar ratio (EtI/PrI=5/5). The mixture was stirred at low temperature overnight and then at 50 °C for 4 days. Then the desilylation was conducted to yield 3-mono-*O*-alkyl cellulose. The peracetylated product **5a'** showed a similar ^{1}H NMR spectrum compared to the product synthesized by NaH (Figure 3.9). The signal of -CH$_2$- group in this spectrum was overlapped by the intense peak of acetyl methyl. The lower intensity of the alkyl methyl peak indicated the inefficiency of the alkylation. The DS of ethyl and propyl moieties are calculated by the integration of alkyl peaks respectively. DS$_{Pr}$ (0.19) is lower than DS$_{Et}$ (0.27), which indicate the lower reactivity of the longer alkyl chain.

However, it should be noted that the difference between the two DS values

(Et/Pr=0.27/0.19=1.42) was decreased compared to the alkylation in the presence of NaH (Et/Pr=0.95/0.15=6.33), where alkylation reagents in an equimolar ratio (5/5) were applied. It can be concluded from the $DS_{total,}$ which is much lower than 1 (0.46) that the alkylation with the presence of *n*-BuLi was less efficient. This might be the reason of the insolubility of the desilylated product in either water or DMSO. The investigation of distribution of the two different ether groups becomes impossible because a 3-*O*-alkyl cellulose chain with DS_{total} around 1 cannot be obtained from this synthetic methodology.
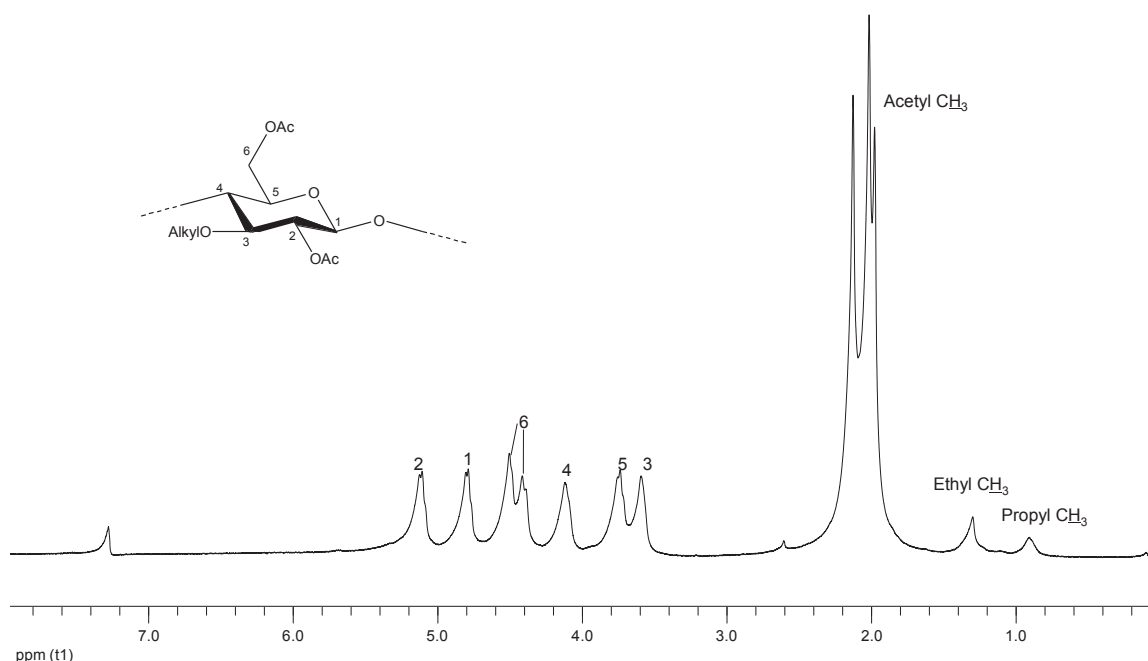
Figure 3.9 ^{1}H NMR of 2,6-di-*O*-acetyl-3-*O*-ethyl (Et)/*n*-propyl (Pr) cellulose synthesized from alkylation with the presence of *n*-BuLi (**5a'**)

3.4 Further solution state analyses of 3-*O*-alkyl celluloses

3.4.1 Characterization of temperature dependant solubility of 3-*O*-alkyl celluloses

3.4.1.1 Turbidimetric measurements of 3-*O*-alkyl celluloses

The measurements of 3-mono-*O*-ethyl cellulose (3EC) and 3-mono-*O*-propyl cellulose (3PC) by turbidimetry were already reported [38, 65]. The comparison with reproduced tests of 3EC, the LCST shows no dependency on the concentration of aqueous solution (in publication 10 %; reproduced 1 %), a temperature of about 60 °C was measured.

3-O-Et/Pr cellulose derivatives (samples **4a-d**) are soluble in water below room temperature. Samples with pronounced methylation (**4e** DS_{Me} 0.99, DS_{Et} 0.08; **4g** DS_{Me} 0.97, DS_{Pr} 0.12) are water insoluble. This finding corresponds to the fact that the 3MC is water insoluble [54]. However, a product with higher DS_{Et} rather than DS_{Me} is water soluble (**4f**) and the aqueous solution possesses an LCST of 71 °C (Table 3.1). The LCST of the 3-O-Me/Pr cellulose **4h** (DS_{Me} 0.46, DS_{Pr} 0.58) in aqueous solution is 38 °C (Table 3.1).

Figure 3.10 summarizes the transmittance of the aqueous solution (1%, w/v) of 3-O-Et/Pr cellulose depending on the temperature. The LCST was found to depend on the ratio of the two alkyl groups bound at position 3. A LCST of 58 °C was detected for sample **4a** (DS_{Et} 0.95, DS_{Pr} 0.15). Increase of DS_{Pr} and decrease of DS_{Et} result in decrease of the LCST, e.g. 44 °C (sample **4b**, DS_{Et} 0.77, DS_{Pr} 0.27), 38 °C (sample **4c**, DS_{Et} 0.54, DS_{Pr} 0.42), and 33 °C (sample **4d**, DS_{Et} 0.27, DS_{Pr} 0.56). It was observed that the redissolution of the precipitate during the cooling cycle was retarded and slower compared with the heating cycle. However, the cooling curves of the cellulose derivatives with higher contents of ethyl groups (**4a**, **4b**) show some strange changes in transmittance. This may be due to the aggregation of the precipitate during the heating cycle, which makes precipitates formed poorly dispersed in solution which thereby increases the transmittance of the liquid.
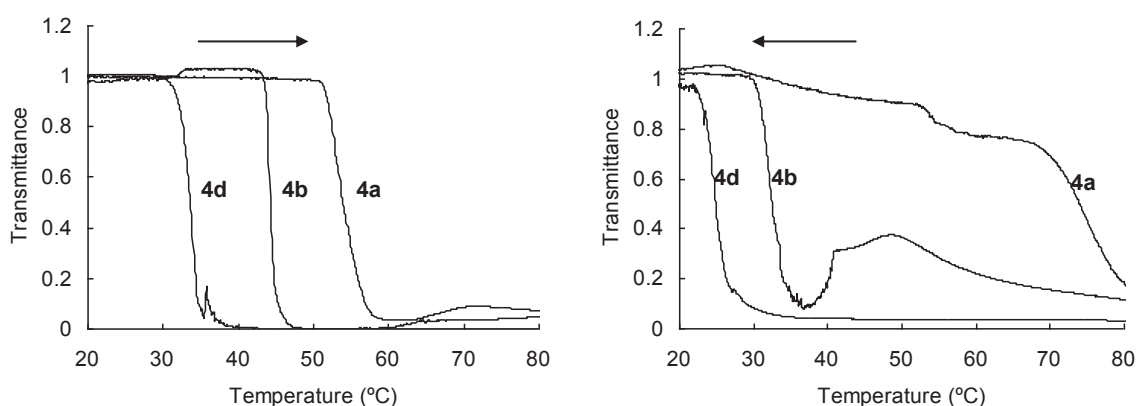
Figure 3.10 Temperature dependent transmittance of 1 % aqueous solutions of 3-O-ethyl (Et)/n-propyl (Pr) cellulose with different DS ratios (**4a**: DS_{Et}/DS_{Pr}=0.95/0.15; **4b**: DS_{Et}/DS_{Pr}=0.77/0.27; **4d**: DS_{Et}/DS_{Pr}=0.27/0.56

3.4.1.2 Turbidimetric measurements of physical mixtures of 3EC and 3PC

In addition, turbidimetric analyses were also conducted with 3EC (sample **4j**, DS 1.07, LCST 60 °C) and 3PC (sample **4k**, DS 1.13, LCST 18 °C), as well as 3EC/3PC mixtures with the comparable molar ratio of Et/Pr moieties as the DS_{Et}/DS_{Pr} of the samples bearing Et and Pr on the same polymer chain (Figure 3.11). The solution of a mixture of 3EC/3PC=0.27/0.56 provided a LCST of 18 °C, which fits the LCST of 3PC; however, the aqueous solution of **4d** with DS_{Et} 0.27 and DS_{Pr} 0.56 has the LCST of 33 °C. It can be concluded that the tuning of LCST of 3-mono-*O*-cellulose ether cannot be realized by physically mixing of two kinds of 3-mono-*O*-alkyl cellulose. The three curves of the turbidimetic measurements of different polymer compositions (**M₁, M₂, M₃**) indicate that all mixtures of 3EC and 3PC solutions have LCSTs in the range of 18-22 °C, and this temperature range corresponds with the LCST of 3PC cellulose according to already published values [65]. However, it should be noted that the high content of 3PC accelerated the rate of flocculation.

Physical mixture		
Sample	3EC	3PC
M₁	0.95	0.15
M₂	0.77	0.27
M₃	0.27	0.56
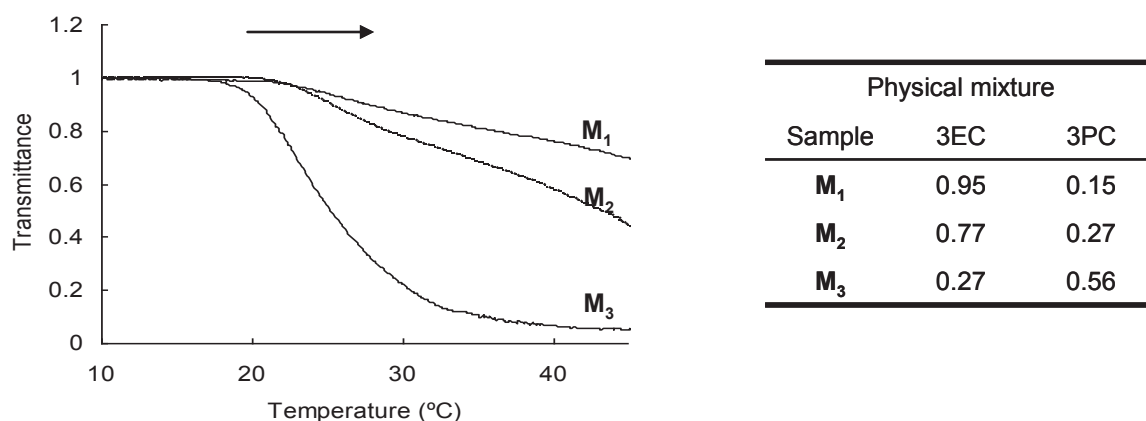
Figure 3.11 Temperature dependent transmittance of 1% aqueous solutions of a mixture of 3-mono-*O*-ethyl cellulose (3EC) and 3-mono-*O*-propyl cellulose (3PC) with different molar ratios

3.4.2 Differential Scanning calorimetry (DSC) of 3-*O*-alkyl cellulose bearing two different ether groups

3.4.2.1 DSC of 3-*O*-alkyl cellulose bearing Et and Pr with different DS ratios

DSC studies have been used to detect thermally induced transitions of aqueous solutions of cellulose ethers. In a first series of tests, measurements of **4a**, **4b**, **4d**, **4k** were carried out. On heating, all samples show a single broad asymmetric endothermic peak (Figure 3.12). This endothermic peak results from the energy requirement of dehydration of the polymer in the aqueous solution: the hydrogen bond structure was broken by heating. The onset of the endothermic peak closely matches the cloud point temperature for each sample.

On cooling, a single exothermic peak was observed. The cooling peak for sample **4a**, **4b**, and **4d**, which is comparable to the endothermic peak, suggests that the process occurring on cooling is the reverse of the one occurring on heating. In this process, disassociation and re-hydration of the molecules (solvation) with the decrease of temperature is involved. Thus, the hydration of the molecules with consequent structuring of water molecules is an exothermic event. The two peaks, for sample **4a**, **4b**, and **4d**, also carry comparable calorimetric enthalpies, which indicate the almost complete reversibility of the process (Table 3.2). An analogous comparison for sample **4k** is rather difficult because part of the exotherm takes place outside the temperature range of the experiment due to the evident retardation of peak emergence, namely hysteresis. Hysteresis, by means of difference in aggregation (heating) and disassociation (cooling) temperature (T_{max}), was negligible for **4b** and **4d** and it becomes noticeable for samples with a high content of propyl moieties (**4k**>**4d**). Hysteresis is quite common in polysaccharide solutions, where it is associated with additional stabilization of the network [104, 105]. A similar explanation is suitable for sample **4k**, where hysteresis might involve "strengthening", as a function of temperature, of the hydrophobic junctions, which allows binding between nearby sites (intra- and interchain interactions).
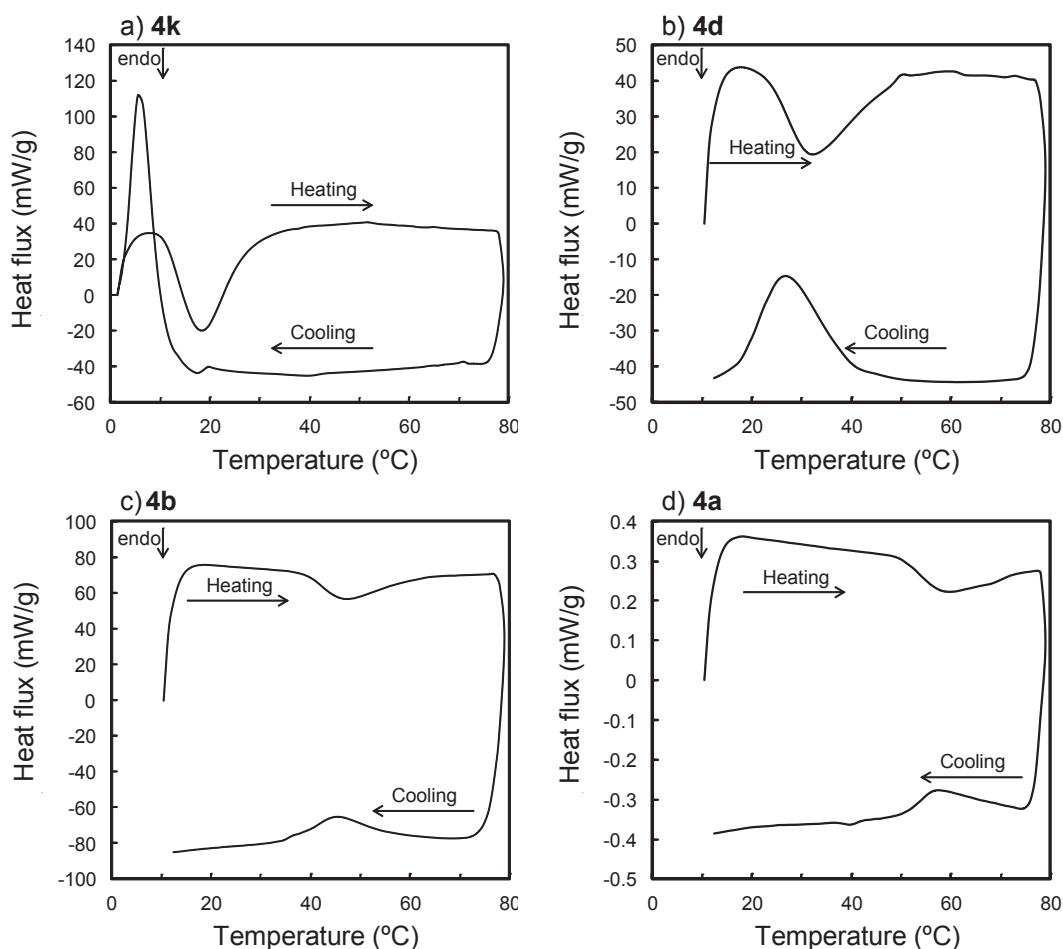
Figure 3.12 Differential Scanning Calorimetry thermograms of: a) **4k**, 3-mono-*O*-propyl cellulose; b) **4d**, 3-*O*-alkyl cellulose with $DS_{Et}/DS_{Pr}=0.27/0.56$; c) **4b**, 3-*O*-alkyl cellulose with $DS_{Et}/DS_{Pr}=0.77/0.27$; d) **4a**, 3-*O*-alkyl cellulose with $DS_{Et}/DS_{Pr}=0.95/0.15$

Second heating-cooling loop, using the same samples was carried out with a higher maximum heating temperature at 110 °C (Figure 3.13). On heating, after the main endothermic transition, and starting at 50 °C, the heat flux function changes in curvature which indicates a different way that the sample absorbs heat (different heat capacity). Comparing to the cooling curves from former measurements with maximum temperatures of 80 °C, the difference is the absence of the exothermic peak during cooling.

A possible explanation for which is that heating to 110 °C is approximately 60 °C above the end of the main transition and allows the structure stabilisation to go to completion, which either suppresses the reversible transition or shifts it to temperatures much lower than the

beginning temperature (1 °C). It would be expected that if the sample **4k** was heated to temperatures slightly above the end of the main transition, then much less hysteresis would occur.

Table 3.2 Transitions parameters for regioselective substituted cellulose ethers: T_{on} = onset temperature; T_{max} = peak temperature; T_{off} = offset temperature and ΔH = enthalpy of the transition

Sample	Heating					Cooling			
	T_{on}	T_{max}	T_{off}	ΔH (J/g product[c])		T_{on}	T_{max}	T_{off}	ΔH (J/g product[c])
3EC[a,b]	51	62	85	14.7	P1	78	58	50	-11.3
					P2	31	24	18	-3.4
4a	51.5	58.9	72.3	6.7		64.3	57.1	51.5	-5.1
4b	39.1	47.0	61.1	11.6		57.9	45.3	34.8	-10.94
4d	22.8	32.1	50.1	21.83		40.4	26.8	18.1	-22.7
4k	10.1	18.4	28.3	36.8		19.8	9.8	-[d]	-[d]

a [72];
b On cooling two separated processes were observed: P1 and P2
c Enthalpy refers to mass of dissolved products
d Data not available
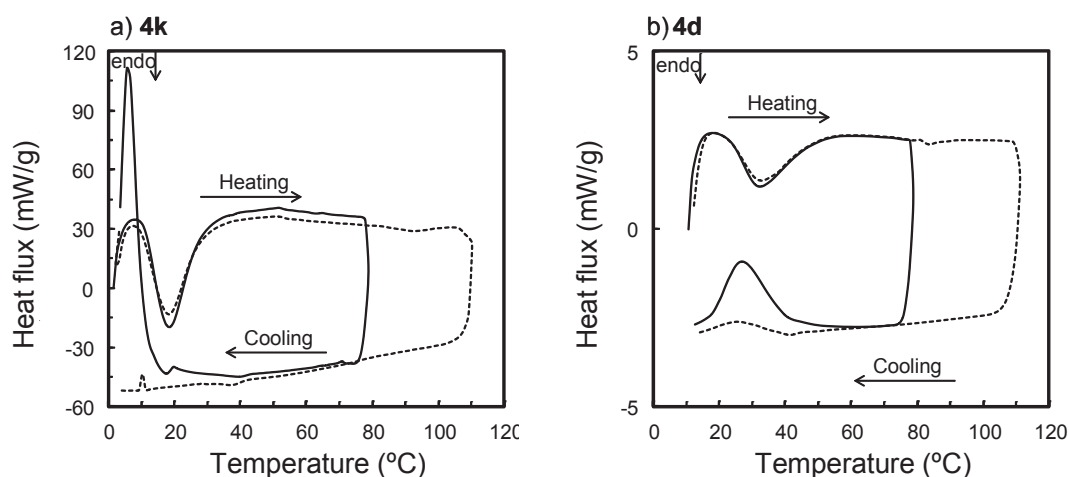
Figure 3.13 Dependence of the exothermic peak on cooling from the maximum heating temperature for sample **4k**, 3-mono-*O*-propyl cellulose (a) and **4d**, 3-*O*-alkyl cellulose with DS_{Et}/DS_{Pr}=0.27/0.56 (b): 78 °C (solid line) and 110 °C (dotted line)

The absence of hysteresis of exothermic peak for both sample **4a** and **4b** (Figure 3.12), where heating to 80 °C is close to the end of the main endothermic peak, favours this hypothesis.

Moreover, the irreversibility of the transition was seen for all the other samples when heated to 110 °C; an example for sample **4d** (Figure 3.13). Based on these results a "critical temperature" was suggested, above which association becomes irreversible and this temperature seems to be a function of the ratio of the two alkyl moieties: a higher the propyl content leads to a lower "critical temperature".

The enthalpy of transition, estimated from the area under the peak, is directly proportional to the DS of propyl group: **4k>4d>4b>4a** (Table 3.2). The present results may reflect the different hydrophobicity of each sample. Assuming the chain length of the two alkyl moieties is directly proportional to their "hydrophobicity" (Pr>Et), the most hydrophobic sample **4k** would aggregate first [106]. Moreover, data reported by Sun *et al*. [72] for 3-mono-*O*-ethyl cellulose (3EC) are not in coherence with the observed trends. In contrast to what is expected, the value reported for the enthalpy of aggregation was higher than sample **4d**. This observation suggests that the increase in enthalpy when ethyl groups are replaced by propyl groups can be explained not only in terms of the "additive effect" due to the higher hydrophobicity of propyl groups compared to ethyl groups, but also distinctive structural factors must be taken into account.

Sun *et al*. observed the separation of two peaks for the disassociation on cooling [72], where the peak at low temperature was attributed to the reformation of the original cellulose structure in solution, based on the Haque *et al*. [67] model. The original cellulose structure in solution involves, the existence of remaining crystallinity due to hydrogen bonding at the unsubstituted position 2 and 6 as shown by Kondo *et al*. [107]. When functionalized with propyl moieties, its chain length might sterically prohibit hydrogen bonding between unsubstituted hydroxyl groups, and therefore suppress the lower exothermic peak of the **4a**, **4b** and **4d**.

3.4.2.2 DSC of 3-*O*-alkyl cellulose bearing Et and Pr with comparable DS_{Et}/DS_{Pr} (**4c**, **4c'**) synthesized by alkylation under different conditions

4c and **4c'** are two samples with comparable DS_{Et} and DS_{Pr} prepared via alkylation under different reaction conditions. The solutions of these two samples are subjected to DSC measurement, in order to evaluate the difference of thermal behaviour of the solutions.

The diagram of **4c** is quite similar to **4b** and **4d** (Figure 3.14a). Heating to 80 °C and then cooling gives a curve with endothermic and exothermic peaks. Moreover, hysteresis of exothermic peak was also observed. A second test with higher maximum temperature at 110 °C shows no exothermic peaks, which is the case also for **4b** and **4d**.
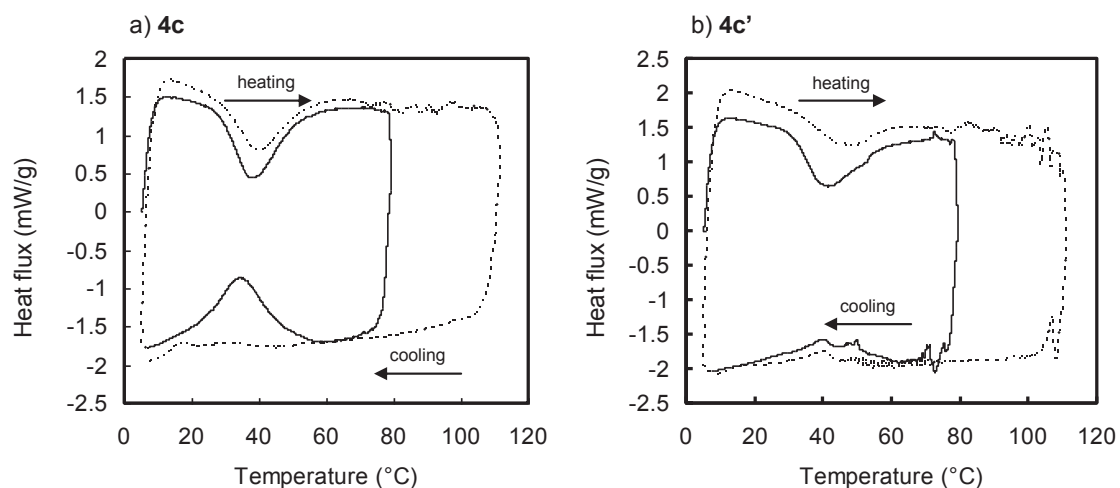
Figure 3.14 Differential Scanning Calorimetry thermograms with different maximum heating temperatures: a) **4c**, 3-*O*-alkyl cellulose with DS_{Et}/DS_{Pr}=0.54/0.42; b) **4c'**, 3-*O*-alkyl cellulose with DS_{Et}/DS_{Pr}=0.59/0.43. 78 °C (solid line), 110 °C (dotted line)

However, **4c'** shows a different diagram (Figure 3.14b): the exothermic process during cooling was much hindered in both two heating-cooling cycles (80 °C and 110 °C), compared to the endothermic process during heating. Due to the lack of the detailed structure information, the difference of solution behaviours between these two products remained mysterious.

3.4.2.3 DSC of 3-*O*-alkyl celluloses bearing Me and Et (**4f**) and Me and Pr (**4h**)

Compared to other samples (**4a-d**, **4k**), **4f** shows very different DSC traces. Heating to 80 °C didn't show any complete endothermic peak, but a trend of endothermic effects was visible starting from 70 °C, which corresponds to the turbidimetry measurement results (Figure 3.15a). The cooling curve shows an exothermic process immediately from 80 °C and then steadily returns to the original value.
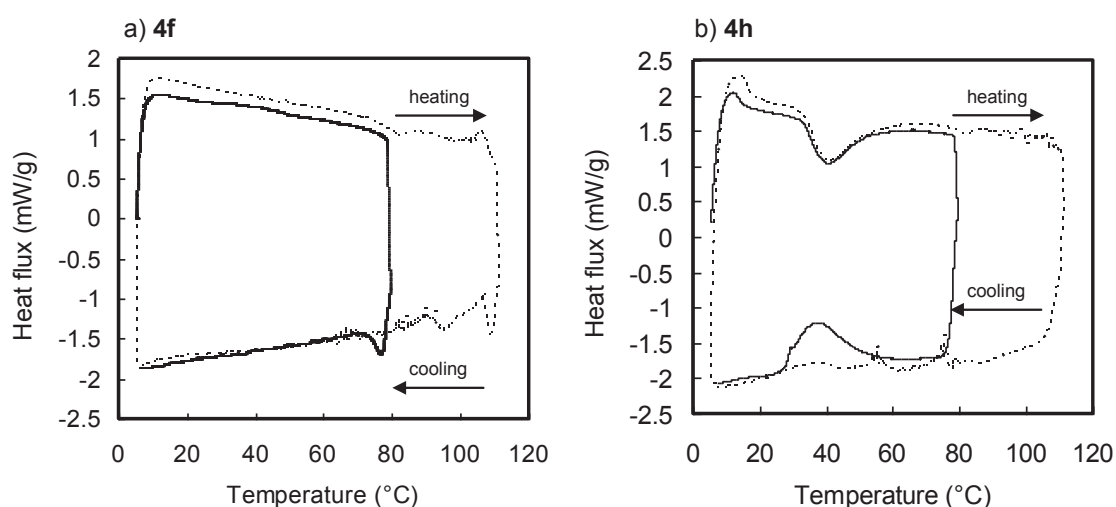
Figure 3.15 Differential scanning calorimetry thermograms with different max. heating temperatures: a) **4f**, 3-*O*-alkyl cellulose with DS_{Me}/DS_{Et}=0.19/0.91; b) **4h**, 3-*O*-alkyl cellulose with DS_{Me}/DS_{Pr}=0.46/0.58. 78 °C (solid line), 110 °C (dotted line)

Heating to 110 °C allows the full appearance of endothermic peak, but the area of the peak is quite small (1 J/g product), which indicates a much lower enthalpy of the endothermic process than for the other samples. However, the cooling curve containing multiple endo- and exothermic peaks are very complicated to interpret.

For sample **4h**, both endothermic and exothermic peaks are clearly found in the heating curve up to 80 °C (Figure 3.15b), with comparable enthalpy values (endo 13.9 J/g product; exo -13.6 J/g product). Still the hysteresis of the exothermic peak was not negligible.

When heating to 110 °C, the heating process didn't show significant changes, but the exothermic peak was absent from the cooling curve, instead, there are two smaller somewhat

noisy peaks at about 75 and 55 °C. Moreover, a very weak broad peak around 35 °C was also observed. It is believed that the two peaks at 75 and 55 °C correlated, at least to a certain extent, to the two "plateau-like" cooling curve of G' and G" obtained from the rheology test (see section 3.3.3.2).

Regarding the "split" exothermic peak of 3EC [72], the peak at the lower temperature 35 °C was due to the reformation of the original cellulose structure in solution.

3.4.3 Rheology of 3-*O*-alkyl celluloses bearing two different ether groups

3.4.3.1 Rheology of 3-*O*-alkyl celluloses bearing Et and Pr with different DS ratios

Small deformation dynamic viscoelastic measurements have been used to monitor structural changes, which accompany the thermally induced aggregation of cellulose ethers in water. Observing Figure 3.16, changes of elastic modulus (G'), loss modulus (G") and tan δ (G"/G'), on heating, for sample **4k** can be seen. At low temperature (~1°C) the rheological properties are typical of a solution with the elastic modulus lower than the viscous modulus (G'<G"). The structural changes occur in two steps, previously reported for methyl cellulose [67, 69, 70]: As the temperature increases, G' firstly increases slowly till 10 °C, above which it changes more rapidly with temperature. The crossover of the moduli, which indicates the border between liquid and gel state, took place at around 5 °C. However, in this temperature range, no signal was observed in the calorimetry measurements. Therefore, this structural change is not related to hydrophobic aggregation.

The onset temperature of the second step of the increase in G', closely matches the onset temperature of the endothermic peak in the calorimetry measurements. On further heating, above 50 °C, G' attains a plateau with a magnitude of 30 kPa. G" changes with similar profile, however, it does not level off at high temperatures but it shows, instead, a steady increase. This section of plateau-like G' curve suggests structural stabilization, in other words, no more

interactions of polymers developed. Therefore, the changes in heat flux curvature above 50 °C in the calorimeter (Figure 3.12a) does not involve hydrophobic dehydration, which leads to more junctions between polymers, but it is instead associated with changes in the loss modulus.
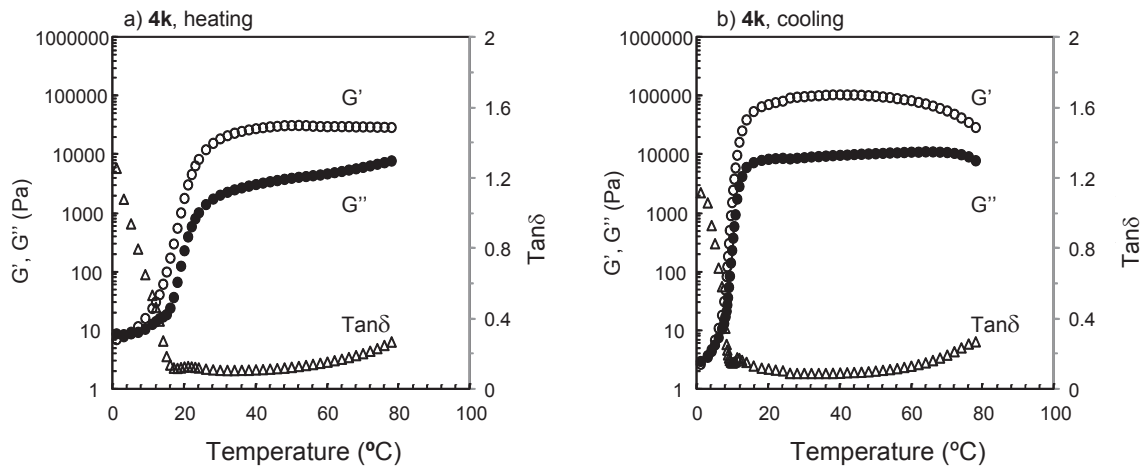
Figure 3.16 Temperature sweep measurement of storage modulus (G') and loss modulus (G'') for **4k**, 3-mono-*O*-propyl cellulose (DS=1.13)

On cooling, the gel-network transforms back to a solution as shown in Figure 3.16b. Interestingly, the magnitude of G' and G'' at the beginning is a little higher than the magnitude at comparable temperature on heating. The structural stabilisation occurs during the last period of heating. As the samples are cooled, the junctions formed become thermodynamically unstable, but the stabilized structure shows slightly higher moduli. From the plateau region the two moduli fall back to almost their original value very fast, confirming the gelation process is fully reversible. Comparison between the onset of network formation on heating and the onset of the network collapse on cooling confirms the hysteresis observed in the calorimeter.

Figure 3.17a shows structural changes on heating for sample **4d**: both moduli increase with a similar shape seen per sample **4k**. The main differences are: the temperature at which the major changes occur and the magnitude of both moduli. The onset of the second step is close

to 30 °C, which is almost 20 °C higher than for **4k**, confirming the trend observed in the calorimetric experiment: the increase of the ethyl group content increases the transition temperature.

The maximum value reached by G' is one order of magnitude lower than **4k**. The presence of a maximum for both moduli is a consequence of the beginning of the macroscopic phase separation occurring at high temperatures, which is a result of heterogeneity of the sample between the two plates in the rheometer. However on cooling, a sign of reversibility is still observed, mirrored by an increase in both moduli upon cooling, which then fell back to their original value with a much less prominent hysteresis than sample **4k** (Figure 3.17b).

The heating curve of sample **4b** is shown in Figure 3.18. The same consideration on the structural development can be made for this sample. The initial decrease of both moduli upon heating to a temperature of about 20 °C is more evident than both sample **4k** and **4d**, as expected for a homogeneous polymer solution [108]. However above 20 °C a two step increase in G' is seen, consistent with the previous samples, only at a higher temperature, which is consistent with what has been reported previously [67].
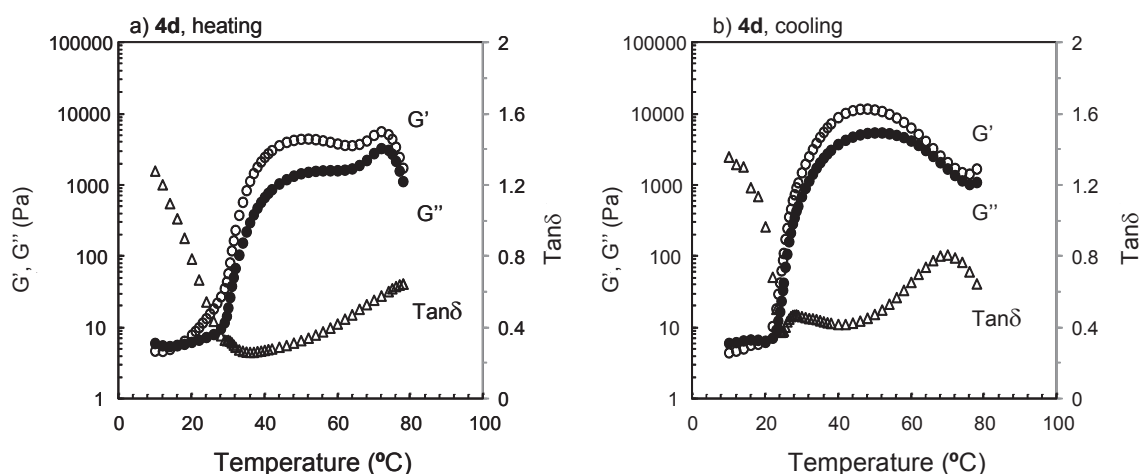
Figure 3.17 Temperature sweep measurement of storage modulus (G') and loss modulus (G") for **4d**, 3-*O*-alkyl cellulose with $DS_{Et}/DS_{Pr}=0.27/0.56$

The decrease of the two moduli upon further heating is more evident than sample **4d** as a

consequence of the more severe two-phase separation, and the decrease stopped where the endotherm signal ends (Figure 3.12c). Hysteresis on cooling was negligible (Figure 3.18b), corresponding to the calorimetric result.
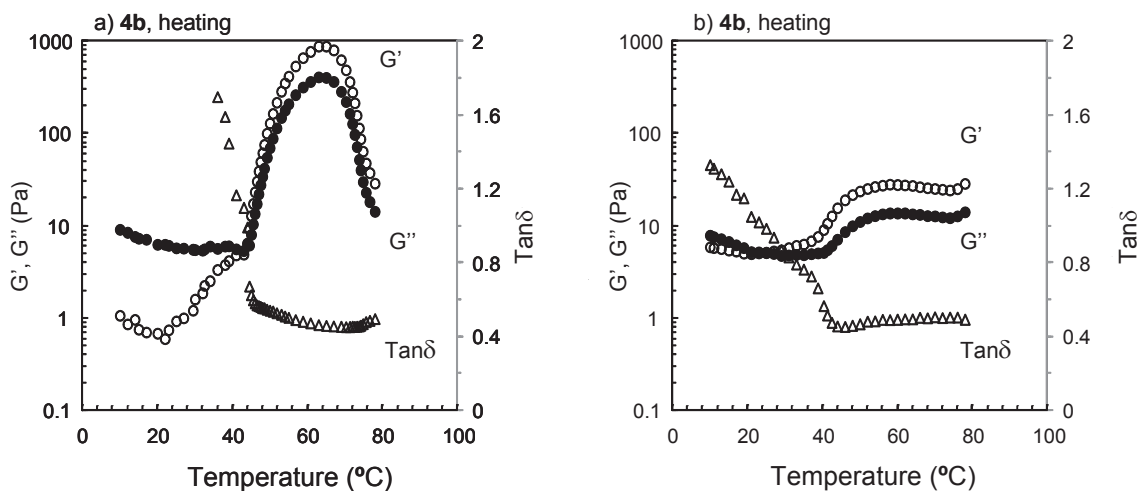
Figure 3.18 Temperature sweep measurement of storage modulus (G') and loss modulus (G") for **4b**, 3-*O*-alkyl cellulose with DS_{Et}/DS_{Pr}=0.77/0.27

Rheological studies reveal the same trends with a further increase in ethyl content of the samples (**4a**, Figure 3.19), a higher temperature is required for gelation, A gel with a lower modulus was observed and the solution became more heterogeneous at high temperatures, again coinciding with the end of the endotherm (Figure 3.12). Initial values of G' are too low to be measured and start to be detected when temperatures approach 40 °C. The onset of the second dramatic increase in modulus is around 56 °C, which is the highest among the samples studied. Above 56 °C the two moduli steeply increase although G' never considerably exceeds G", which is an indication that the solution is less gel-like.

3.4.3.2 Rheology of 3-*O*-alkyl celluloses bearing Et and Pr with comparable DS_{Et}/DS_{Pr} (**4c**, **4c'**) synthesized by alkylations under different conditions

The two samples with comparable content of ethyl and propyl moieties **4c**, **4c'** were also studied by rheology, using an oscillary shear mode (10 rad/s) and a temperature sweep

(1 °C/min) from 1 °C to 75 °C and then back. First, during the heating process, similar trends of change in the curves of G' and G'' to the former samples were found (Figure 3.20).
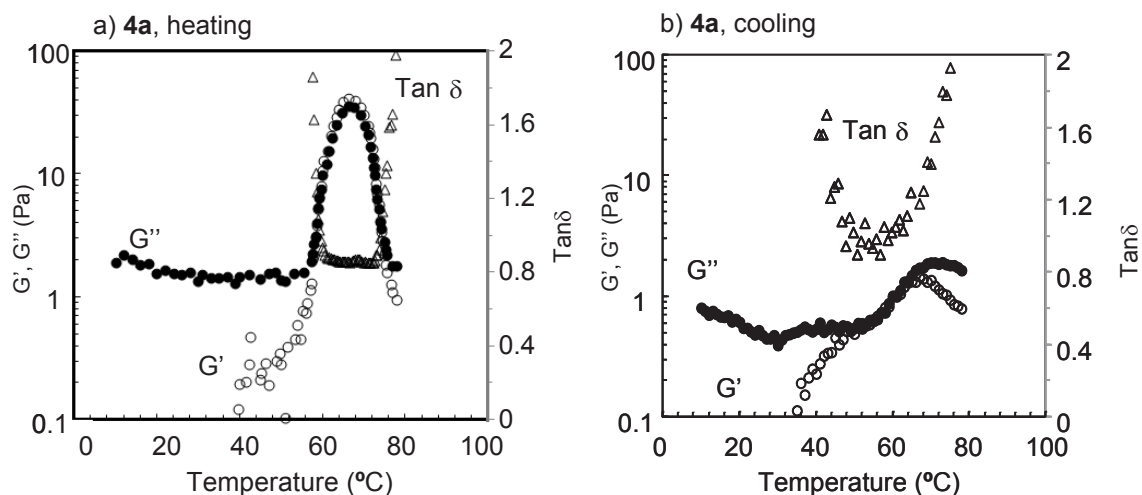
Figure 3.19 Temperature sweep measurement of storage modulus (G') and loss modulus (G'') for **4a,** 3-*O*-alkyl cellulose with DS_{Et}/DS_{Pr}=0.95/0.15

For both **4c** and **4c'**, the onset temperatures of increase in G' and G'' are comparable and correspond to the calorimetric measurements. However, an obvious difference is the shapes of the curves: **4c'** curve is more plateaux-like, similar to the former sample **4b**, whereas an extremely short or peak-like "stabilization area" was found for the **4c**, which is similar to the sample with higher ethyl moiety content **4a**. Moreover, the maximum G' value of these two samples shows a significant difference: **4c** (about 3800 Pa) is almost 4 times of that of **4c'** (1000 Pa).

Since the DS_{Et} and DS_{Pr} are comparable for **4c** and **4c'**, and the concentrations of the solutions are also the same (6.2%), the difference in G'and G'' was believed to be related to the detail structure of these two samples. Because **4c** and **4c'** were synthesized from different reaction conditions which could lead to different substructure in polymer backbone (way of distribution of the ethyl and propyl groups, conformation of polymer chain in solution).
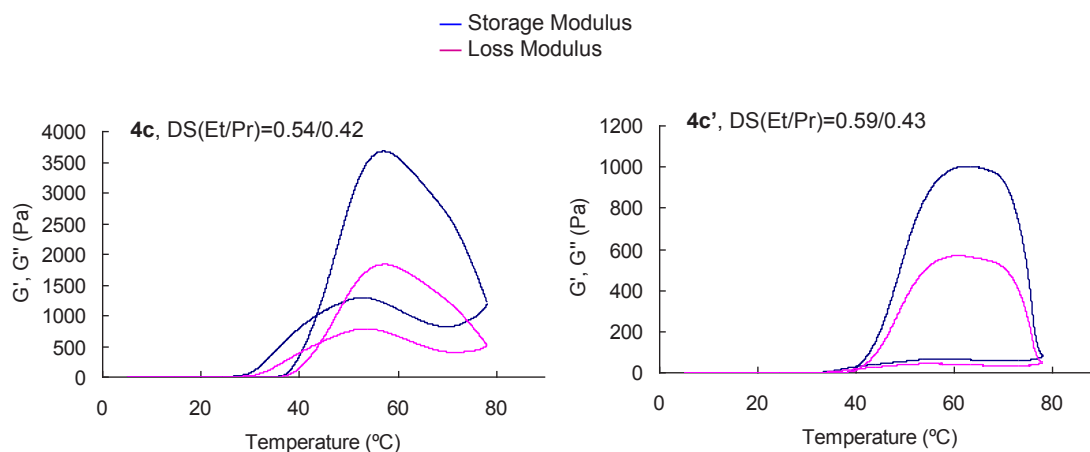
Figure 3.20 Temperature sweep measurement of storage modulus (G') and loss modulus (G'') for **4c** and **4c'** synthesized under different conditions (**4c**, 50 °C; **4c'**, r. t. with catalyst)

When cooling, it should be noted that, the sample **4c** showed a non negligible hysteresis with G' and G'' falling back to their original values. Surprisingly, the reversibility of G' and G'' of **4c'** cannot be observed in the cooling process, which is difficult to interpret with the present results.

3.4.3.3 Rheology of 3-*O*-alkyl celluloses bearing Me and Et (**4f**) and Me and Pr (**4h**)

Both moduli of **4f** show very different curves compared to other samples (Figure 3.21): G' and G'' decreases, unlike the increasing trends of the other samples; the cross over point was around 40 °C, which also indicate the gel-like property above this temperature. The increase of both moduli didn't take place until 70 °C, which fits perfectly the LCST measured by turbidimetry. The dramatic increase in moduli stopped sharply at highest heating temperature 75 °C, which is insufficient for G' and G'' to reach the maximum value, higher temperature are required. However, the properties of the aqueous solution and the limitation of the equipment prohibit further heating which would lead to the formation of bubbles in the solution.
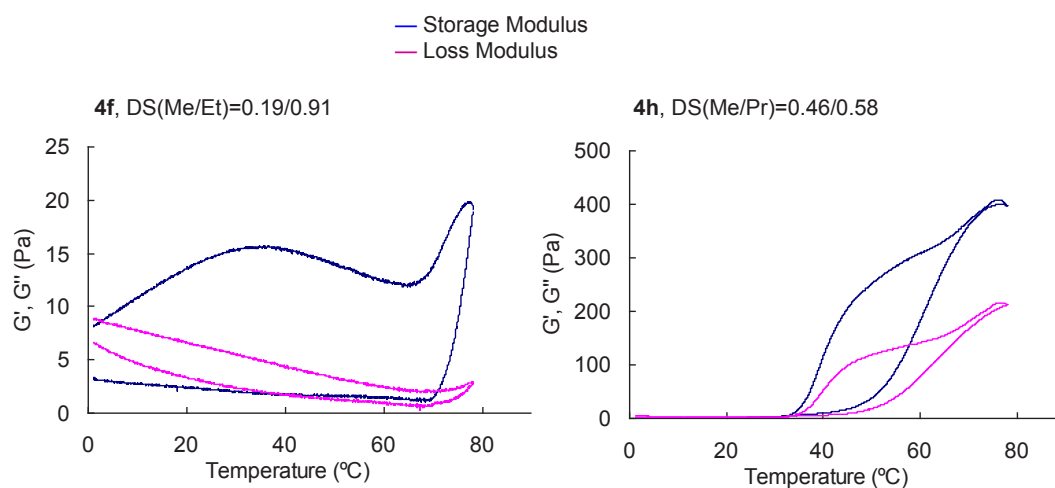
Figure 3.21 Temperature sweep measurement of storage modulus (G') and loss modulus (G'') for **4f**, 3-*O*-alkyl cellulose with DS_{Me}/DS_{Et}=0.19/0.91 and **4h**, 3-*O*-alkyl cellulose with DS_{Me}/DS_{Pr}=0.46/0.58

The values of G' obtained by cooling are difficult to explain but it finally fell close to the starting value. While the G'' showed a better reversibility, unlike the other samples, the G'' of **4f** returned to the original value with an increasing trend. In general, a detailed and reasonable interpretation for the G' and G'' curves are still unavailable. Through observation of the remaining solution on the plate of rheometer, it is believed that the phase separation is more predominant than for the other samples, which could be associated with the curves of G' and G''.

The G' and G'' curves of the sample **4h** showed a much better reversibility of dissolution and more homogenously gel-like system above the LCST (Figure 3.21b). The heating curve is similar to other samples except **4f**. However, one should notice that further heating to a temperature higher than 80 °C is required to allow the maximum value of G' and G'' to appear. For the same reason as the case of **4f**, further heating is impossible for the aqueous solution of **4h**.

Upon cooling of **4h**, both moduli decreased with decreasing temperature, but unlike the heating process, the decrease occurred in a two-stepped way: cooling from 75 °C, the decrease of G' and G'' was obviously slowed down, characterized by a gradually reduced

slope of the curves at around 65 °C; from 45-50 °C the decrease of G' and G" became faster again and finally came back to the starting value. This "two plateau" cooling curve implies different phases of the formation of a polymer network.

3.4.4 Dynamic light scattering (DLS) of 3-*O*-alkyl cellulose bearing Et and Pr with comparable DS_{Et}/DS_{Pr} (**4c**, **4c'**) synthesized by alkylation under different conditions

In order to investigate the difference of the DP_n of the two cellulose ethers with comparable DS values of ethyl and propyl groups (**4c**, **4c'**), further experiments were carried out including DLS. As speculated in 3.2.1, for sample **4c** and **4c'** synthesized by alkylation under different conditions, the aggregation might take place during the desilylation. Therefore, the DP values calculated from SEC are not reliable.

3.4.4.1 DLS of the aqueous solution of samples **4c**, **4c'**

In the first set of measurements, the aqueous solution of **4c** and **4c'** were measured at concentrations of 10 mg/mL and 5 mg/mL, but the size distribution of the particle (hydrodynamic radius, R_h) shows little difference when the temperature was raised. It is supposed that these two concentrations might be too high for the DLS measurement.

As the test of a dilute solution gave reasonable trends of change in size distributions, the aqueous solutions of the two cellulose ethers (0.5 mg/mL) were measured and the particle size distribution was recorded at different temperatures, namely at 25, 30, 35, 40 °C. In Figure 3.22, it is observed that an increase in temperature yields in increase of the size, which is proportional to the temperature for both two samples. Moreover, the distribution peaks are almost monodisperse at lower temperatures.

However, the peak began to split into two at higher temperatures, **4c** at 40 °C, **4c'** at 45 °C. This can be explained by the kinetic effect: the equilibrium time might be too short for the

formation of large particles or aggregates or the partial settling of bigger particles, so that two size distributions were detected.
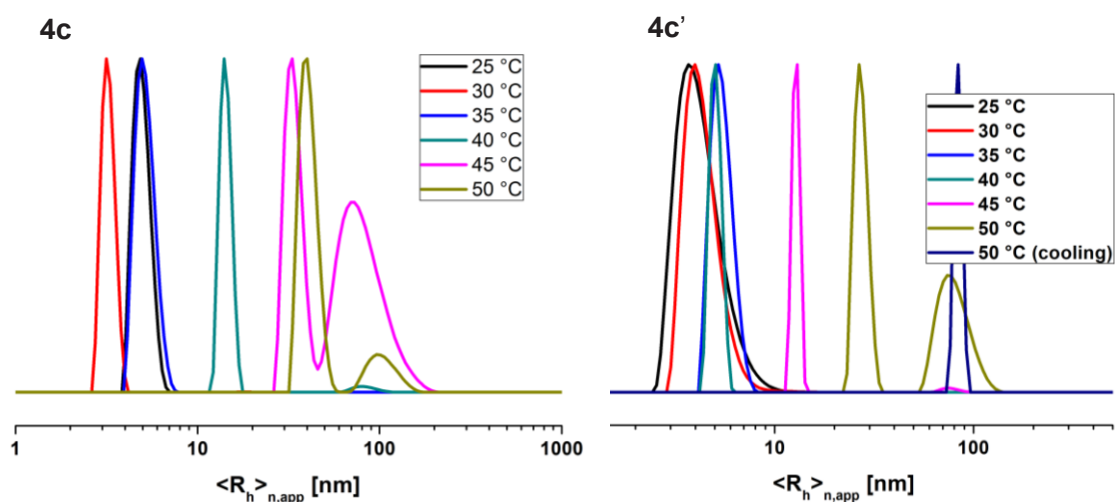
Figure 3.22 Particle size distribution in water measured by dynamic light scattering of 3-*O*-Et/Pr cellulose synthesized under different conditions **4c** (left, 50 °C) and **4c'** (right, r. t. with catalyst) at different temperatures

But if more time was provided, the small particles had sufficient time to form larger particles or aggregates. This assumption can be proved by the monodisperse peak of **4c'** during the cooling circle (50 °C cooling).

Generally, the hydrodynamic radius of two products shows no significant difference at various temperatures. Thus, it can be concluded that the solution behaviours of **4c** and **4c'** in water, are comparable at different temperatures.

3.4.4.2 DLS of samples **4c**, **4c'** dissolved in DMA/LiCl

The solution behaviour of the cellulose derivatives in DMA/LiCl was also studied, due to the magnitude different DP_n results of **4c** and **4c'**, which were obtained by SEC in DMA/LiCl. The solutions are prepared at concentration of 1 mg/mL according to the procedure of SEC sample preparation. The temperature of measurement was set at 40 °C, which is the column temperature used for the SEC measurements. The size distribution is shown in Figure 3.23.
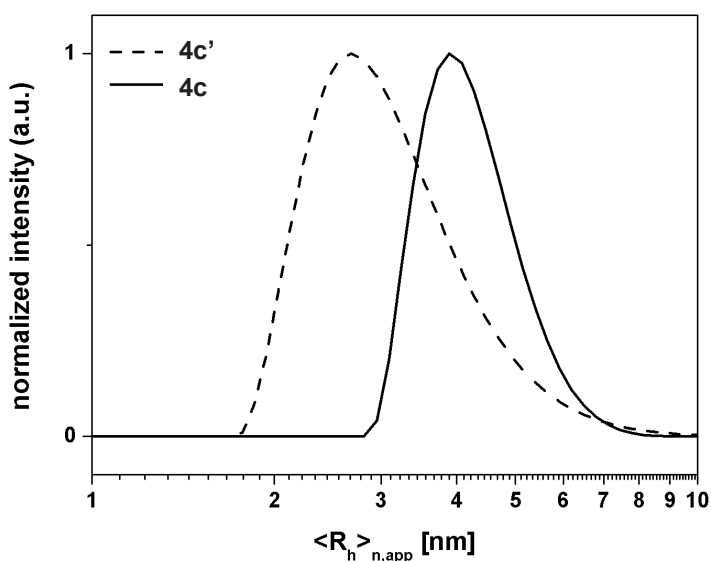
Figure 3.23 Particle size distribution measured in DMA/LiCl at 40 °C by dynamic light scattering (DLS) of 3-*O*-Et/Pr cellulose synthesized via alkylation at 50 °C without phase transfer catalyst (**4c**) and at r. t. with catalyst (**4c'**)

The particle size of **4c** and **4c'** slightly deviates and a higher value for **4c'** is observed, which is in a good agreement with the higher molar mass expected from the SEC in DMA. A three-fold increase in molar mass does not always need the hydrodynamic radius of the polymer coils to increase, as observed in the literature [109]. This result in comparison to the observations in water shows the different solvation of the different cellulose derivates in different solvents.

Therefore, through the DLS measurements carried out in different solvents, it can be concluded that the particle size distribution only gives a hint for the magnitude difference of apparent DP of **4c** and **4c'**, which are calculated from SEC measurements. Thus, other factors that are able to influence the SEC test must be considered.

3.4.5 Capillary viscosity of 3-*O*-alkyl celluloses with comparable DS_{Et}/DS_{Pr} (**4c**, **4c'**) synthesized by alkylation under different conditions

Conventionally, the conformation of polymer chains can be studied by capillary viscometry.

Polymer chain conformations of the two cellulose ethers could be crucial for understanding the difference in degree of polymerization depending on the synthesis conditions: the conformation of the polymer may influence the retention time when passing through the column.

The intrinsic viscosity was obtained by concentration extrapolation. The reduced viscosity and inherent viscosity of solutions at different concentration were measured in an Ostwald capillary, and the values were plotted as a function of concentration. According to the Huggins equation (1) and Kraemer equation (2), in ideal case, the linear trends line would cross at one point at y axis, and the y value of this point would be the intrinsic viscosity [110].

$$\eta_{red} = \frac{1 - \eta_r}{c} = k_H [\eta]^2 c + [\eta]$$ (1) Huggins equation

$$\eta_{inh} = \frac{\ln \eta_r}{c} = -k_K [\eta]^2 c + [\eta]$$ (2) Kraemer equation

η_{red}: reduced viscosity; η_{inh}: inherent viscosity; η_r: relative viscosity

Aqueous solution of sample **4c** and **4c'** were submitted to this measurement. The values of reduced viscosity (η_{red}) and inherent viscosity (η_{inh}) were plotted as a function of concentration, as shown in Figure 3.24:

As discussed in section 3.2.2, due to the restriction of SEC column temperature (no lower than 30 °C), the number average molar mass calculated from SEC in aqueous solution are unavailable. The calculation according to Mark-Houwink-Kuhn-Sakurada equation is impossible. Therefore, the conformation of polymer chains of sample **4c** and **4c'** cannot be assessed.
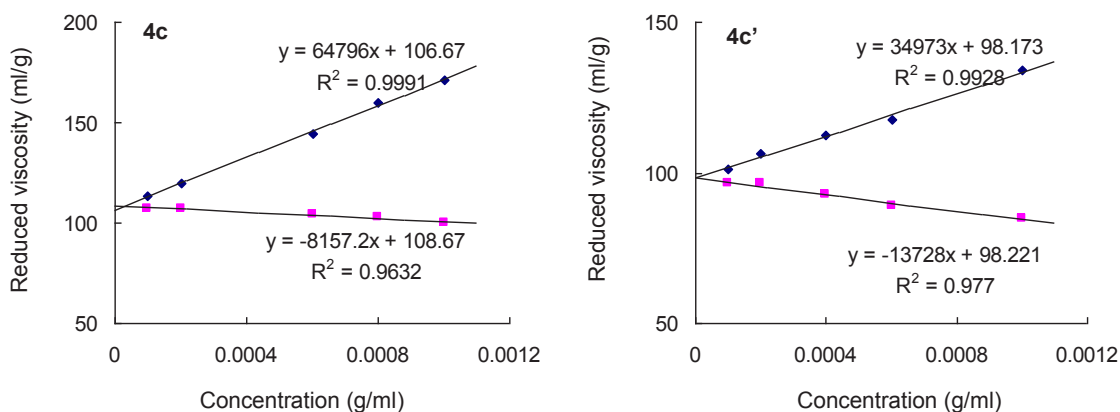
Figure 3.24 Plots of reduced viscosity and inherent viscosity of aqueous solution of 3-*O*-ethyl (Et)/*n*-propyl (Pr) cellulose synthesized via different conditions **4c** (50 °C) and **4c'** (r. t. with catalyst) against concentration

Other parameters were evaluated further. Firstly, Huggins and Kraemer constants were calculated by equation (1) and (2) respectively. Then with the obtained intrinsic viscosity values, coil density (ρ) was calculated by approximation equation (3) [111]:

$$[\eta] = 2.5 \frac{1}{\rho} \tag{3}$$

The k_H, k_K and ρ values are shown in Table 3.3:

Table 3.3: Huggins and Kraemer constant as well as coil density of **4c** and **4c'**

Sample	k_H	k_K	ρ (g/ml)
4c	5.7	0.7	0.023
4c'	3.6	1.4	0.025

The calculated coil density values of **4c** and **4c'** are comparable. The k_H values of both samples deviate largely from the ideal case in good solutions of polymers (k_H 0.2-0.8). This unusual Huggins constant could be found in solutions where the solute molecules have a tendency to associate, forming either well-defined structures or aggregates, particularly for polysaccharides and oligomerizing proteins [112]. However, it is still difficult to conclude regarding the difference of the k_H value of **4c** and **4c'**, further investigation must be made to

understand the solution behaviour of the molecules of **4c** and **4c'**, which were synthesized under different alkylation conditions.

3.4.6 Investigation of distribution of two ether groups (Et, Pr) of 3-*O*-alkyl celluloses with comparable DS_{Et}/DS_{Pr} (**4c**, **4c'**) synthesized by alkylations under different conditions by mass spectrometry (MS)

As speculated, the huge difference in DP_n of sample **4c** and **4c'** might be due to the different distribution of two ether groups along the polymer backbone. Thus, samples **4c** and **4c'** were analyzed by advanced techniques developed by Mischnick *et al.* (mentioned in section 2.5.3) in order to obtain the information of the distribution of two ether groups, namely "block-wise" structure or randomly distributed structures.

3.4.6.1 Gas chromatography combined with flame ionization detector mass spectrometry (GC-FID/MS) measurements of complete hydrolyzed sample **4c** and **4c'**

The two samples were degraded by acid catalyzed hydrolysis and then reduced into monomers by $NaBD_4$ and finally acetylated with acetic anhydride. D-Pinitol was used as internal standard to calculate the recovery of sample material. Figure 3.25 shows the GC chromatogram of compounds with different retention time. The assignments of the peaks were determined by GC combined with flame ionization detector mass spectrometry (FID/MS) analysis.

From this chromatogram, the two peaks with most important intensity correspond to the 3-*O*-Et and 3-*O*-Pr. In spite of other significant inferior peaks of other substitution pattern, the regioselective functionalization pattern of **4c** and **4c'** were confirmed, which is in accordance with the results from NMR spectroscopy.
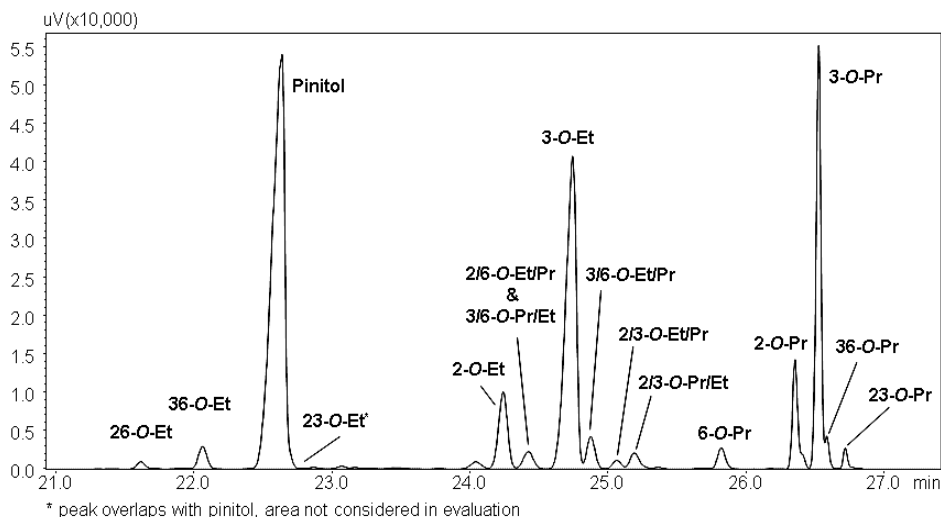
Figure 3.25 Gas chromatogram of alditol acetates obtained from sample **4c**. Peaks are assigned according to the ethylated or propylated positions, respectively (e.g. 3/6-*O*-Et/Pr means an ethyl in position 3 and propyl in position 6, 2,6-*O*-Et means ethyl substituent in both position 2 and 6)

Relative monomer composition (molar) of the samples **4c** and **4c'** was obtained by GC-FID/MS analysis of corresponding alditol acetates respectively. The results are shown in Table 3.4. The evaluation peak areas were corrected according to the effective carbon response (ECR) concept.

Table 3.4 Relative monomer composition (mol %) of the samples **4c** and **4c'**

	Et (mono)	Pr (mono)	Et (di)	Pr (di)	Et/Pr (mix)	DS	%Et total	%Pr total	%Et (mono)	%Pr (mono)
4c-1	47.59	36.47	3.60	3.08	9.26	1.16	55.82	44.18		
4c-2	49.95	37.05	2.95	2.44	7.61	1.13	56.71	43.29		
4c-3	49.69	36.81	3.11	2.62	7.77	1.14	56.68	43.32		
average	**49.08**	**36.78**	**3.22**	**2.72**	**8.21**	**1.14**	**56.40**	**43.60**	**57.17**	**42.83**
4c'-1	50.81	33.15	4.06	2.93	9.05	1.16	59.40	40.60		
4c'-2	52.35	35.03	3.31	1.33	7.97	1.13	59.65	40.35		
average	**51.58**	**34.09**	**3.69**	**2.13**	**8.51**	**1.14**	**59.52**	**40.48**	**60.21**	**39.79**

The DS value calculated and the molar percentage of mono substituted, which correspond to the results calculated from NMR spectra. The statistical distribution of the substituents in the oligomers was calculated, and the percentage of monomers with different ether groups (Et, Pr)

from GC analysis (Table 3.4) were taken for calculation. The results are shown in Table 3.5. These calculated results are going to be compared with the experimental results obtained by ESI-IT-MS in the next section (Table 3.6 and 3.7).

3.4.6.2 Analysis of partially hydrolyzed sample **4c** and **4c'** by electrospray ionization ion trap mass spectrometry (ESI-IT-MS)

Before the analysis of ESI-IT-MS, all the free OH groups of the cellulose ether must be fully peralkylated. In order to differ from ethyl and propyl, the sample **4c** and **4c'** were both perdeuteromethylated by CD_3I. The IR spectra of these products indicated there is almost no absorbance of OH (not shown), so they were applied for the following procedure, in which, the two perdeuteromethylated samples were partially hydrolyzed by acid catalyzed hydrolysis (1 mol/L trifluoracetic acid, 25 min, 120 °C) and afterwards labeled by reductive amination with *meta*-aminobenzoic acid.

Table 3.5 Calculated ethyl and propyl constitution (%) in oligomers with DP 2-5

DP	Subst. pattern	4c	4c'
2	Et/Et	32.68	36.25
	Et/Pr	48.97	47.92
	Pr/Pr	18.34	15.83
3	3Et	18.69	21.83
	2Et/Pr	42.00	43.27
	Et/2Pr	31.46	28.60
	3Pr	7.86	6.30
4	4Et	10.68	13.14
	3Et/1Pr	32.01	34.74
	2Et/2Pr	35.97	34.44
	1Et/3Pr	17.97	15.17
	4Pr	3.37	2.51
5	5Et	6.11	7.91
	4Et/1Pr	22.88	26.15
	3Et/2Pr	34.28	34.56
	2Et/3Pr	25.68	22.84
	1Et/4Pr	9.62	7.55
	5Pr	1.44	1.00

The mass spectrometric analysis of labeled compounds bears the advantage of measuring in negative ion mode. Analytes can be detected as anions [M-H]⁻ and the ionization is independent of adduct formation with sodium ions or other cations [96, 113, 114]. Whereas the adduct formation depends on the number and position of substituents the labeled compounds can be compared more reliable since every molecule carries one acid function and deprotonation is independent of the substituent pattern. Polarity of the analytes, which also influences the ion yield in the ESI process, is similar and leveled off by the effect of the tag introduced. Average DS values of each oligomeric fraction (of certain DP) can be used to check whether the results are representative, since it is only then in agreement with the DS of the starting material.

The oligomeric mixture obtained from partial hydrolysis was infused directly into the mass spectrometer by syringe pump. The mass spectrum was shown in Figure 3.26
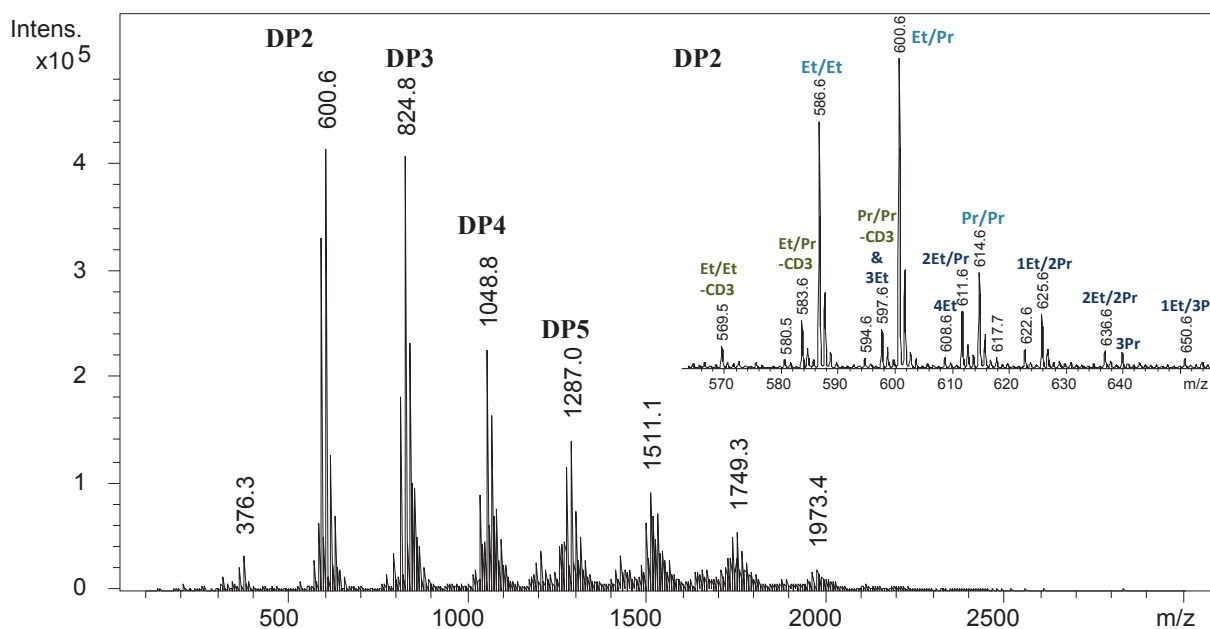
Figure 3.26 ESI-IT-MS spectrum of perdeuteromethylated sample **4c'** after partial hydrolysis and reductive amination with *meta*-aminobenzoic acid (mABA)

In this mass spectrum, oligomers with DP 2 and 3 had higher intensity. Not only mono

substitution patterns were observed, but also other substitution patterns with higher DS were visible. Therefore signals from these substitution patterns are applied for calculation of DS of the particular DP. Besides perdeuteromethylated oligomers, small amounts of oligomers with free OH groups were also detected, but these signals were not used for the evaluation.

To obtain reliable results each sample was measured three times with different methods, in voltages of ion optics and ion traps (detail in experimental part, section 4.6), because these measurement parameters can influence the ion yield and the relative intensities. However this was not observed for the presented samples. The relative intensities from the mass spectra are shown in Table 3.6 and 3.7.

Table 3.6. Relative intensities (Int.) of [M-H]$^-$ ions of DPs 2-5 of perdeuteromethylated sample **4c**, measured by three ESI-MS methods

DP	n(Et)	n(Pr)	n(CD$_3$)	m/z	Int. method 1	Int. method 2	Int. method 3
2	2	0	4	586	31.20	33.71	34.61
2	1	1	4	600	51.38	47.75	47.30
2	0	2	4	614	17.42	18.54	18.09
3	3	0	6	810	20.83	21.45	24.42
3	2	1	6	824	43.03	39.93	38.42
3	1	2	6	838	29.75	31.76	30.64
3	0	3	6	852	6.38	6.87	6.52
4	4	0	8	1034	12.18	11.95	14.06
4	3	1	8	1048	35.37	33.59	30.92
4	2	2	8	1062	30.26	33.81	34.10
4	1	3	8	1076	17.78	16.04	16.39
4	0	4	8	1090	4.41	4.60	4.53
5	5	0	10	1258	7.32	6.78	8.62
5	4	1	10	1272	24.11	24.17	22.25
5	3	2	10	1286	32.55	32.23	34.25
5	2	3	10	1300	21.69	22.90	20.27
5	1	4	10	1314	10.22	9.36	9.37
5	0	5	10	1328	4.11	4.57	5.25

One should notice that the experimental results from three ESI-MS measurements (Table 3.6 and 3.7) of each sample were averaged, since they did not show strong deviations, only slight scattering that lies within the measuring inaccuracy.

It is quite clear that for both samples, the experimental results of compositions of oligomers with DP_n didn't deviate significantly from the calculation results, which implies that for both **4c** and **4c'** the distribution of ethyl and propyl groups along the backbone is rather random than block-wise. In the case of a block-wise distribution of the two ether groups, the experimental content of homo-substituted oligomers (for example oligomer $DP_n=2$ with 2 ethyl group or 2 propyl group) would be higher than the calculated results.

Table 3.7. Relative intensities (Int.) of [M-H]⁻ ions of DPs 2-5 of perdeuteromethylated sample **4c'**, measured by three ESI-MS methods

DP	n(Et)	n(Pr)	n(CD$_3$)	m/z	Int. method 1	Int. method 2	Int. method 3
2	2	0	4	586	36.64	37.47	39.00
2	1	1	4	600	49.21	47.65	44.34
2	0	2	4	614	14.15	14.88	16.67
3	3	0	6	810	22.73	20.54	26.00
3	2	1	6	824	45.12	46.57	41.47
3	1	2	6	838	26.15	26.96	25.74
3	0	3	6	852	6.00	5.93	6.80
4	4	0	8	1034	14.64	15.35	14.64
4	3	1	8	1048	35.86	39.13	41.33
4	2	2	8	1062	32.87	28.79	27.94
4	1	3	8	1076	11.67	13.46	13.28
4	0	4	8	1090	4.96	3.27	2.81
5	5	0	10	1258	10.41	10.19	8.73
5	4	1	10	1272	29.58	26.97	28.37
5	3	2	10	1286	32.89	33.44	36.20
5	2	3	10	1300	20.21	17.68	18.38
5	1	4	10	1314	6.91	8.73	8.32
5	0	5	10	1328	0.00	2.98	0.00

The comparison of experimental results (Table 3.6 and 3.7) and calculation results (Table 3.5) can be demonstrated by the diagrams in Figure 3.27.

3.4.7 Cryo-transmission electron microscopy (TEM) of 3-*O*-alkyl celluloses

Microscopy provides a direct way to gain structural information which may be crucial for

interpreting the properties of polymers [115]. During the course of these studies, transmission electron microscopy was carried out because of its efficiency for the observation of microstructures.
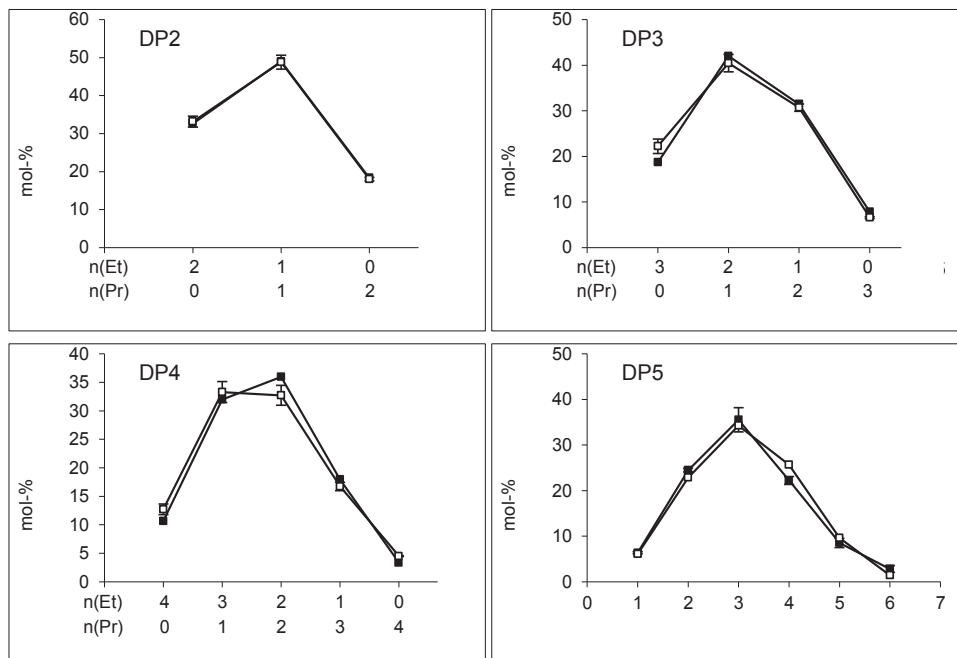
a)
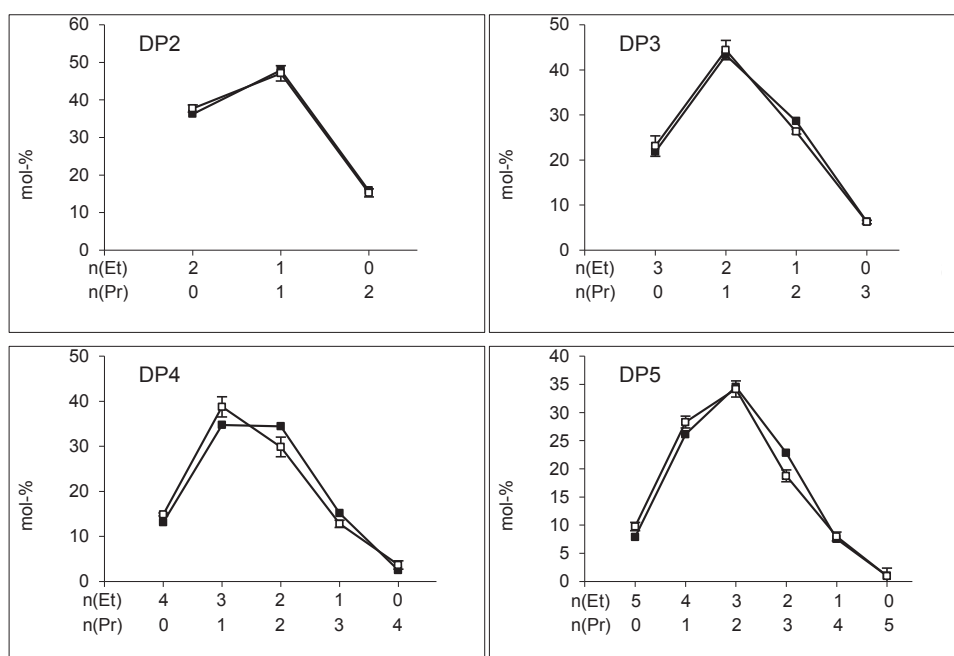
b)

Figure 3.27. Comparison of experimental (□) and calculated (■) distribution of ethyl and propyl of sample **4c** (a), and sample **4c'** (b)

3.4.7.1 Cryo-transmission electron microscopy (TEM) of 3-O-alkyl celluloses with comparable DS_{Et}/DS_{Pr} (**4c**, **4c'**) but synthesized by alkylations under different conditions

Based on the Micro DSC curves, different temperatures were chosen for sample preparation. Figure 3.28 showed the structures of **4c** and **4c'** under different temperatures: around 20 °C hardly any structures or particles are visible; as the temperature was increased to 35-40 °C small particles were observed already; at higher temperatures of 42-47 °C, irregular large aggregates are visible. From the comparison of the microscopy photos of these two samples at different temperatures, no significant differences in their structures were observed.
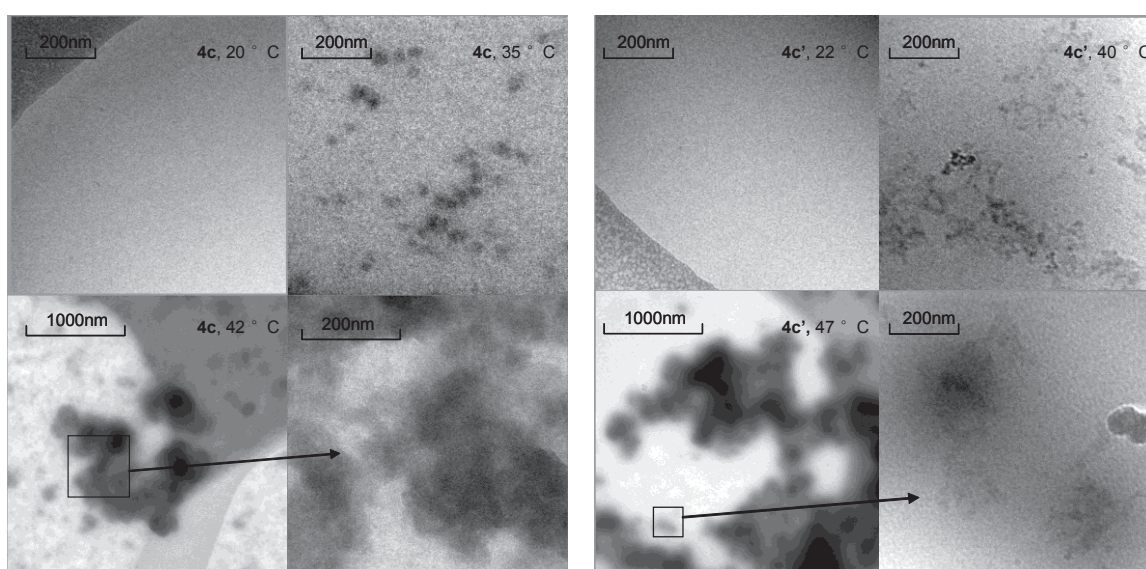
Figure 3.28 TEM images of 3-O-ethy/propyl cellulose (**4c** and **4c'**) synthesized under different conditions at different temperatures

3.4.7.2 Cryo-TEM observation of physical mixture of 3-mono-O-ethyl cellulose (3EC) and 3-mono-O-propyl cellulose (3PC)

Mixture M_1 (3EC/3PC=0.95/0.15) was observed at different temperatures (Figure 3.29).

At 5 °C, the sample shows no structures (not shown); at 25 °C, small aggregates began to form (which could also be sheets and fibrillar structures); when heated to 48 °C, a network-like structure with micelles was formed; at 54 °C, both large aggregates and small micellar aggregation were clearly observed. Thus, an obvious difference in temperature

dependant structure between 3-*O*-Et/Pr and mixture of 3EC and 3PC was observed.

3.5 Solid state analysis of 3-*O*-alkyl celluloses

3.5.1 X-ray diffraction (WAXRD) of 3-*O*-alkyl celluloses bearing two different ether groups

T. Kondo *et al.* has reported the investigation of the hydrogen bonding of different regioselectively substituted cellulose ethers by wide angle X-ray diffraction (WAXRD): 3-mono-*O*-methyl cellulose has the most crystallinity than regioselective methyl cellulose with other functionalization patterns (6-mono-*O*-methyl cellulose, 2,3-di-*O*-methyl cellulose) [107]. Thus, it is of great interest to study the crystallinity of 3-*O*-alkyl celluloses bearing two different ether groups.
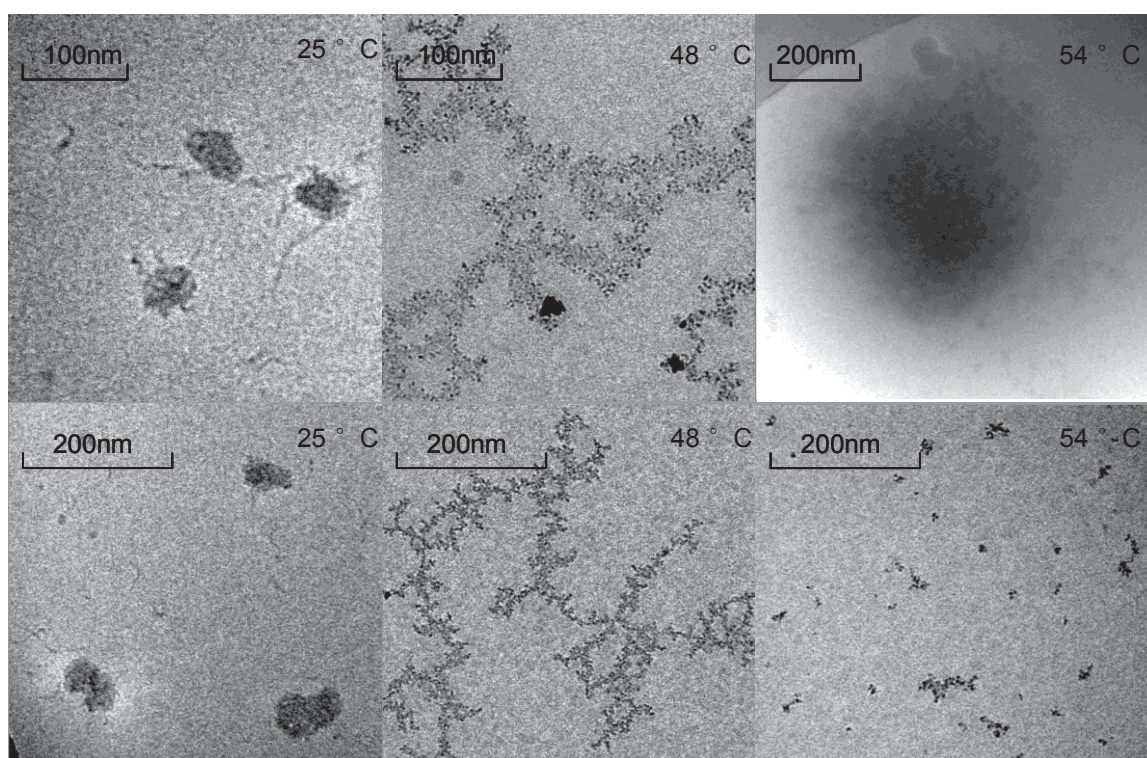
Figure 3.29 TEM images of 3-mono-*O*-ethyl cellulose (3EC) and 3-mono-*O*-propyl cellulose (3PC) (**4c** and **4c'**) mixture with molar ratio 3EC/3PC=0.95/0.15 at different temperatures

As shown in Figure 3.30a, in spite of the same main peak at 20°, the diffractogram of **4e** (Me/Et=0.99/0.08) shows a small peak at about 12° which is comparable to the diffractogram

of 3MC [107]; whereas **4g** (Me/Pr=0.97/0.12) only gives a broadening of the main peak at same position. It can be concluded that when the DS ratio of Me/Et and Me/Pr is comparable, products substituted with propyl groups have a decreased crystallinity. The same trends were observed in the case of **4e** and **4f** shown in Figure 3.30b. In this case the conclusion would be: when it is always methyl and ethyl groups are introduced in position 3, the crystallinity of products with larger DS_{Et} will also be reduced.
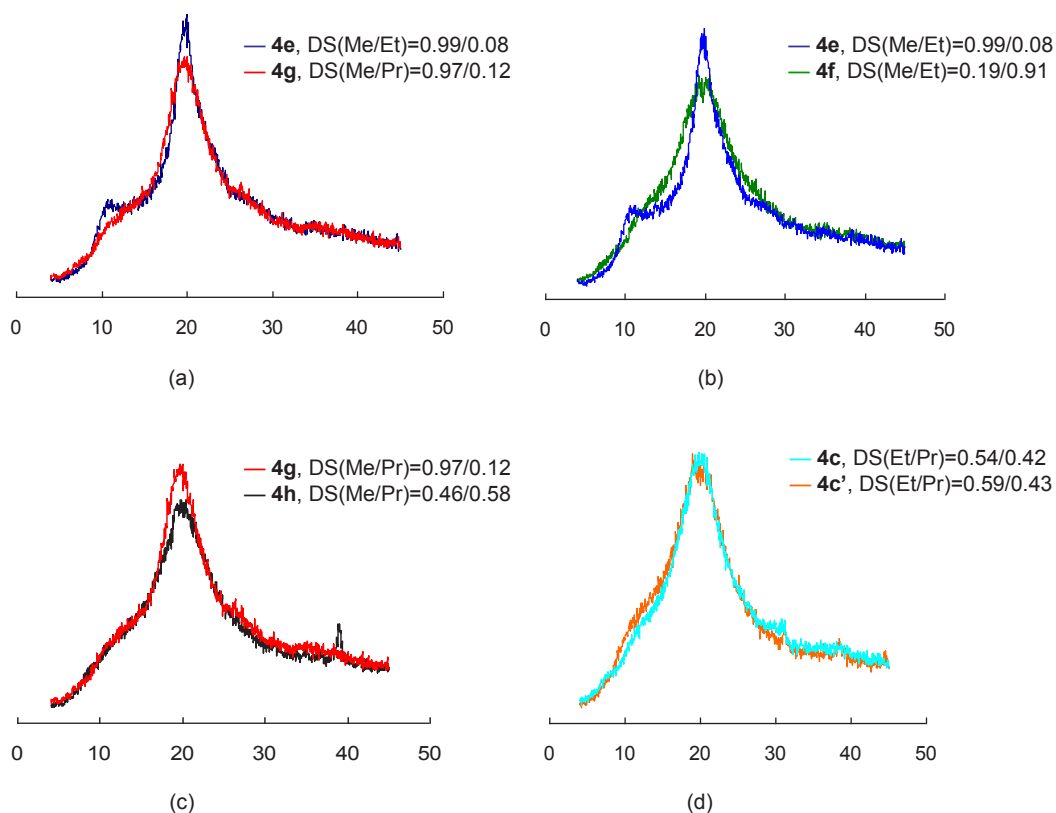
Figure 3.30 Wide angle X-ray diffraction of 3-*O*-methyl/ethyl cellulose **4e**, **4f**, 3-mono-*O*-methyl/propyl cellulose **4g**, **4h**, and regioselective cellulose derivatives synthesized via different conditions **4c** (50 °C) and **4c'** (r. t. with catalyst)

However, the comparison of **4g** and **4h** (Figure 3.30c) with different DS ratios of methyl and propyl moieties show no significant differences. The small peak at about 39° may due to cavities formed during the sample preparation (chapiter 4.16). Still the intensity of the main peak of **4h** with larger DS_{Pr} seems to be slightly weakened. Thus, further evaluation of their crystallinity is necessary.

4c and **4c'** were also measured by WAXRD (Figure 3.30d). Almost two identical diffractograms were observed. Thus, different reaction conditions used for alkylation cause no influence on the crystallinities of the final products with comparable DS_{Et}/DS_{Pr}.

3.5.2 Dynamic mechanical thermal analysis of 3-*O*-alkyl celluloses bearing two different ether groups (Me, Et, Pr)

Dynamic mechanical thermal analysis (DMTA) is a useful tool for mechanical properties characterization, especially for polymer materials. It is reported that the side chain relaxation information of cellulose esters can be obtained by this method [116], which could also be meaningful for the investigation of the side chain distribution of the two focused sample **4c** and **4c'** which were synthesized using different alkylation conditions.

The two water-insoluble samples **4e** and **4g** were measured. The temperature sweep was set from -100 °C to 150 °C. As shown in Figure 3.31a, b, the peak of tanδ of the curve **4g** shifted to lower temperature (66 °C) compared to that of **4e** (79 °C). And these two peaks were assigned to the glass transition temperature. So it can be concluded that even the DS of the longer alkyl chain (Et or Pr) is low, the increase of one carbon can cause a significant decrease of glass transition temperature.

As mentioned, the main purpose of the DMTA test is to investigate the side chain relaxation, or in other words, the alpha transition. However, no such transition described in former published article was observed in the diagrams. The reason could be the chain length of alkyl groups (methyl-C1, ethyl-C2, propyl-C3) is not as high as that of cellulose laurate (C12) mentioned in this article.

3.6 Synthesis of 3-mono-*O*-acetyl cellulose

As mentioned in 2.2.2.2, the protection of position 2 and 6 by *tert*-butyldimethylsilyl

(TBDMS) were also efficient, but the desilylation is easier than TDMS cellulose. Therefore, 2,6-di-*O*-TBDMS cellulose was chosen as an intermediate for the synthesis of 3-mono-*O*-acetyl cellulose. The synthesis of 2,6-di-*O*-TBDMS cellulose was according to the published article [59].

(a) **4e**, DS(Me/Et)=0.99/0.08   (b) **4g**, DS(Me/Pr)=0.97/0.12
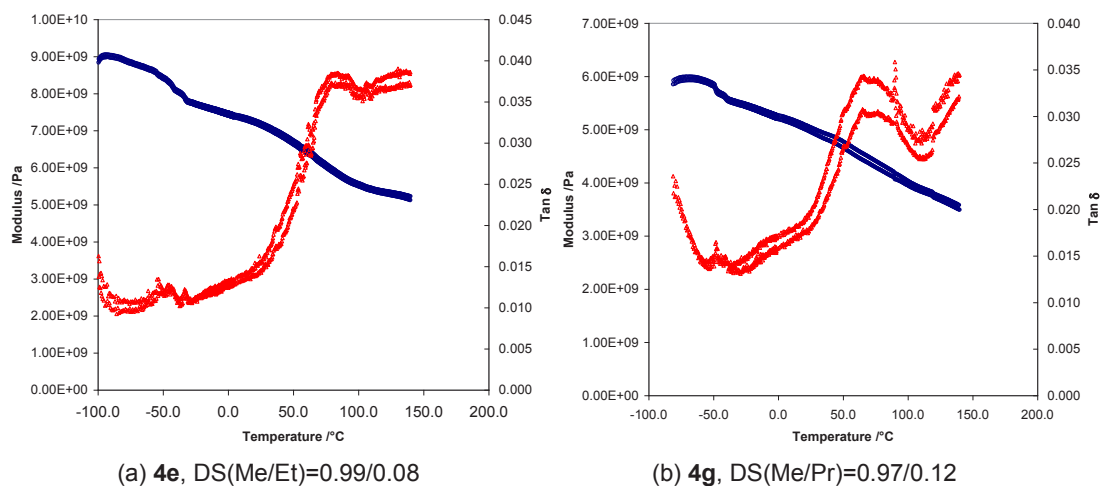
Figure 3.31 Temperature dependant change in modulus (blue) and tan δ (red) of 3-*O*-methyl/ethyl cellulose with DS_{Me}/DS_{Et}=0.99/0.08 **4e**, 3-*O*-methyl/propyl cellulose with DS_{Me}/DS_{Pr}=0.97/0.12 **4g**

3.6.1   Desilylation   of   2,6-di-*O*-TBDMS-3-mono-*O*-acetyl   cellulose   catalysed   by tris(4-bromophenyl)aminium hexachloroantimonate (TBPA$^+$• SbCl$_6^-$)

In order to yield 3-mono-*O*-acetate via 2,6 silyl protected cellulose, a primary silyl ether (position 6) and a secondary ether (position 2) must both be cleaved. A suitable reported catalyst is tris(4-bromophenyl)aminium hexachloroantimonate (TBPA$^+$• SbCl$_6^-$) [117]. Thus the proposed synthesis route is shown in Scheme 3.3.

The desilylation products were characterized directly by NMR spectroscopy in DMSO-d6. Both ^{1}H and ^{13}C NMR spectra showed significant peaks of remaining silyl group peaks, as well as the signals from acetyl groups and the protons of AGU (Figure 3.23). As a result, the content of silyl groups after treatment of TBPA$^+$• SbCl$_6^-$ is indeed reduced but still non-negligible.
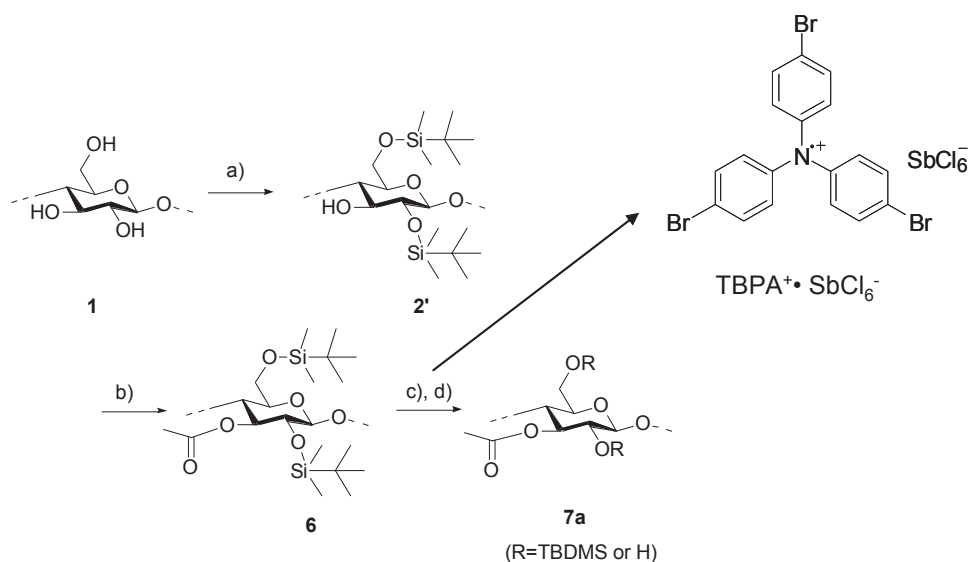
Scheme 3.3 Synthesis of 3-mono-*O*-acetyl cellulose by tris(4-bromophenyl)aminium hexachloroantimonate (TBPA$^+$• SbCl$_6^-$): a) *tert*-butyldimethylsilyl chloride, imidazole, DMA/LiCl, r. t., 24 h; b) acetic anhydride, pyridine, 4-*N,N*-dimethylaminopyridine (DMAP, cat.) THF, 50 ºC, 4 d; c) tris(4-bromophenyl)aminium hexachloroantimonate (TBPA$^+$• SbCl$_6^-$), CHCl$_3$/MeOH=5/1 (v/v), 50 ºC, 24 h; d) tris(4-bromophenyl)aminium hexachloroantimonate (TBPA$^+$• SbCl$_6^-$), DMSO, 50 °C, 24 h
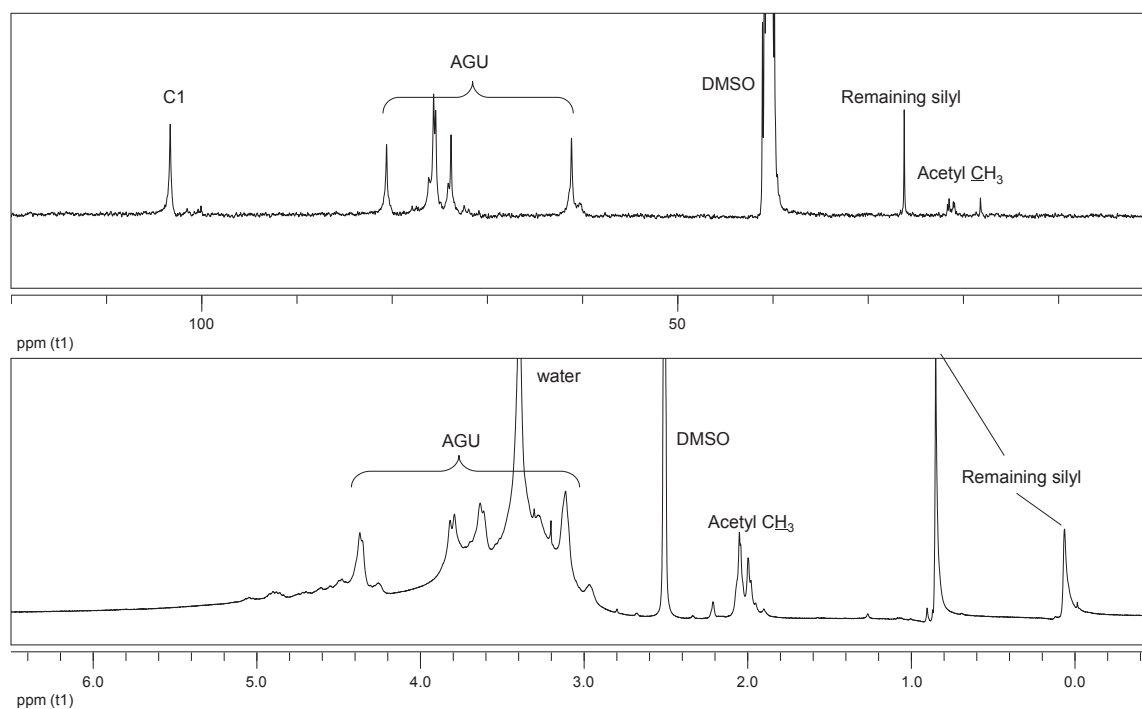
Figure 3.32 ^{13}C and ^{1}H NMR in DMSO-d6 of 3-*O*-acetyl cellulose synthesized by tris(4-bromophenyl)aminium hexachloroantimonate (TBPA$^+$• SbCl$_6^-$)

One should also note that in both ^{13}C and ^{1}H NMR spectra, the peaks for acetyl group are

very weak, which implies also the partial cleavage of acetyl group during the desilylation reaction.

3.6.2 Desilylation of 2,6-di-*O*-TBDMS-3-mono-*O*-acetyl cellulose by fluoride HF/pyridine, CsF, SelectFluor®

In general, the reaction conditions for these desilylation reagents HF/pyridine, CsF, SelectFluor® are similar. Since the solubility of 3-*O*-acetyl-2,6-*O*-TBDMS cellulose is limited, tetrahydrofuran was chosen as the solvent for desilylation. Regarding the highly corrosive properties of HF, the temperature of desilylation by HF/pyridine was set at room temperature, while the other two were set at 50 °C (Scheme 3.4).
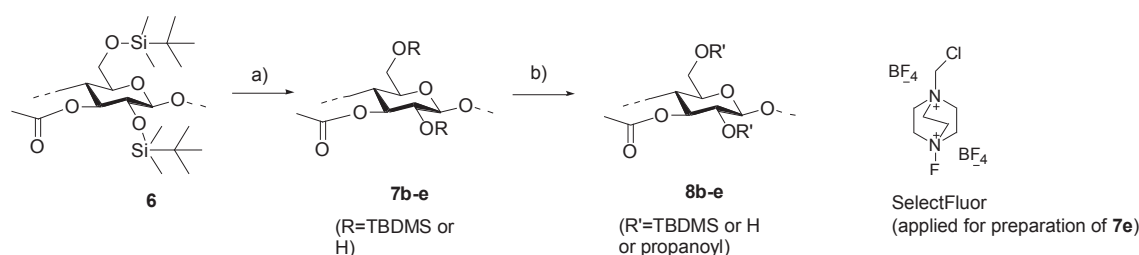
Scheme 3.4. Desilylation by fluorides to yield 3-mono-*O*-acetyl cellulose: a) fluorides (HF/pyridine-**7b**; CsF-**7c, d**; SelectFluor®-**7e**), THF or DMSO, r.t. or 50 ºC, 24 h; b) propanoic anhydride, 4-*N,N*-dimethylaminopyridine, pyridine, 80 °C, 24 h

The conditions and the results of each reaction are summarized in Table 3.8:

Table 3.8. Reagents used and reaction conditions for desilylation

Sample	Reagent	Solvent	Temperature (°C)	Results
7b	HF/pyridine	THF	25	degraded, incomplete desilylation
7c	CsF	THF	50	degraded, incomplete desilylation
7d	CsF	DMSO	50	incomplete desilylation
7e	SelectFluor	THF	50	degraded, incomplete desilylation

The product was perpropanoylated and then measured by NMR spectroscopy in CDCl$_3$ at 60 °C. Surprisingly, in spite of remaining silyl peaks, all three products showed no significant peaks for the anhydrousglucose unit (AGU) which are normally significant at this

temperature.
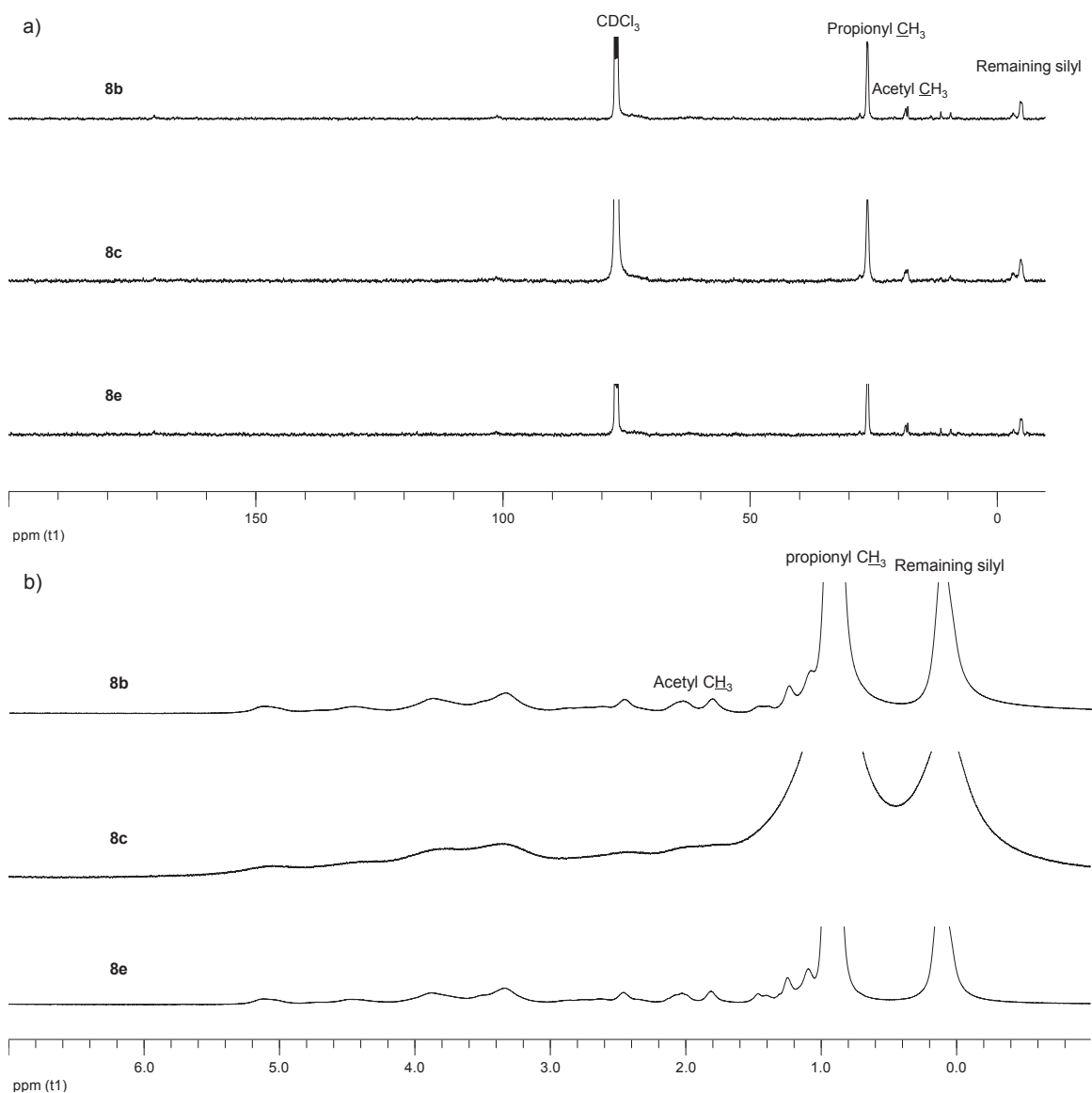
Figure 3.33 ^{13}C (a) and ^{1}H NMR (b) spectra in CDCl$_3$ of perpropanoylated products **8b**, **8c**, **8e**

It is suggested that the majority part of cellulose derivative was finally degraded by the fluoride reagent, with an inefficient desilylation. The degraded products were washed and filtered away by water during the work up procedure.

For alternative conditions, desilylation by CsF in dimethylsulfoxide was reported [118], so similar reaction was carried out in DMSO. Surprisingly, the perpropanoylated product **8d** showed a much better cellulose structure characterized by NMR spectroscopy. In both ^{1}H and ^{13}C spectra, the peaks are well attributed. However, non-negligible signals of silyl group still

exists around 0 ppm, and the peaks for acetyl CH$_3$ and acetyl carbonyl were hardly visible in both ^{1}H and ^{13}C spectra which implies the loss of acetyl from position 3. These facts proved that the desilylation is incomplete, and moreover that the acetyl was not remaining during the desilylation.
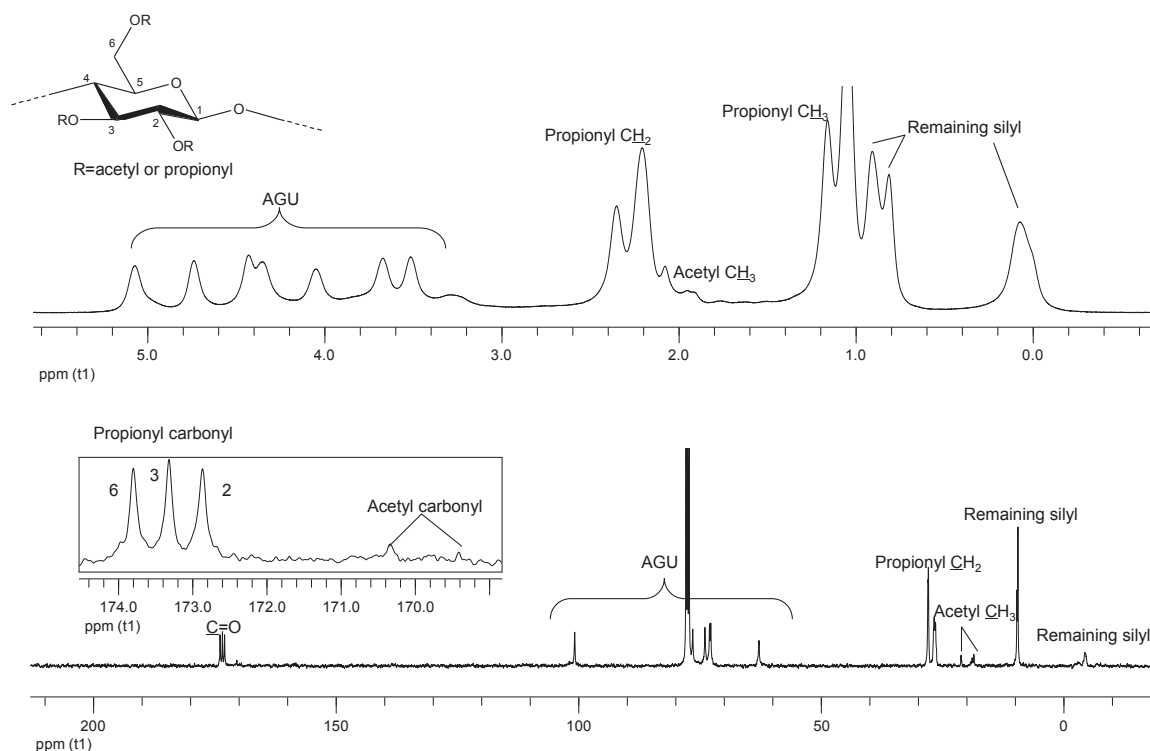
Figure 3.34 ^{13}C and ^{1}H NMR in CDCl$_3$ of perpropanoylated products of desilylation **7d** with CsF in DMSO at 50 °C

In this part of work, the desilylation of 3-mono-*O*-acetyl-2,6-di-*O*-TBDMS cellulose by TBPA$^+$• SbCl$_6^-$, HF/pyridine, CsF, Selecfluor are proved to be incomplete, because of the non negligible silyl signals around 0 ppm and 1 ppm. Second, the fluorides with high nucleophile F$^-$ caused an obvious degradation of polymer except in the case of CsF in DMSO. In this case, the NMR spectra imply that the desilylation was incomplete and the acetyl groups were cleavaged.

4. Experimental part

4.1 Materials

Microcrystalline cellulose **1** (Avicel PH-101, Sigma–Aldrich, DP_n 117) was dried under vacuum over potassium hydroxide for 3 h at 105 °C and lithium chloride (Fluka) was dried under vacuum over potassium hydroxide for 3 h at 150 °C. Sodium hydride (Fluka) was used after washing a suspension in mineral oil (60%) with *n*-hexane and *n*-pentane and drying at room temperature under argon gas flow. DMA (Fluka), anhydrous THF (Aldrich) and pyridine (Fluka) were stored over molecular sieves (size 3 Å). All other chemicals were used as received.

3MC (sample **4i**, DS 1.05) [54], 3EC (sample **4j**, DS 1.07) [38], 3PC (sample **4k**, DS 1.13) [65] and 2,6-di-*O*-(*tert*-Butyldimethylsilyl) cellulose (**2'**) [59] were prepared according to the published procedures.

4.2 3-*O*-Alkyl cellulose

4.2.1 Synthesis of 2,6-di-*O*-TDMS cellulose **2**

Microcrystalline cellulose **1** (100 g, 617 mmol) was slurried in 2532 mL DMA in a 5 L reaction vessel and heated to 130 °C for 3 h. The mixture was cooled to 100 °C and LiCl (200 g, 4718 mmol, 7.6 mol/mol AGU) was added. A clear solution was obtained after stirring overnight at 30 °C. Imidazole (200 g, 2938 mmol, 4.8 mol/mol AGU) was added to the solution, followed by TDMS-Cl (500 mL, 2548 mmol, 4.1 mol/mol AGU). The mixture was allowed to react for 24 h at 100 °C under vigorous mechanical mixing. After cooling to room temperature, the reaction mixture was poured into 3 L water. The well dispersed product was filtered off, washed 2 times with 600 mL water and then 6 times with 400 mL ethanol, the product was dried in a vacuum oven at 60 °C.

Yield: 273 g (99%).

Silicon content: 27.19%.

DS$_{Si}$ 2.06.

FT-IR (KBr, cm^{-1}): 3504 νOH, 2960 2872 νC-H, 1466 δC-H, 1252 νSi-C, 1152-1037 νC-O-C, 833 778 νSi-C.

SEC in THF: $\overline{M}_n$ 42556 g/mol, DP$_n$ 94.

The product is soluble in *n*-hexane, toluene, THF, and chloroform.

4.2.2 2,6-di-*O*-TDMS-3-*O*-Et/Pr cellulose **3c** and **3c'**

3c: To 2,6-di-*O*-TDMS cellulose 2 (13.26 g, 29.7 mmol) dissolved in dry THF (130 mL), sodium hydride (7.6 g, 292 mmol, 10 mol/mol modified AGU) was added under vigorous mechanical mixing. After 1 h, PrI (23.2 mL, 237.4 mmol, 8 mol/mol modified AGU) and EtI (4.8 mL, 59.4 mmol, 2 mol/mol modified AGU) were added drop wise. The solution solidified accompanied with an obvious exothermic effect. The mixture was stirred overnight until the paste became liquid. The mixture was allowed to react at 50 °C for 4 d under mechanical stirring. The remaining sodium hydride was destroyed by the addition of 20 mL isopropanol, followed by adding 10 mL of water. The product was precipitated in buffer solution (14.68 g Na$_2$HPO$_4$·12H$_2$O and 3.54 g KH$_2$PO$_4$ in 1 L distilled water) and filtered off, washed 2 times with 200 mL ethanol and dispersed, then washed again 4 times with 200 mL water, and 4 times with 200 mL ethanol. The pale yellow product was dried under vacuum at 40 °C.

Yield: **3c** 12.29 g (94%)

FT-IR (KBr, cm^{-1}): 3452 νOH (very weak), 2963 2873 νC-H, 1468 δC-H, 1379 δCH$_3$, 1255 νSi-C, 1089 1044 νC-O-C, 832 777 νSi-C.

SEC in tetrahydrofuran (THF): **3c** $\overline{M}_n$ 21453 g/mol, DP$_n$ 49

3c': The procedure is almost comparable to that of **3c**, the only difference is the addition of tetra-*n*-butylammonium iodide (TBAI, 0.12 g) after overnight stirring of the reaction mixture.

Then the system was allowed to react at room temperature for 4 days under mechanical stirring. The work up is identical to that of **3c**.

Yield: **3c'** 12.18 g (89%)

FT-IR spectrum is comparable to that of **3c**

SEC in tetrahydrofuran (THF): **3c'** $\overline{M}_n$ 15911 g/mol, DPn 33.

These two products are soluble in *n*-hexane, toluene, THF and chloroform.

4.2.3 Alkylation with the presence of *n*-BuLi as base **3a'**

The solution of 2,6-di-*O*-TDMS cellulose **2** (1 g, 2.2 mmol) in dry THF (20 mL), was cooled to -78 °C by mixture of isopropanol and dry ice under vigorous mechanical mixing. 11.2 mL (22.4 mmol) *n*-BuLi in hexane (0.775 g/mL) was added dropwise by syringe under atmosphere of argon. After 30 min, ethyl iodide (0.9 mL, 1.75 g, 11.2 mmol) and propyl iodide (1.1 mL, 1.90 g, 11.2 mmol) were carefully added by syringe under protecting gas, an obvious gas generation could be observed, and the clear solution turned into a non-transparent paste. The mixture was allowed to react in isopropanol/dry ice bath and the temperature was slowly raised to room temperature overnight, and then reacted at 50 °C for 4 days. Isopropanol (5 mL) was dropped into the mixture to destroy the excess of *n*-BuLi, which could be confirmed by adding the same amount of distilled water. Then the hexane was evaporated under reduced pressure, the residue was poured into 100 mL distilled water, well dispersed, and then filtered off, the solid was washed 4 times by water (20 mL each time), then by ethanol (20 mL each time) and dried under vacuum at 40 °C to yield a light yellow solid.

Yield: 1.06 g (quantitative)

DS$_{Et}$ 0.27, DS$_{Pr}$ 0.19 (determined by ^{1}H-NMR spectroscopy after peracetylation)

4.2.4 3-*O*-Et/Pr cellulose **4c**

To 2,6-di-*O*-TDMS-3-*O*-Et/Pr cellulose **3c** (12.17 g, 26.4 mmol) dissolved in THF (183 mL), TBAF·3H$_2$O (32.3 g, 105.6 mmol, 4 mol/mol modified AGU) was added, and the mixture was allowed to react for 24 h at 50 °C under stirring. After cooling to room temperature, the polymer was precipitated with ethanol/isopropanol 2:1 (v/v), filtered off, washed with isopropanol and dried in vacuum. The precipitate was dissolved in dimethyl sulfoxide (DMSO, 59 mL) and treated with TBAF·3H$_2$O (3.49 g) for 24 h at 50 °C. After cooling to room temperature, the polymer was precipitated with 800 mL diethyl ether/isopropanol 2:1 (v/v), filtered off, washed 4 times with 50 mL diethyl ether/isopropanol 2:1 (v/v) and dried under vacuum. The crude product was dissolved in 50 ml DMSO and reprecipitated in 300 mL diethyl ether/isopropanol 2:1 (v/v). The product was washed with diethyl ether/isopropanol 2:1 (v/v) and dried in vacuum at 40 °C.

Yield: 2.46 g (47%).

DS$_{Et}$ 0.54, DS$_{Pr}$ 0.42 (determined by ^{1}H-NMR spectroscopy after peracetylation).

SEC in DMA/LiCl: $\overline{M}_n$ 41477 g/mol, DP$_n$ 212.

The product is soluble in DMSO, DMA, *N,N*-dimethyl formamide (DMF), and water.

4.2.5 2,6-di-*O*-Acetyl-3-*O*-Et/Pr cellulose **5c**

To 3-mono-*O*-Et/Pr cellulose (**4c**, 0.2 g, 1 mmol) dissolved in dry pyridine (6 mL), 6 mL (63.5 mmol, 63 mol/mol modified AGU) acetic anhydride and 0.02 g (0.2 mmol, 0.2 mol/mol modified AGU) 4-*N,N*-dimethylaminopyridine were added. The mixture was allowed to react for 20 h at 80 °C and then 3 h at 100 °C under stirring and exclusion of moisture. After cooling to room temperature, the product was precipitated with 50 mL isopropanol, filtered off, washed 6 times with 50 mL isopropanol, and dried under vacuum at 40 °C.

Yield: 0.3 g, quantitative.

SEC in THF, **5c**: $\overline{M}_n$ 54866 g/mol, DP_n 272;

^{1}H-NMR (400 MHz, CDCl$_3$, ppm): 0.85 (-O-CH$_2$CH$_2$C$\underline{H}_3$), 1.07 (-O-CH$_2$C$\underline{H}_3$), 1.48 (-O-CH$_2$C$\underline{H}_2$CH$_3$), 2.07 (-COC$\underline{H}_3$), 3.41 (H-3), 3.43 (H-5), 3.63(H-4), 3.53, 3.75 (-O-C$\underline{H}_2$CH$_3$, -O-C$\underline{H}_2$CH$_2$CH$_3$), 4.16 (H-6α), 4.36 (H-6β), 4.44 (H-1), 4.78 (H-2).

^{13}C-NMR (CDCl$_3$, ppm): 170.0, 169.0 (C=O), 100.8 (C-1), 80.6 (C-3), 77.5 (C-4), 73.9 (C-2, 5), 67.5 (-O-$\underline{C}$H$_2$CH$_3$, -O-$\underline{C}$H$_2$CH$_2$CH$_3$), 62.6 (C-6), 23.1 (-O-CH$_2$$\underline{C}H_2CH_3$), 20.5 (-CO$\underline{C}H_3$), 15.2 (-O-CH$_2$$\underline{C}H_3$), 10.2 (-O-CH$_2CH_2$$\underline{C}H_3$).

FT-IR (KBr, cm^{-1}): 2978 2937 2900 νC–H, 1748 νC=O, 1441 δC-H, 1375 δC-H$_3$, 1231, 1047 νC-O-C.

The product is soluble in chloroform, pyridine, and ethyl acetate.

4.3 Synthesis of 3-mono-*O*-acetyl cellulose

4.3.1 3-mono-*O*-acetyl-2,6-di-*O*-TBDMS cellulose **6**

To 2,6-di-*O*-TBDMS cellulose **2**' (10 g, 29.7 mmol) dissolved in dry THF (300 mL), acetic anhydride (50 ml, 539 mmol, 21 mol/mol modified AGU), pyridine (50 ml) and 4-*N,N*-dimethylaminopyridine (DMAP, 0.2 g, 1.6 mmol) were added whilst vigorously mixing it with a mechanical mixer, and the mixture was allowed to react at 50 °C for 4 d. The product was precipitated in 1200 ml methanol and dispersed, then washed 4 times with 200 mL water, and 4 times with 200 mL ethanol. The pale yellow product was dried under vacuum at 40 °C.

Yield: **6** 8.62 g (78%)

FT-IR (KBr, cm^{-1}): 3440 (weak) νOH, 2960 2865 νC-H, 1769 νC=O, 1473 δC-H, 1371 δCH$_3$, 1256 νSi-C, 1122 1041 νC-O-C, 837 778 νSi-C.

The product is soluble in chloroform and THF.

4.3.2 Desilylation of 3-mono-*O*-acetyl-2,6-di-*O*-TBDMS cellulose **6** with TBPA$^+\bullet$ SbCl$_6^-$ as catalyst **7a**

To 2,6-di-*O*-TBDMS cellulose **6** (0.5 g) dissolved in chloroform (30 mL), 6 ml methanol was carefully added by syringe under vigorous mixing. The solution was stirred at room temperature overnight. Then tris(4-bromophenyl)aminium hexachloroantimonate (TBPA$^+\bullet$ SbCl$_6^-$, 0.2 g) was added and the mixture was allowed to react at 50 °C for 24 h. The product was precipitated in 120 ml water and filtered off. Then it was washed 4 times with 50 mL water, and 4 times with 50 mL methanol. The white product was dried under vacuum at 40 °C. The vacuum-dried product was dissolved in DMSO (10 ml), then TBPA$^+\bullet$ SbCl$_6^-$ (0.2 g) was added and the mixture was allowed to react at 50 °C for 24 h. The work up procedure was repeated to yield a white product.

Yield: 0.13 g (55%)

^{1}H-NMR (400 MHz, DMSO-d6, ppm): 0.05 (Si-(CH$_3$)$_2$, TBDMS), 0.84 (-(CH$_3$)$_3$, TBDMS), 2.04 (-COC$\underline{H}_3$), 2.90-5.00 (AGU).

^{13}C-NMR (100 MHz, DMSO-d6, ppm): 170.0, 169.0 (C=O), 103.2 (C-1), 80.5 (C-3), 75.5 (C-4), 73.7(C-2, 5), 61.0 (C-6), 21.3, 20.8 (-CO$\underline{C}$H$_3$), -3.3 (C-$\underline{C}$H$_3$ silyl), -4.5 (Si-$\underline{C}$H$_3$).

FT-IR (KBr, cm^{-1}): 3512 νOH, 2957 2886 νC-H, 1763 νC=O, 1473 δC-H, 1363 δCH$_3$, 1256 νSi-C, 1123 1041 νC-O-C, 837 778 νSi-C.

The product is soluble in DMSO.

4.3.3 Desilylation 3-mono-*O*-acetyl-2,6-di-*O*-TBDMS cellulose **6** with HF/pyridine as catalyst **7b**

To 2,6-di-*O*-TBDMS cellulose **6** (0.5 g) dissolved in THF (50 ml) in a PTFE (polytetrafluoroethylene) flask, hydrogen fluoride in pyridine was added drop wise by syringe. The mixture was allowed to react at room temperature for 24 h. The product was precipitated

in 150 ml NaHCO$_3$ aqueous solution and filtered off. Then it was washed 4 times by 50 ml water, and 4 times by 50 ml methanol. The white product was dried under vacuum at 40 °C. The desilylation by CsF and SelectFluor® is similar to this described procedure.

Yield: 0.51 g (quantitative)

4.3.4 Perpropanoylation 8b

To product **7b** (0.1 g) dispersed in pyridine (6 ml), propionate anhydride (6 ml) and 4-*N,N*-dimethylaminopyridine (DMAP) was added. The mixture was heated to 80 °C and allowed to react for 24 h. The product was precipitated in 70 ml NaHCO$_3$ aqueous solution and filtered off, then washed 4 times by 20 ml water, 4 times by 20 ml methanol. The light yellow product was dried under vacuum at 40 °C.

Yield: 0.09 g (90%)

The product is soluble in chloroform.

^{1}H-NMR (400 MHz, CDCl$_3$, ppm): 0.07 (Si-(CH$_3$)$_2$, TBDMS), 0.82, 0.91 (C-(CH$_3$)$_3$, TBDMS), 1.05, 1.16(-CH$_3$ propionyl), 2.11 (weak, -COC$\underline{H}_3$), 2.21, 2.36 (-CH$_2$- propionyl), 3.52 (H-3), 3.69 (H-4), 4.07 (H-α), 4.37 (H-6β), 4.44 (H-1), 4.75 (H-2), 5.09 (H-3).

^{13}C-NMR (100 MHz, CDCl$_3$, ppm): 173.8, 173.3, 172.9 (C=O), 100.6 (C-1), 76.2 (C-4), 73.7 (C-5), 72.7 (C-3), 72.5 (C-2), 62.6 (C-6), 27.7, 26.1 (-CH$_2$-, propionyl), 20.8 (weak, -COC$\underline{H}_3$), 9.1 (-CH$_3$, propionyl), -3.3 (weak, C-(C$\underline{H}_3$)$_3$, TBDMS), -4.7 (weak, Si-(C$\underline{H}_3$)$_2$, TBDMS).

FT-IR (KBr, cm^{-1}): 3504 νOH, 2956 2858 νC-H, 1761 νC=O, 1473 δC-H, 1363 δCH$_3$, 1256 νSi-C, 1123 1041 νC-O-C, 837 779 νSi-C.

4.4 Fourier transform infrared spectroscopy (FT-IR)

FT-IR spectra were recorded on a Nicolet Avatar 370 DTGS spectrometer using the KBr technique. The KBr disks were dried under vacuum at 120 °C for 30 min before measurement.

4.5 Nuclear magnetic resonance spectroscopy (NMR)

The ^{1}H and ^{13}C NMR spectra were acquired with Bruker Avance 250 (250 MHz) or Avance 400 (400 MHz) spectrometers in deuterated chloroform (CDCl$_3$) or DMSO-d6 at 60 °C. The DS of the alkyl moieties was calculated from the peak area obtained by integration of the ^{1}H-NMR spectra. The DS$_{Me}$, DS$_{Et}$, and DS$_{Pr}$ were calculated by equation (4) and (5).

$$DS_{Me} = \frac{9 \cdot I_{AGU} - 7 \cdot I_{Ac} - 13 \cdot I_{CH_3}}{3 \cdot I_{AGU} + 3 \cdot I_{AGU} + I_{CH_3}} \qquad (4)$$

$$DS_{Et(Pr)} = \frac{16 \cdot I_{CH_3}}{3 \cdot I_{AGU} + 3 \cdot I_{Ac} + I_{CH_3}} \qquad (5)$$

I_{AGU} is the peak area of the AGU (anhydroglucose unit) peaks from 3.2 to 4.7 ppm.

I_{Ac} is the peak area of the methyl of the acetyl moiety at 2.06 ppm.

I_{CH_3} is the peak area of the Me group of Et moiety (1.07 ppm) or Pr moiety (0.85 ppm).

For 2,6-di-O-acetyl-3-mono-O-Et/Pr, DS$_{Et}$ and DS$_{Pr}$ were calculated by equation (6).

$$DS_{Et} + DS_{Pr} = 3 - \frac{13}{2 + 3 \cdot \dfrac{I_{AGI}}{I_{Ac}}} \qquad (6)$$

I_{AGU} is the peak area of the AGU peaks from 3.2 to 4.7 ppm.

I_{Ac} is the peak area of the methyl group of the acetyl moiety at 2.06 ppm.

I_{CH_3} (Et) and I_{CH_3} (Pr) correspond to the integral value of the methyl group of the ethyl moiety (1.07 ppm) or n-propyl (0.85 ppm) moiety respectively.

4.6 Gas chromatography combined with flame ionization detector mass spectrometry (GC-FID/MS) and electrospray ionization ion trap mass spectrometry (ESI-IT-MS)

Complete hydrolysis: As a first step the monomer composition of the two samples was determined by GC-FID/MS to obtain detailed information about the substitution pattern on the monomer level. Therefore the samples were degraded to monomers by acid catalyzed hydrolysis then reduced to alditols by $NaBD_4$ and finally acetylated with acetic anhydride. D-Pinitol was used as an internal standard to calculate the recovery of the sample material.

Partial hydrolysis: 15-20 mg of each sample was weighed in a Schlenck flask, dried under vacuum for several hours and then dissolved in 2 mL DMSO. To the dissolved material 200 mg of powdered NaOH (30 eq./OH) and 54 µL CD_3I (5 eq./OH) was added. After 12 hours another 25 µL of CD_3I was added and the mixture was stirred for 4 hours. Afterwards, excess alkylation reagent was removed under vacuum and the samples were isolated by liquid/liquid extraction with dichloromethane and water. 2 mg of each sample was partially hydrolyzed by acid catalyzed hydrolysis (1 M trifluoroacetic acid, 25 min, 120 °C) and afterwards labelled by reductive amination with *meta*-aminobenzoic acid.

GC/FID-MS analysis was carried out on a GC-2010 (Shimadzu) equipped with a ZB-5MS column (Phenomenex, length=29 m, i.d. =0.25 mm) and hydrogen as carrier gas, in order to analysis the monomers. To be able to assign all of the peaks, one sample was also measured by GC-MS (GC5890A, Hewlett Packard) with electron impact ionization (EI).

ESI-IT mass spectra were recorded on a HCT Ultra ETDII (Bruker Daltonics, Bremen, Germany), equipped with an ion trap (IT) mass analyzer. Samples were introduced directly with a syringe at a flow of 200 µL min^{-1}. The parameter settings for different methods of measurement mentioned in 3.4.6.2 were shown in Table 4.1:

Table 4.1 Parameter settings for different methods of measurement

Parameters	Method 1	Method 2	Method 3
Dry temperautre	300 °C		
Nebulizer pressure	10 psi [a]		
Dry gas flow rate	5 L/min		
HV [b] Capillary	3500 V		
HV [b] End Plate Offset	-500 V		
Capillary Exit	-280 V		
Skimmer	-40.0 V		
Octupole 1 DC [c]	-8.00 V		
Octupole 2 DC [c]	-2.70 V	-5.65 V	-3.67 V
Octu. RF [d] amplitude	200.0 Vpp [e]	254.4 Vpp [e]	200.0 Vpp [e]
Lens 1	5.0 V		
Lens 2	60.0 V		
Trap drive	100.6	140.9	140.9

a. pounds per square inch; b. high voltage; c. direct current potential; d. radio frequency potential; e. volt per peak

4.7 Preparation for aqueous solution for SEC, Micro DSC, rheology measurements, capillary viscosimetry, DLS, and cryo-TEM

The cellulose ethers were dissolved in distilled water by storing in a fridge at 4 °C for 24 h. Then the solutions were centrifuged at 5-7 °C to remove particles and insoluble impurities. An aliquot from the supernatant was then dried at 80 °C to calculate the dry weight concentrations. An aqueous solution with the desired concentration was obtained by dilution.

4.8 Size exclusion chromatography (SEC)

Sample preparation (in DMA/LiCl): cellulose ether (20 mg) was added to anhydrous DMA (0.5 mL) in a vial with a magnetic stirrer. After heating of the suspension to 130 °C for 1.5 h, the mixture was allowed to cool to 80 °C. Dried LiCl (42 mg) was added; after cooling, the sample was maintained for 1 h at 50 °C and subsequently at room temperature overnight whilst stirring. After stepwise dilution (DMA; 1.5 mL) of the cellulose solution, an aliquot of 0.1 mL was filled up to 1 mL with DMA to adjust the cellulose concentration to 1 mg/mL and LiCl concentration to 2.1 mg/mL.

Equipment: A JASCO SEC (Size exclusion chromatography) system was applied consisting of a degasser DG 980-50, pump PU 980, UV detector 975 (λ=354 nm), refractive index detector 930, column oven, and guard column. Separation was carried out using three SDV-Gel columns (106, 104, and 103 Å, Polymer Standards Service, Mainz, Germany) at 40 °C. The calibration standard was polystyrene or pullulan.

4.9 Lower critical solution temperature (LCST) measurement

LCST measurements were conducted with a turbidimetric photometer TEPPER Analytik (Germany, λ = 670 nm) by heating the aqueous solutions of cellulose (1%, w/w) from 5 to 90 °C and cooling back to 5 °C with a heating/cooling rate of 1 °C/min. The transmittance at the initial temperature was set to 100%. The LCST was estimated by applying the tangents to the turbidity curves of the samples (heating curves) and determination of the temperature at the intersection point.

4.10 Differential scanning calorimetry (DSC)

Thermal characteristics of cellulose ether aqueous solutions were determined using SETARAM micro DSC-III calorimeter (Caluire, France). About 850 mg of each sample solution, with distilled water as a reference, were sealed into DSC cells. The volume of water reference is calculated from the exact concentration of each solution, in order to match the heat capacity of the sample. Both the sample and reference cells were allowed to equilibrate at 10 °C for 1 h. Temperature was then raised from 10 to either 78 or 110 °C at heating rate of 1 °C/min and then lowered immediately to 10 °C at the same rate. In case of solution of 3-mono-*O*-propyl cellulose the starting temperature was lowered to 1 °C, to take into consideration the low temperature of the endothermic transition. Enthalpy values (ΔH), onset temperature T_{on}, peak temperature T_m and end temperature T_{off} of the transition were

calculated using Setaram software with an interpolated baseline.

4.11 Rheology measurements

Dynamic viscoelastic measurements were carried out on a controlled stress rheometer (MCR 301, Anton Parr, Austria). A 25 mm diameter parallel plate geometry and 1 mm as gap were used. All measurements were performed under oscillatory shear mode at an angular frequency of 10 rad/s and a shear strain ensuring operation within the linear viscoelastic regime. To prevent dehydration during the measurements a thin layer of low viscosity silicone oil was placed on the periphery surface of the solution. The storage modulus (G') and loss modulus (G") were monitored employing the same heating rate (1 °C/min) and temperature ranges as for the differential scanning calorimeter experiment.

4.12 Viscosity measurement

The reduced viscosity of aqueous solution in different concentrations was measured by capillary viscometer: PVS 1/2, Lauda, with an Ostwald capillary type Ic (K=0.02663 mm^2/s^2, Schott-Instruments, Mainz, Germany). The temperature was controlled by a water bath at 20 °C（±0.01 °C) for measurements of aqueous solutions.

4.13 Dynamic light scattering

DLS was performed at a scattering angle of 90° on an ALV CGS-3 instrument (ALV-Laser Vertriebsgesellschaft GmbH, D-63225 Langen, Germany) and a He–Ne laser operating at a wavelength of $\lambda = 633$ nm at 25 °C. Aqueous sample solution (0.5 mg/ml) was measured at different temperature: 25, 30, 35, 40, 45, 50 °C. The CONTIN algorithm was applied to analyze the correlation functions obtained. Apparent hydrodynamic radius of the particles was calculated according to the Stokes–Einstein equation. All CONTIN plots are

number-weighted.

4.14 Cryo TEM

For cryo-TEM a volume of 4 μL of the alkyl cellulose solution (after heating) was placed onto a grid covered by a perforated carbon support foil (Quantifoil Micro Tools Jena). The grid was blotted by a self-made auto-controlled blotting system equipped with a climatic chamber and then plunged rapidly into liquid ethane. The frozen sample was transferred with the Gatan-626 single tilt cryotransfer system into the cryo-electron microscope Philips-CM120.

4.15 Dynamic mechanical thermal analysis

DMTA was conducted at both frequency of 1 and 10 Hz with mechanical analyzers (DMA8000, from Perkin Elmer, USA). A material pocket technique 35-37 mm in single cantilever geometry, at a heating rate of 2 K/min was used. The sample powders were distributed evenly inside the pocket, and the pocket was folded shut and submitted to the measurements.

4.16 Wide angle X-ray diffraction

The WAXRD measurements of solid samples were carried out by X-ray diffractometer (Bruker AXS D5005) equipped with a copper tube operating at 40 kV and 50 mA produced CuKα radiation of 0.154 nm wave length. Solid samples were placed on a holding plate with a round cavity (1 mm depth) and squeezed in order to form a compact solid layer. Measuring temperature was maintained at 20 °C. The infraction angle swept from 4 to 45°.

Table 4.2 Summary of ^{1}H and ^{13}C NMR of cellulose derivatives discussed

Sample	Chemical shift (ppm) Glucose unit						Me	Et		n-Pr			Ester group			Silyl
	H1	H2	H3	H4	H5	H6	H7	H7	H8	H7	H8	H9	CH$_3$^{Ac}	CH$_2$^{Pro}	CH$_3$^{Pro}	TBDMS
5a-d	4.44	4.78	3.41	3.63	3.43	4.16, 4.36	-	3.48, 3.74	0.97	3.48, 3.74	1.38	0.75	2.00	-	-	-
5e, f	4.49	4.80	3.42	3.60	3.47	4.17, 4.35	3.44	3.53, 3.79	1.08	-	-	-	2.08	-	-	-
5g, h	4.51	4.80	3.35	3.62	3.49	4.14, 4.36	3.41	3.52, 3.72	-	3.52, 3.72	1.45	0.83	2.05	-	-	-
7a	2.90-5.00^a						-	-	-	-	-	-	2.04	-	-	0.05, 0.84
8b	4.44	4.75	5.09	3.69	3.52	4.07, 4.37	-	-	-	-	-	-	2.08^b	2.28	1.10	0.07, 0.86

Sample	Chemical shift (ppm) Glucose unit					Me	Et		n-Pr			Ester group			C=O on position:			Silyl
	C1	C2,5	C3	C4	C6	C7	C7	C8	C7	C8	C9	CH$_3$^{Ac}	CH$_2$^{Pro}	CH$_3$^{Pro}	2	3	6	TBDMS
5a-d	100.8	73.9	80.6	77.5	62.6	-	67.5	15.2	67.5	23.1	10.2	20.5	-	-	170	-	169	-
5e, f	100.8	73.2	80.7	77.6	62.6	59.6	67.6	15.3	67.6	-	-	20.6	-	-	170	-	169	-
5g, h	100.8	73.1	80.6, 82.6^c	77.5	62.7	59.5	-	-	67.6^d	23.2	10.3	20.6	-	-	170	-	169	-
7a	103.2	73.7	80.5	75.5	61.0	-	-	-	-	-	-	21.0^b	-	-	170.1	-	170.0	-4.5, -3.3
8b	100.6	C5:72.5 C2:73.7	72.7	76.2	62.6	-	-	-	-	-	-	20.8^b	27.7, 26.1	9.1	173.8	173.3	172.9	-4.1, -3.3

5a-d: 2,6-*O*-acetyl-3-*O*-Et/Pr cellulose; **5e**, **f**: 2,6-*O*-acetyl-3-*O*-Me/Et cellulose; **5g**, **h**: 2,6-*O*-acetyl-3-*O*-Me/Pr cellulose; **7a**: product after desilylation of 2,6-*O*-TBDMS-3-*O*-acetyl cellulose; **8b**: product after desilylation and then propanoylation of 2,6-*O*-TBDMS-3-*O*-acetyl cellulose; CH$_3$^{Ac}: CH$_3$ of acetyl; CH$_3$^{Pro}, CH$_2$^{Pro}: CH$_3$ and CH$_2$ of propanoyl.

a. not assigned in detail; b. very weak ; c. one peak 80.6 for **5g**, two peaks 80.6 (C3-Pr) and 82.6 (C3-Me) for **5h**; d. not observed in the spectrum for **5h**

5. Summary

The synthesis of 3-*O*-alkyl cellulose bearing two different ether groups was accomplished by simultaneous alkylation of 2,6-di-*O*-thexyldimethylsilyl (TDMS) cellulose in the presence of tetrabutylammonium iodide (TBAI) as a phase transfer catalyst. Every combination of two reagents out of methyl iodide (MeI), ethyl iodide (EtI) and *n*-propyl iodide (PrI) were used as alkylation reagents for the synthesis of 3-*O*-methyl/ethyl, 3-*O*-ethyl/propyl and 3-*O*-methyl/propyl cellulose. The degree of substitution (DS) of each moiety could be controlled by the molar ratio of alkylation reagents to modified anhydroglucose units; a higher molar ratio of alkyl iodide leads to a higher DS of the corresponding alkyl ether. Alkyl moieties with shorter chain lengths show a higher reactivity: Me>Et>Pr. The structure of 2,6-di-*O*-acetyl-3-mono-*O*-alkyl cellulose was characterized by Fourier transform infrared (FT-IR) and nuclear magnetic resonance (NMR) spectroscopies.

Measurements of temperature dependent turbidity of the aqueous solutions of 3-*O*-alkyl cellulose bearing two different ether groups indicated that the lower critical solution temperature (LCST) depends on the DS ratio of the alkyl moieties. The results obtained by temperature dependent turbidity photometry can be confirmed by differential scanning calorimetry (DSC). The DSC measurements also revealed the reversibility of the inter- and intrachain hydrophobic interaction. The hysteresis of the exothermic peaks during the cooling process became noticeable when the propyl content increases.

The polymer degradation was studied by comparing the number average degree of polymerization (DP_n) values of each intermediate within the three-step synthesis that may cause a decrease of DP_n beginning from cellulose via 2,6-di-*O*-TDMS cellulose to 3-*O*-alkyl cellulose. However, it was also observed that the DP_n of 3-*O*-alkyl celluloses which were calculated from size exclusion chromatography (SEC) measurments were significantly influenced by the alkylation conditions. From the results of SEC measurements in solution of

dimethylacetamide (DMA)/LiCl (column temperature 40 °C), 3-O-alkyl cellulose prepared by alkylation at 50 °C without any catalyst has a DP_n value that is higher than the DP (117) of the microcrystalline cellulose used as starting material, and products synthesized by alkylation at room temperature in presence of a phase transfer catalyst possessed comparably lower DP_n values. The DP_n calculation from the results of SEC measurements in water solution became impossible because the molecules already began to aggregate prior to chromatography.

Small deformation dynamic viscoelastic measurements of polymer aqueous solution revealed a different behaviour depending on the applied alkylation conditions. The aqueous solution of 3-O-alkyl celluloses synthesized under different alkylation conditions showed one magnitude difference in G' (storage modulus) and G" (loss modulus).

The dynamic light scattering (DLS) measurements in DMA/LiCl also implies the difference of particle size distribution at 40 °C (column temperature of SEC in DMA/LiCl). The product synthesized by alkylation at 50 °C without catalyst shows a slightly larger particle size distribution than the product prepared from alkylation at room temperature with catalyst. However, the DLS measurements in water revealed that the particle size distributions of the aqueous solution of these two samples are comparable at various temperatures.

Regarding the distribution of substituents along the cellulose backbone, these two 3-O-alkyl celluloses synthesized under different alkylation conditions were investigated by mass spectroscopy. Firstly, the complete hydrolysis product of cellulose derivative was analysed by gas chromatography coupled with mass spectroscopy (GC-MS), and randomly substituent distribution was calculated for certain monomer composition, which serves as a reference structure. Then the oligomeric mixture with different monomer compositions obtained by partially hydrolysed polymers was studied by electrospray ionization ion trap mass spectrometry (ESI-IT-MS). Compared to the theoretical calculation values, experimental results of ESI-IT-MS showed no significant differences. That means different alkylation

conditions give statistical distributions of different ethers groups along the polymer backbone.

Moreover, further research into the properties of 3-*O*-alkyl cellulose ethers should be continued. For instance, the aqueous solutions of 3-mono-*O*-propyl cellulose and 3-*O*-ethyl/propyl cellulose with high DS_{Pr} formed strong gels above the LCST. Further studies on the rheological properties appear to be very promising for exploiting their potential application in the pharmaceutical field.

Another topic of this presented work is the synthesis of novel 3-*O* cellulose esters, which have not previously been investigated. The key step of the preparation of 3-*O*-acetyl cellulose is the desilylation under mild conditions. Two types of catalysts were studied: fluorides including hydrogen fluoride/pyridine (HF), cesium fluoride (CsF), 1-Chloromethyl-4-fluoro-1,4-diazoniabicyclo[2.2.2]octane bis(tetrafluoroborate) (Selecflour) and tris(4-bromophenyl)aminium hexachloroantimonate (TBPA$^+$• SbCl$_6^-$). However, both of these catalysts are proved to be inefficient: either a high extent of polymer degradation (desilylation by fluorides) or an incomplete desilylation (desilylation by TBPA$^+$• SbCl$_6^-$) was achieved.

The main problem is the poor solubility of 3-mono-*O*-acetyl-2,6-di-*O*-TBDMS cellulose, which restricts the selection of the catalyst for desilylation. Thus, other solvents or solvent systems as well as alternative catalysts should be considered.

In general, regioselective derivatives of cellulose are ideal to understand the structure property relationships of functionalized polysaccharides depending on different functionalization patterns in detail.

Zusammenfassung

3-*O*-Alkylcellulosen mit zwei unterschiedlichen Alkylgruppen wurden durch simultane Umsetzung von 2,6-di-*O*-Thexyldimethylsilyl(TDMS)cellulose mit Alkyliodiden in Gegenwart von Natriumhydrid sowie nachfolgende Abspaltung der TDMS-Gruppen synthetisiert. Die Struktur der peracetylierten Produkte wurde mittels Fouriertransformations-Infrarotspektroskopie (FT-IR) und kernmagnetischer Resonanzspektroskopie (NMR) untersucht. Der durchschnittliche Substitutionsgrad (DS) beider Ethersubstituenten konnte durch das molare Verhältnis der Alkylierungsmittel zur modifizierten Anhydroglucoseeinheit gesteuert werden: ein größeres Molverhältnis führt zu einem höheren DS.

Messungen der temperaturabhängigen Trübung der wässrigen Polymerlösung ergaben, dass die untere kritische Lösungstemperatur (LCST) durch das Verhältnis der unterschiedlichen Ethersubstituenten gesteuert werden kann. Dieses Ergebnis konnte mittels differenzkalorimetrischer Methoden (DSC) bestätigt werden.

Der Polymerabbau während dieser Mehrstufensynthese über 2,6-di-*O*-TDMS-Cellulose zur 3-*O*-Alkylcellulose wurde durch den Vergleich der zahlenmittleren Polymerisationsgrade (DP_n) der Zwischenverbindungen untersucht. Darüber hinaus wurde gezeigt, dass der durch gelpermeationschromatographische Messungen in *N,N*-Dimethylacetamid/LiCl ermittelte DP_n der 3-*O*-Alkylcellulosen signifikant von den Reaktionsbedingungen der Alkylierung abhängt. Die DP_n-Werte einer bei 50°C ohne Katalysator und einer bei Raumtemperatur in Gegenwart eines Phasentransferkatalysators veretherten Probe unterscheiden sich um eine Größenordnung. Rheologische Messungen bestätigten ebenfalls das unterschiedliche Verhalten der Proben. Viskoelastische Messungen der wässrigen Polymerlösungen bei unterschiedlichen Temperaturen zeigten, dass sowohl G' (Speichermodul) als auch G'' (Verlustmodul) beider Proben sich um eine Größenordnung unterscheiden. Anscheinend

ist der Aufbau beider Polymere hinsichtlich der Sequenz entlang der Polymerkette unterschiedlich. Die Zusammensetzung der modifizierten Proben wurde daher mittels Gaschromatographie/Massenspektrometrie untersucht. Allerdings ergaben sich hieraus keine Unterschiede zwischen den Zusammensetzungen beider Proben. D.h., der Vergleich experimenteller Ergebnisse mit theoretischen Berechnungen lässt auf eine statistische Verteilung der unterschiedlich 3-*O*-alkylierten Wiederholungseinheiten schließen.

Die Synthese von 3-*O*-Acetylcellulose wurde mit dem Ziel untersucht, geeignete Desilylierungsbedingungen zu finden. Allerdings konnten keine in der niedermolekularen organischen Chemie etablierten Reaktionsbedingungen auf Cellulosederivate übertragen werden.

6. References

[1] K. Lindhorst, *Essentials of Carbonhydrate Chemistry and Biochemistry*, 3rd edition, **2007**, Wiley

[2] p 114-124 and 124-136, Th. Heinze, T. Liebert, *"Celluloses and Polyoses/Hemicelluloses"*, in K. Matyjaszewski and M. Möller (eds.), *Polymer Science: A Comprehensive Reference*, Vol 10, pp. 83-152, **2012**, Elsevier BV, Amsterdam

[3] *Chemical Functionalization of Cellulose in Polysaccharides: Structural Diversity and Functional Versatility*, S. Dumitriu (ed.), **2004**, Marcel Dekker, New York, Basel, Hong-Kong

[4] S. C. Fox, B. Li, D. Xu, K. J. Edgar, *Biomacromolecules* **2011**, *12*, 1956

[5] D. Klemm, B. Heublein, H.-P. Fink, A. Bohn, *Angew. Chem. Int. Ed.*, **2005**, *44*, 3358

[6] p 97-98, Th. Heinze, T. Liebert, *"Celluloses and Polyoses/Hemicelluloses"*, in K. Matyjaszewski and M. Möller (eds.), *Polymer Science: A Comprehensive Reference*, Vol 10, pp. 83-152, **2012**, Elsevier BV, Amsterdam

[7] C. F. Schönbein, *Ber. Naturforsch. Ges.*, Basel, **1847**, *7*, 27

[8] p 419 – 459, K. Balser, L. Hoppe, T. Eichler, M. Wendel, A.-J. Astheimer, *Ullmann's Encyclopedia of Industrial Chemistry, Vol. A5*, W. Gerhartz, Y. S. Yamamoto, F. T. Campbell, R. Pfefferkorn, J. F. Rounsaville (eds.), **1986**, VCH, Weinheim

[9] L. J. Tanghe, R. Brewer, *J. Anal. Chem.*, **1955**, *40*, 350

[10] p170, J. March, *Advanced Organic Chemistry: Reactions, Mechanisms, and Structure*, **1992**, Wiley Interscience, New York

[11] p 115, Th. Heinze, T. Liebert, *Celluloses and Polyoses/Hemicelluloses*, in K. Matyjaszewski and M. Möller (eds.), *Polymer Science: A Comprehensive Reference*, Vol 10, pp. 83-152, **2012**, Elsevier BV, Amsterdam

[12] p 200, R. T. Bogan, R. J. Brewer, in *Encyclopedia of Polymer Science and engineering*,

H. F. Mark, N. M. Bikales, C. G. Overberger *et al.* (eds.), John Wiley & sons, **1985**, New York

[13] T. Morooka, M. Norimoto, T. Yamada, N. Shiraishi, *J. Appl. Polym. Sci.*, **1984**, *29*, 3981

[14] p 38-60, K. J. Edgar, T. J. Pecorini, W. G. Glasser, *Cellulose Derivatives:Modification, Characterization and Nanostructures*, Th. Heinze, W. G. Glasser (eds.), ACS Syposium Series, *688*, **1998**

[15] J. W. Brewstern C. J. Ciotti, *J. Am. Chem. Soc.*, **1955**, *77*, 6214

[16] J. E. Sealy, C. E. Frazier, G. Samaranayaske, W. G. Glasser, *J. Polym. Sci. Part B Polym. Phys.*, **2000**, *38*, 486

[17] H. A. Staab, *Angew. Chem.*, **1962**, *74*, 407

[18] G. Höfler, W. Steglich, H. Vorbrüggen, *Angew. Chem.*, **1978**, *90*, 602

[19] K. J. Edgar, C. M. Buchanan, J. S. Debenham *et al.*, *Prog. Polym. Sci.*, **2001**, *26*, 1605

[20] W. Suida, *Monatsh. Chem.*, **1905**, *26*, 413

[21] D. Traill, *J. Soc. Chem. Ind. Trans.*, **1934**, LIII, 338T;

[22] R. E. Montona, *Pap. Trade J. (Tappi Section)*, **1936**, 35

[23] p 208, D. Klemm, B. Philipp, T. Heinze, U. Heinze, W. Wagenknecht, *Comprehensive Cellulose Chemistry; Volume 2: Functionalization of Cellulose*, **1998**, WILEY-VCH Verlag GmbH

[24] p. 125-126, Th. Heinze, T. Liebert, "*Celluloses and Polyoses/Hemicelluloses*", in K. Matyjaszewski and M. Möller (eds.), *Polymer Science: A Comprehensive Reference*, Vol 10, pp. 83-152, **2012**, Amsterdam: Elsevier BV

[25] D. A. Sitch, *J. Text. Inst. Trans.*, **1953**, *44*, T407

[26] H. Ke, J. Zhou, L. Zhang, *Polym. Bull.*, **2006**, *56*, 349

[27] P. Mischnick, *J. Carbohydr. Chem.*, **1991**, *10*, 711

[28] U. Erler, P. Mischnick, A. Stein, D. Klemm, *Polym. Bull.*, **1992**, *29*, 349

[29] D. Klemm, A. Stein, *J. Macromol. Sci. Pure Appl. Chem.*, **1995**, *A32,* 899

[30] p 128, Th. Heinze, T. Liebert, *"Celluloses and Polyoses/Hemicelluloses"*, in K. Matyjaszewski and M. Möller (eds.), *Polymer Science: A Comprehensive Reference*, Vol 10, pp. 83-152, **2012**, Amsterdam: Elsevier BV

[31] E. Heymann, *Trans. Faraday Soc.*, **1935**, *31*, 846

[32] p 220, D. Klemm, B. Philipp, T. Heinze, U. Heinze, W. Wagenknecht, *Comprehensive Cellulose Chemistry; Volume 2: Functionalization of Cellulose*, **1998** WILEY-VCH Verlag GmbH

[33] P. Basque, A. de Gunzbourg, P. Rondeau, A. M. Ritcey, *Langmuir*, **1996**, *12*, 5614

[34] C. L., McCormick, P. A. Callais, B. H. Jr. Huchinson, *Macromolecules*, **1985**, *18*, 2394

[35] Th. Heinze, R. Dicke, A. Koschella, A. H. Kull, E. A. Klohr, W. Koch, *Macromol. Chem. Phys.*, **2000**, *201*, 627

[36] J. Cai, L. Zhang, *Macromol. Biosci.*, **2005**, *5*, 539

[37] R. P. Swatloski, S. K. Spear, J. D. Holbrey, R. D. Rogers, *J. Am. Chem. Soc.* **2002**, *124*, 4974

[38] A. Koschella, D. Fenn, Th. Heinze, *Polym. Bull.*, **2006**, *57*, 33

[39] M. Karakawa, Y. Mikawa, H. Kamitakahara, F. Nakatsubo, *J. Polym. Sci., Part A: Polym. Chem.*, **2002**, *40*, 4167

[40] C. Deus, H. Friebolin, E. Siefert, *Makromol. Chem.*, **1991**, *192*, 75

[41] C. L. McCormic, P. A. Callais, *Polymer*, **1987**, *28*, 2317

[42] K. Rahn, M. Diamantoglou, D. Klemm *et al.*, *Angew. Makromol. Chem.*, **1996**, *238*, 143

[43] A. Koschella, T. Leermann, M. Brackhagen, Th. Heinze, *J. Appl. Polym. Sci.*, **2006**, *100*, 2142

[44] Helfrich, B., Koester, H., *Ber. Dtsch. Chem. Ges.*, **1924**, *57*, 587

[45] p. 327, J. W. Green, *"Triphenylmethyl ethers"*, in: *Methods of Carbohydrate Chemistry*, vol. 111, chap. 57, R. L.Whistler, J. W. Green, J. N. BeMiller, M. L. Wolfrom(eds.),

Academic Press, **1963**, New York, London

[46] M. Yalpani, *Tetrahedron*, **1985**, *41*, 2957

[47] T. R. Dawsey, C. L. McCormick, *J. Macromol. Sci. Rev. Macromol. Chem. Phys.*, **1990**, *C30*, 405

[48] T. Kondo, D. G. Gray, *Carbohydr. Res.*, **1991**, *220*, 173

[49] J. A. Camacho Gomez, U. W. Erler, D. Klemm, *Macromol. Chem. Phys.*, **1996**, *197*, 953

[50] D. Klemm, Th. Heinze, B. Philipp, W. Wagenknecht, *Acta. Polym.*, **1997**, *48*, 277

[51] A. Koschella, D. Klemm, *Macromol. Symp.*, **1997**, *120*, 115

[52] D. Klemm, M. Schnabelrauch, A. Stein, M. Niemann, H. Ritter, *Makromol. Chem.*, **1990**, *191*, 2985

[53] H. Kern, S. Choi, G. Wenz, J. Heinrich, L. Ehrhardt, P. Mischnick, P. Garidel, A. Blume, *Carbohydr. Res.*, **2000**, *326*, 67

[54] A. Koschella, T. Heinze, D. Klemm, *Macromol. Biosci.*, **2001**, *1*, 49

[55] J. Ugelstad, T. Ellingsen, A. Berge, *Acta. Chem. Scand.*, **1966**, *20*, 1593

[56] C. M. Starks, *J. Am. Chem. Soc.*, **1971**, *93*, 195

[57] A. W. Herriott, D. Picker, *J. Am. Chem. Soc.*, **1975**, *97*, 2345

[58] B. B.-A. Bar-Nir, J. F. Kadla, *Carbohydr. Polym.*, **2009**, *76*, 60

[59] Th. Heinze, A. Pfeifer, K. Petzold, *BioResources*, **2008**, *3*, 79

[60] T. Kondo, *Carbohydr. Res.*, **1993**, *238*, 231

[61] H. Kamitakahara, A. Koschella, Y. Mikawa, F. Nakatsubo, Th. Heinze, D. Klemm, *Macromol. Biosci.*, **2008**, *8*, 690

[62] A. Nakagawa, C. Ishizu, V. Sarbova, A. Koschella, T. Takano, Th. Heinze, H. Kamitakahara, *Biomacromolecules.*, **2012**, *13*, 2760

[63] A. Koschella, D. Fenn, N. Illy, Th. Heinze, *Macromol. Symp.*, **2006**, *244*, 59

[64] N. Illy, *Diploma thesis*, FSU Jena **2006**

[65] Th. Heinze, A. Pfeifer, V. Sarbova, A. Koschella, *Polym. Bull.*, **2011**, *66*, 1219

[66] K. Petzold, D. Klemm, B. Heublein, W. Burchard, G. Savin, *Cellulose*, **2004**, *11*, 177

[67] A. Haque, E. R. Morris, *Carbohydr. Polym.*, **1993**, *22*, 161

[68] N. Sarkar, *Carbohydr. Polym.*, **1995**, *26*, 195

[69] M. Hirrien, J. Desbrières, M. Rinaudo, *Carbohydr. Polym.*, **1996**, *31*, 243

[70] p 332-348, J. Desbrières, M. Hirrien, M. Rinaudo, *Cellulose Derivatives:Modification, Characterization and Nanostructures*, ACS Syposium Series, *688*, **1998**, Th. Heinze, W. G. Glasser (eds.)

[71] K. Nishinari, K. E. Hofmann, H. Moritaka, K. Kohyama, *Macromol. Chem. Phys.*, **1997**, *198*, 1217

[72] S. Sun, T. J. Foster, W. MacNaughtan, J. R. Mitchell, D. Fenn, A. Koschella, Th. Heinze, *J. Polym. Sci., Part B: Polym. Phys.*, **2009**, *47*, 1743

[73] N. Sarkar, *J. App. Poly. Sci.*, **1979**, *24*, 1073

[74] A. Haque, R. K. Richardson, E. R. Morris, M. J. Gidley, D. C. Caswell, *Carbohydr. Polym.*, **1993**, *22*, 175

[75] L. Li, P. M. Thangamathesvaran, C. Y. Yue, K. C. Tam, X. Hu, Y. C. Lam, *Langmuir*, **2001**, *17*, 8062

[76] L. Li, *Macromolecules*, **2002**, *35*, 5990

[77] T. Funami, Y. Kataoka, M. Hiroe, I. Asai, R. Takahashi, K. Nishinari, *Food Hydrocolloid.*, **2007**, *21*, 46

[78] K. Kobayashi, C.-I. Huang, T. P. Lodge, *Macromolecules*, **1999**, *32*, 7070

[79] R. N. Ibbett, K. Philp, D. M. Price, *Polymer*, **1993**, *33*, 4087

[80] J. Desbrières, M. Hirrien, S. B. Ross-Murphy, *Polymer*, **2000**, *41*, 2451

[81] T. Kato, M. Yokoyama, A. Takahashi, *Coll. & Polym. Sci.*, **1978**, *256*, 15

[82] T. Iwata, J.-I. Azuma, K. Okamura, *Carbohydr. Res.*, **1992**, *224*, 277

[83] D. Xu, K. J. Edgar, *Biomacromolecules*, **2012**, *13*, 299

[84] D. Xu, K. Voiges, T. Elder, P. Mischnick, K. J. Edgar, *Biomacromolecules*, **2012**, *13*, 2195

[85] Y. Yang, J. Cui, L. Zhu, Y. Sun, Y. Wu, *Synlett.*, **2006**, *8*, 1260

[86] J. S. Yadav, B. V. Subba Reddy, C. Madan, *New J. Chem.*, **2000**, *24*, 853

[87] Z. Jiang, Y. Wang, *Tetrahedron Lett.*, **2003**, *44*, 3859

[88] J. Li, D. Menche, *Synthesis*, **2009**, *11*, 1904

[89] K. C. Nicolaou, S. P. Setitz, M. R. Pavia, N. A. Petasis, *J. Org. Chem.*, **1979**, *44*, 4011

[90] C. M. Hayward, D. Yohannes, S.J. Danishefsky, *J. Am. Chem. Soc.*, **1993**, *115*, 9345

[91] A. Padwa1, G. Haffmanns, M. Tomas, *Tetrahedr. Lett.*, **1983**, *24*, 4303

[92] S. Tasadaque A. Shah, S. Singh, P. J. Guiry, *J. Org. Chem.* **2009**, *74*, 2179

[93] p 10, W. M. Groenewoud, *Characterisation of Polymers by Thermal Analysis*, **2001**, Elsevier, Netherlands

[94] p 271, E. Schröder, G. Müller, K.-F. Arndt, *Polymer Characterization*, **1989**, Akademie-Verlag Berlin

[95] p 118-130, P. Mischnick, *Cellulose Derivatives:Modification, Characterization and Nanostructures*, ACS Syposium Series, *688*, **1998**, Th. Heinze, W. G. Glasser (eds.)

[96] J. Cuers, I. Unterieser, W. Burchard, R. Adden, M. Rinken, P. Mischnick, *Carbohydr. Res.*, **2012**, *348*, 55

[97] Th. Heinze, T. Liebert, A. Koschella, *Esterification of Polysaccharides*, **2006** Springer Verlag Heidelberg

[98] K. Schumann, A. Pfeifer, Th. Heinze, *Macromol. Symp.*, **2009**, *280*, 86

[99] E. Rohleder, Th. Heinze, *Macromol. Symp.*, **2010**, *294*, 107

[100] p 201-216, B. Saake, St. Horner, J. Puls, *Cellulose Derivatives:Modification, Characterization and Nanostructures*, ACS Syposium Series, *688*, **1998**, Th. Heinze, W. G.

Glasser (eds.)

[101] Th. Heinze, *Macromol. Chem. Phys.*, **1998**, *199*, 2341

[102] p 61-72, T. Liebert, Th. Heinze, *Cellulose Derivatives:Modification, Characterization and Nanostructures*, ACS Syposium Series, *688*, **1998**, Th. Heinze, W. G. Glasser (eds.)

[103] T. Liebert, D. Klemm, Th. Heinze, *J. Macromol. Sci. Pure Appl. Chem.*, **1996**, *A33*, 613

[104] E. R. Morris, D. A. Rees, G. Robinson, *J. Molecul. Bio.*, **1980**, *138*, 349

[105] C. Rochas, M. Rinaudo, *Biopolym.,* **1984**, *23*, 735

[106] P. I. Privalov, S. J. Gill, *Pure Appl. Chem.*, **1989**, *61*, 1097

[107] T. Kondo, A. Koschella, B. Heublein, D. Klemm, T. Heinze, *Carbohydr. Res.*, **2008**, *343*, 2600

[108] M. C. Williams, *AIChE Journal,* **1975**, *21*, 1

[109] B. V. K. J. Schmidt, T. Rudolph, M. Hetzer, H. Ritter, F. H. Schacher, C. Barner-Kowollik, *Polym. Chem.*, **2012**, *3*, 3139

[110] H.-G. Elias, *Macromolecules, Vol 3: Physical Structures and Properties*, Weinheim, Wiley-VCH, **2008**

[111] B. Vollmert, *Grundriss der Makromolekularen Chemie*, **1962**, Springer-Verlag

[112] R. Pamies, J. G. Hernádez Chifre, M. C. López Matínez, J. G. Torre, *Colloid. Polym. Sci.*, **2008**, *286*, 1223

[113] I. Unterieser, P. Mischnick, *Carbohydr. Res.*, **2011**, *346*, 68

[114] I. Unterieser, J. Cuers, K. Voiges, J. Enebro, P. Mischnick, *Rapid. Commun. Mass Spectrom.*, **2011**, *25*, 2201

[115] A. Nakagawa, F. Steiniger, W. Richter, A. Koschella, Th. Heinze, H. Kamitakahara, *Langmuir*, **2012**, *28*, 12609

[116] J. E. Sealey, G. Samaranayake, J. G. Todd, W. G. Glasser, *J. Polym. Sci. Part B: Polym. Phys.*, **1996**, *34*, 1613

[117] Y. Xu, S. Tang, J. Han, X. She, X. Pan, *Tetrahedr. Lett.* **2008**, *49*, 3634

[118] A. Hosomi, H. Iguchi, J.-I. Sasaki, H. Sakurai, *Tetrahedr. Lett.*, **1982**, *23*, 551

1) ^{1}H and ^{13}C NMR spectra of 2,6-di-O-acetyl-3-mono-O-ethyl/propyl cellulose with DS$_{Et}$/DS$_{Pr}$=0.95/0.15 **5a**
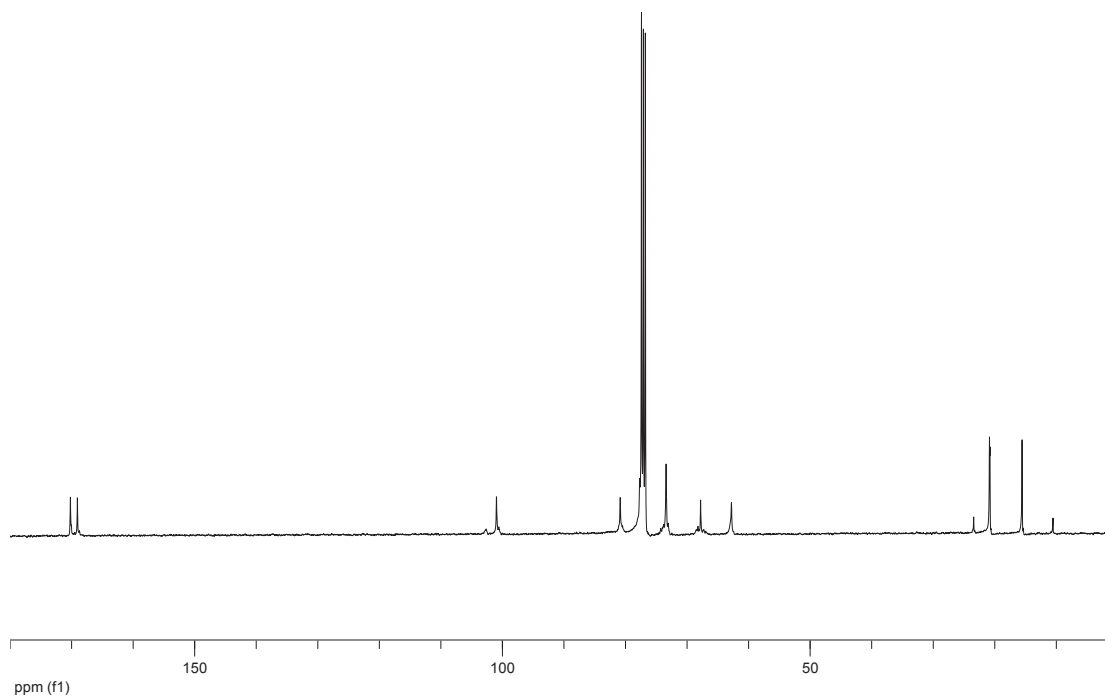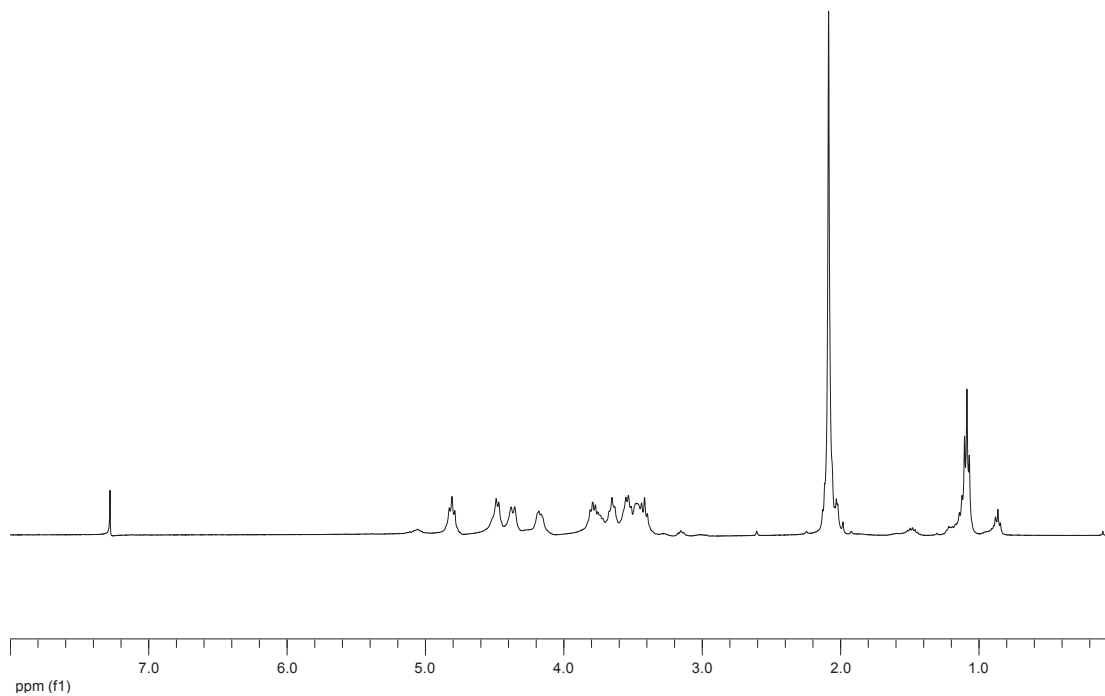
2) ^{1}H and ^{13}C NMR spectra of 2,6-di-*O*-acetyl-3-mono-*O*-ethyl/propyl cellulose with DS$_{Et}$/DS$_{Pr}$=0.77/0.27 **5b**
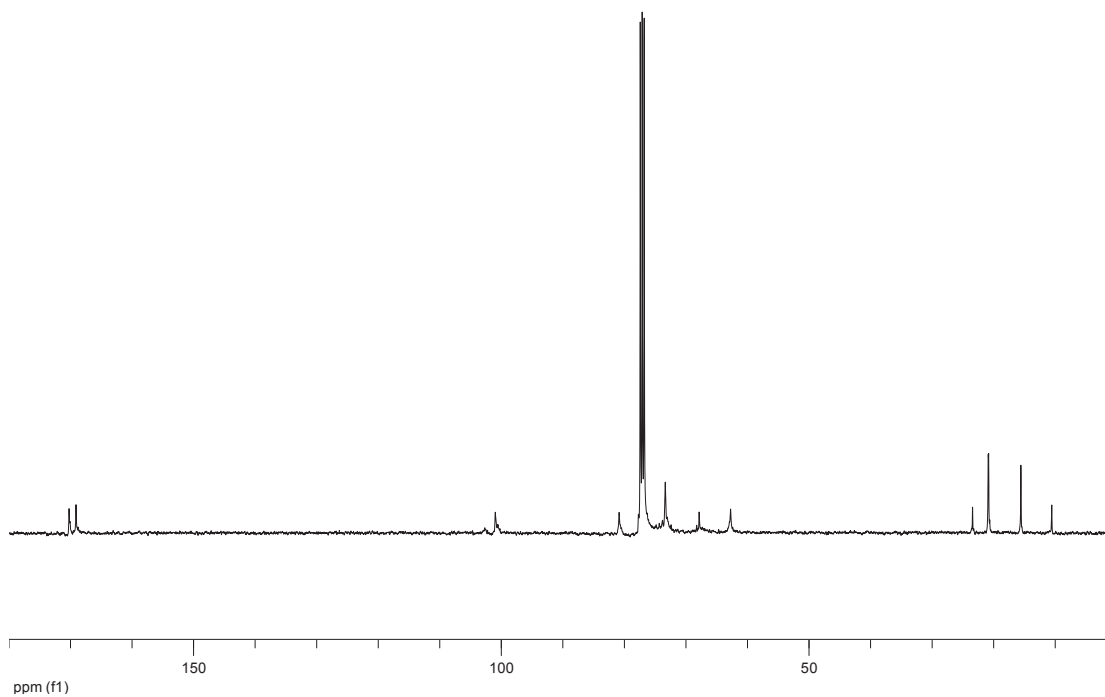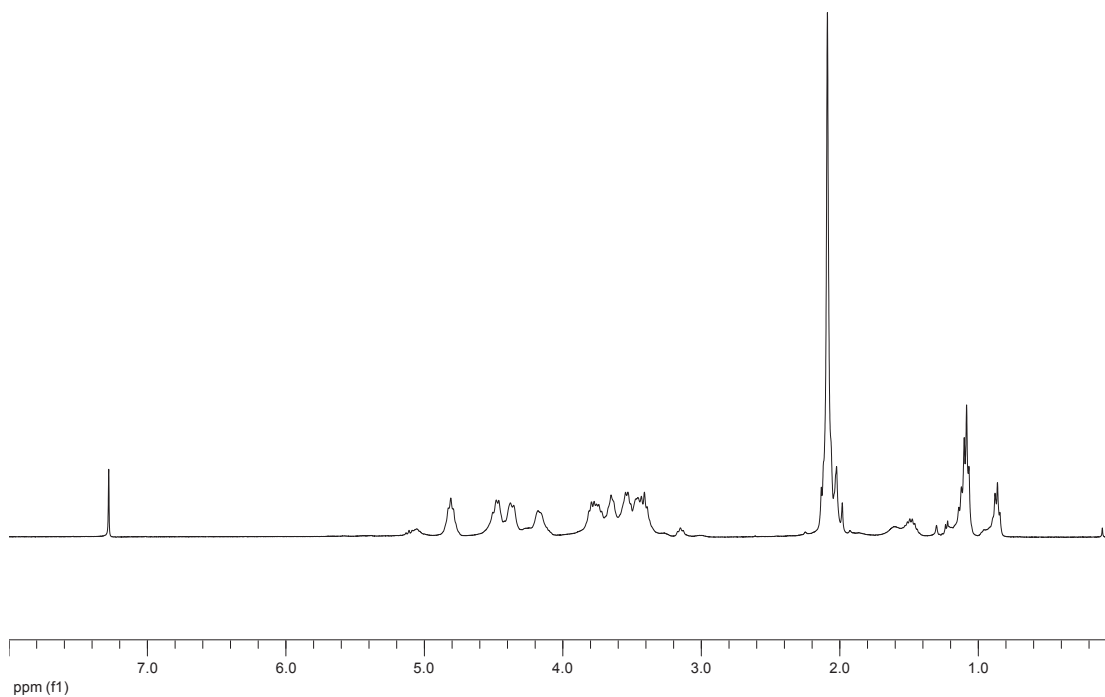
3) ^{1}H and ^{13}C NMR spectra of 2,6-di-*O*-acetyl-3-mono-*O*-ethyl/propyl cellulose with DS$_{Et}$/DS$_{Pr}$=0.27/0.56 **5d**

3) ^{1}H and ^{13}C NMR spectra of 2,6-di-*O*-acetyl-3-mono-*O*-ethyl/propyl cellulose with DS$_{Et}$/DS$_{Pr}$=0.27/0.56 **5d**
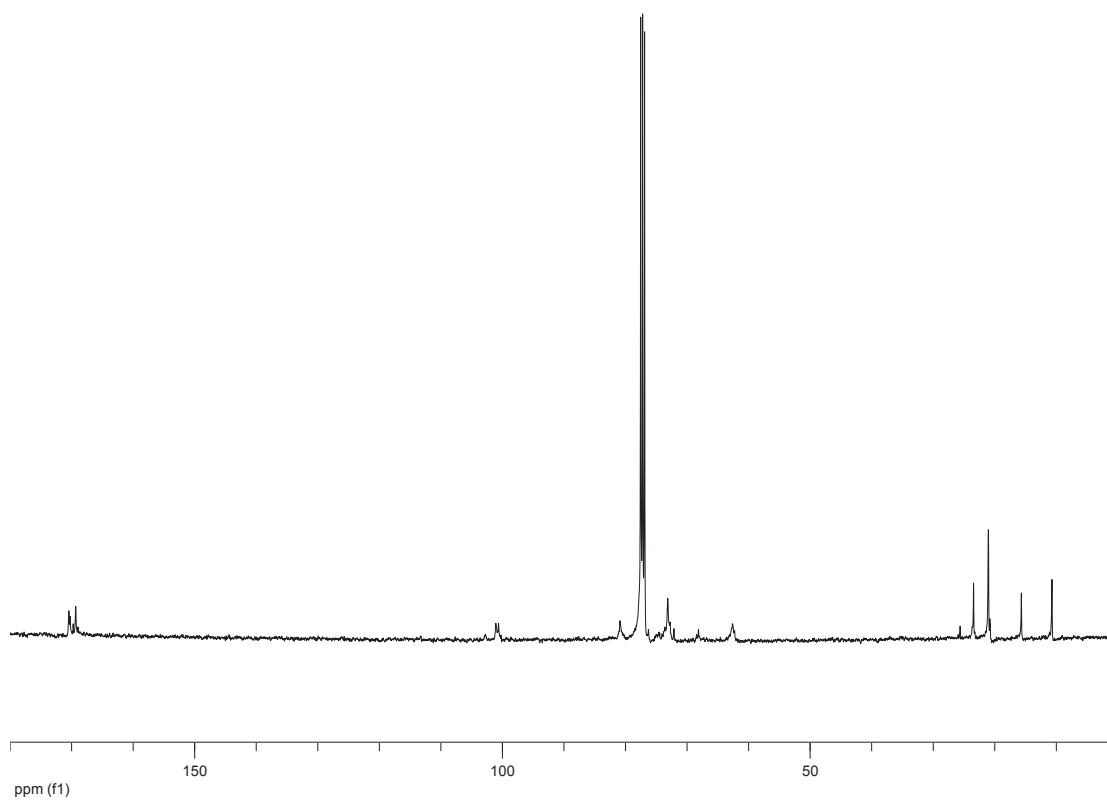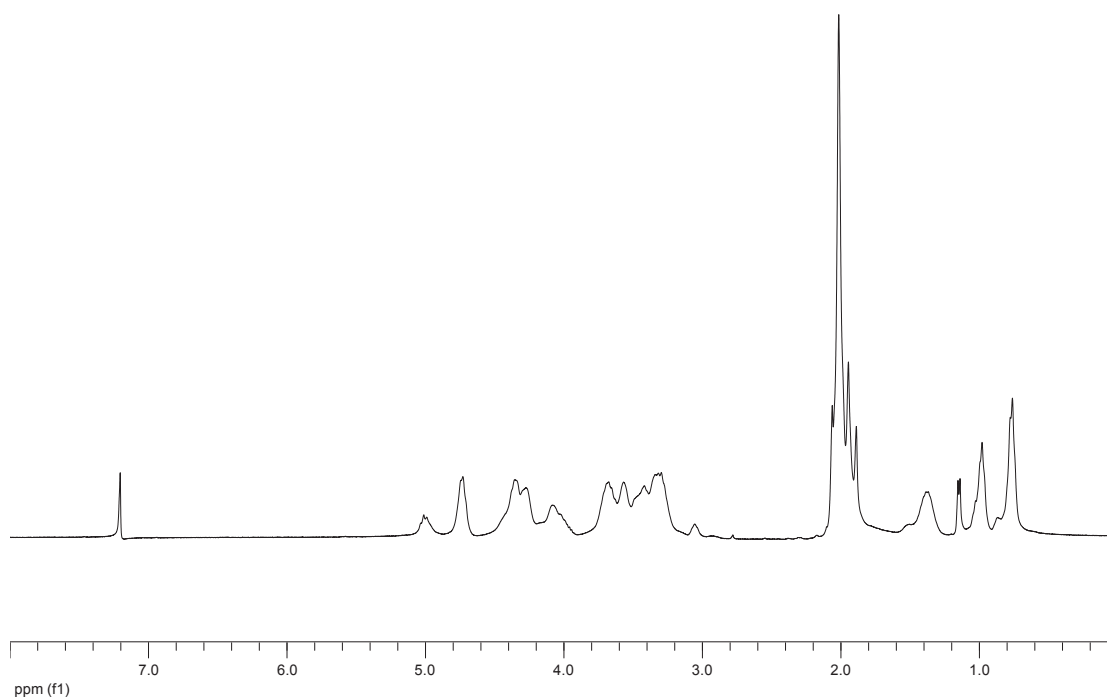
4) ^{1}H and ^{13}C NMR spectra of 2,6-di-*O*-acetyl-3-mono-*O*-methyl/ethyl cellulose with DS$_{Me}$/DS$_{Et}$=0.99/0.08 **5e**
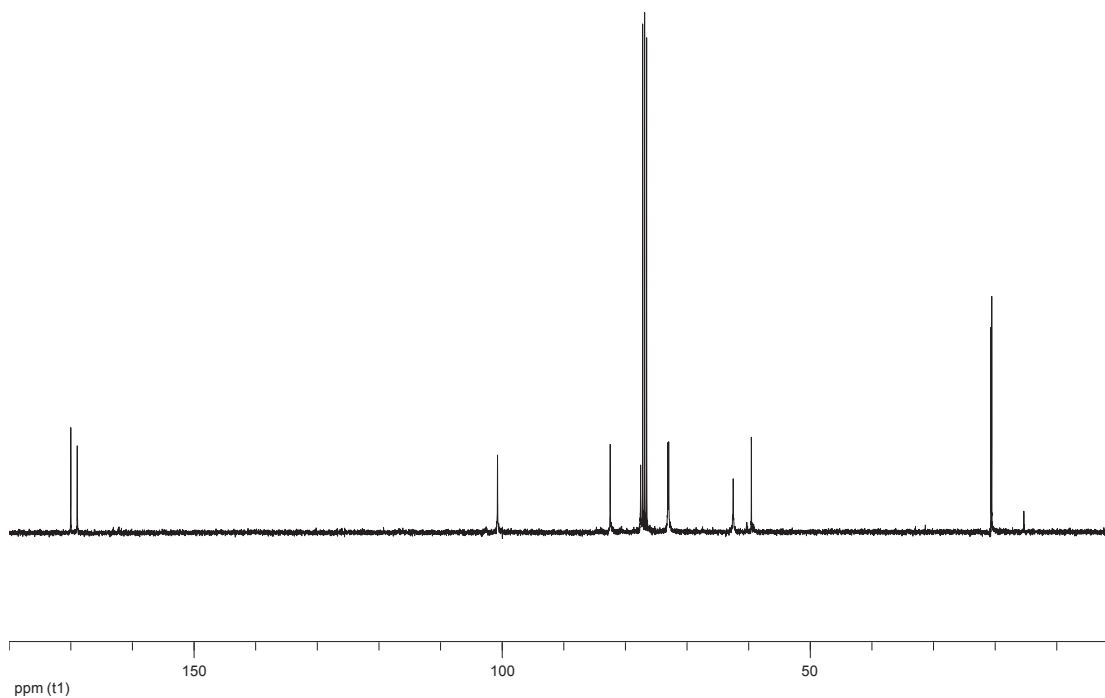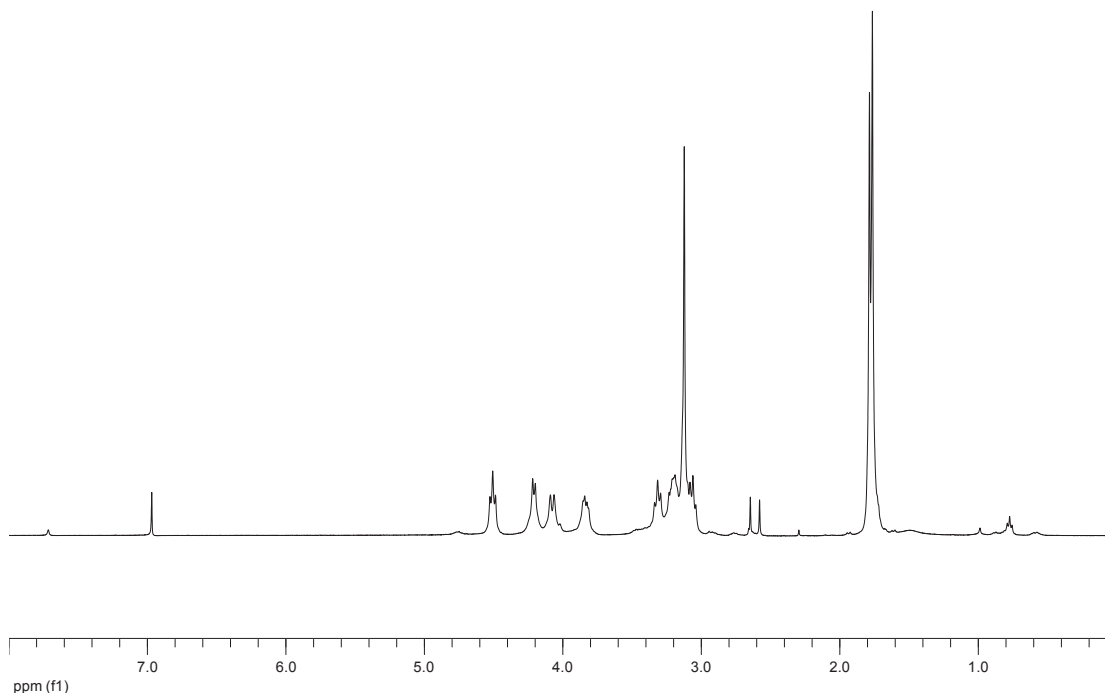
5) ^{1}H and ^{13}C NMR spectra of 2,6-di-*O*-acetyl-3-mono-*O*-methyl/ethyl cellulose with DS$_{Me}$/DS$_{Et}$=0.19/0.91 **5f**
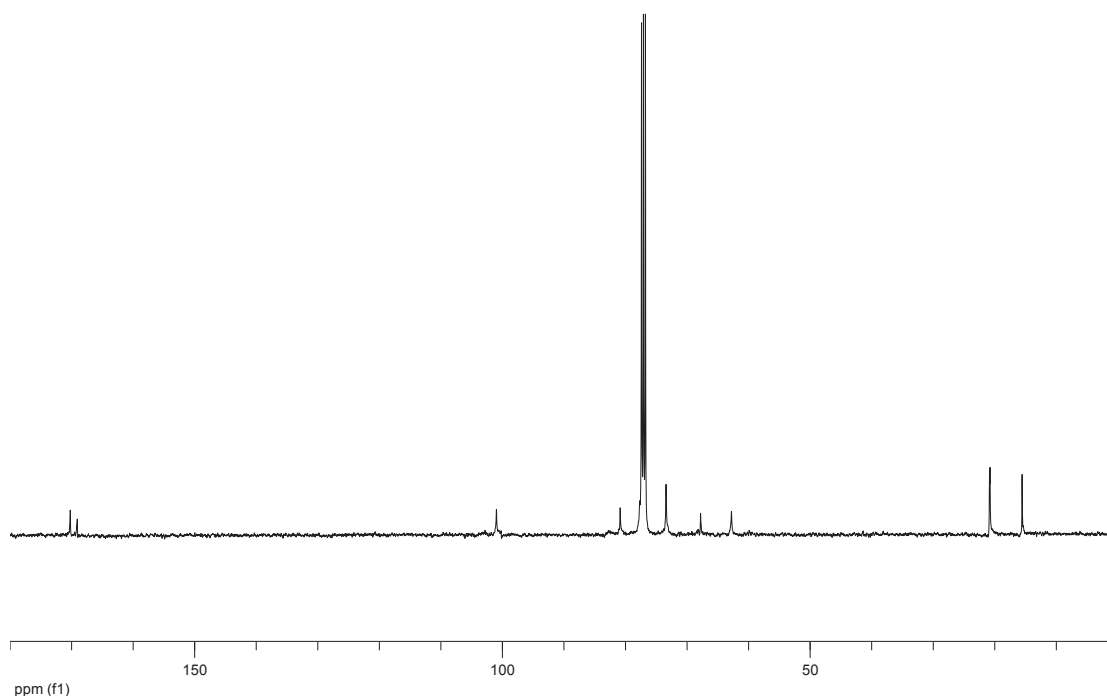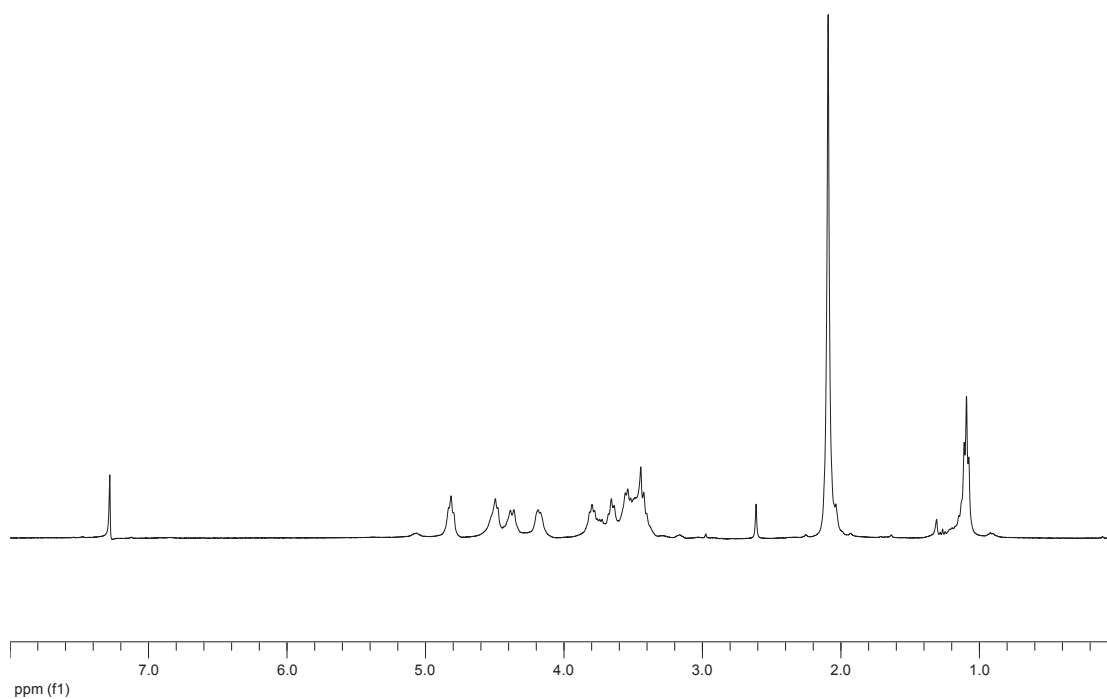
6) ^{1}H and ^{13}C NMR spectra of 2,6-di-*O*-acetyl-3-mono-*O*-methyl/propyl cellulose with DS$_{Me}$/DS$_{Pr}$=0.97/0.12 **5g**
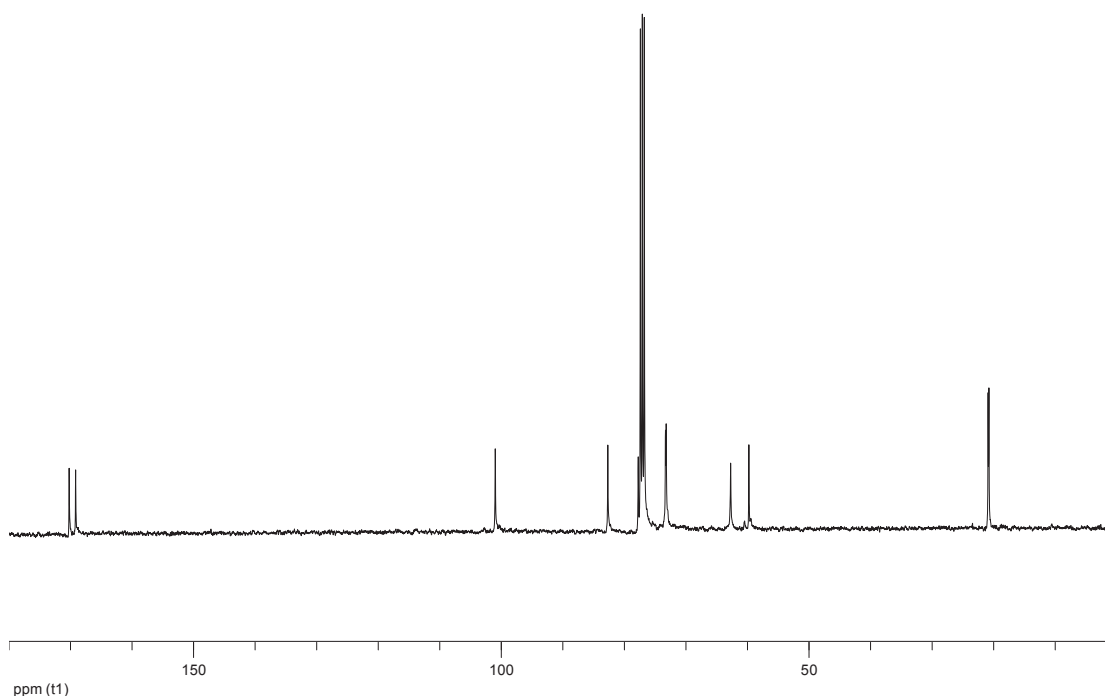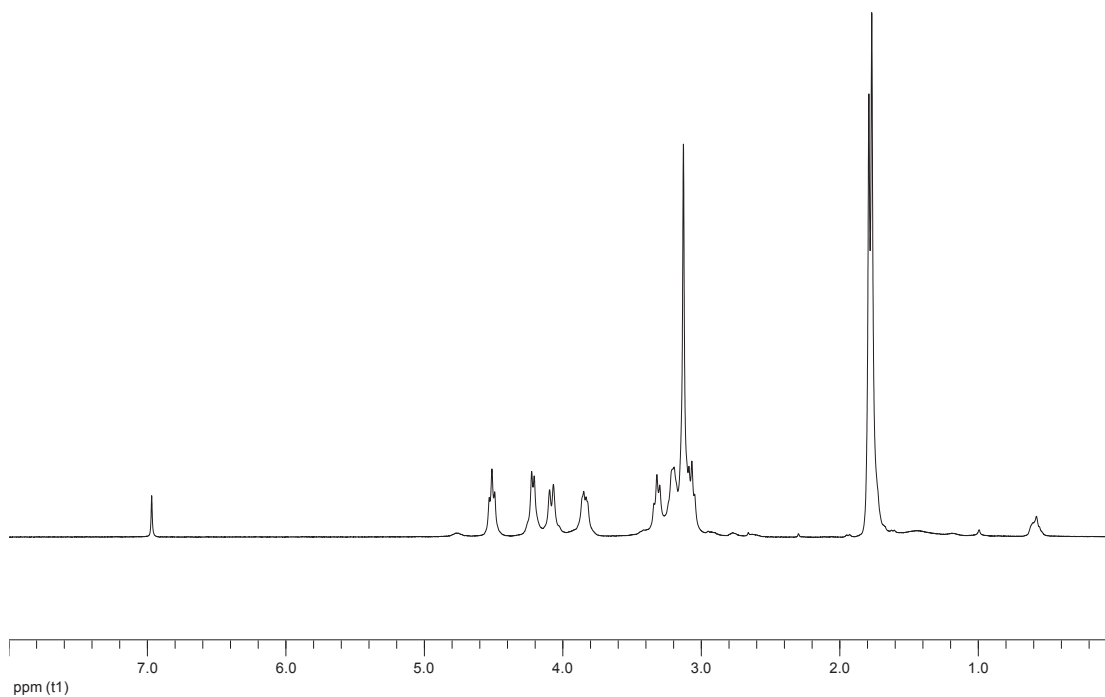
7) ^{1}H and ^{13}C NMR spectra of 2,6-di-*O*-acetyl-3-mono-*O*-methyl/propyl cellulose with DS$_{Me}$/DS$_{Pr}$=0.46/0.58 **5h**
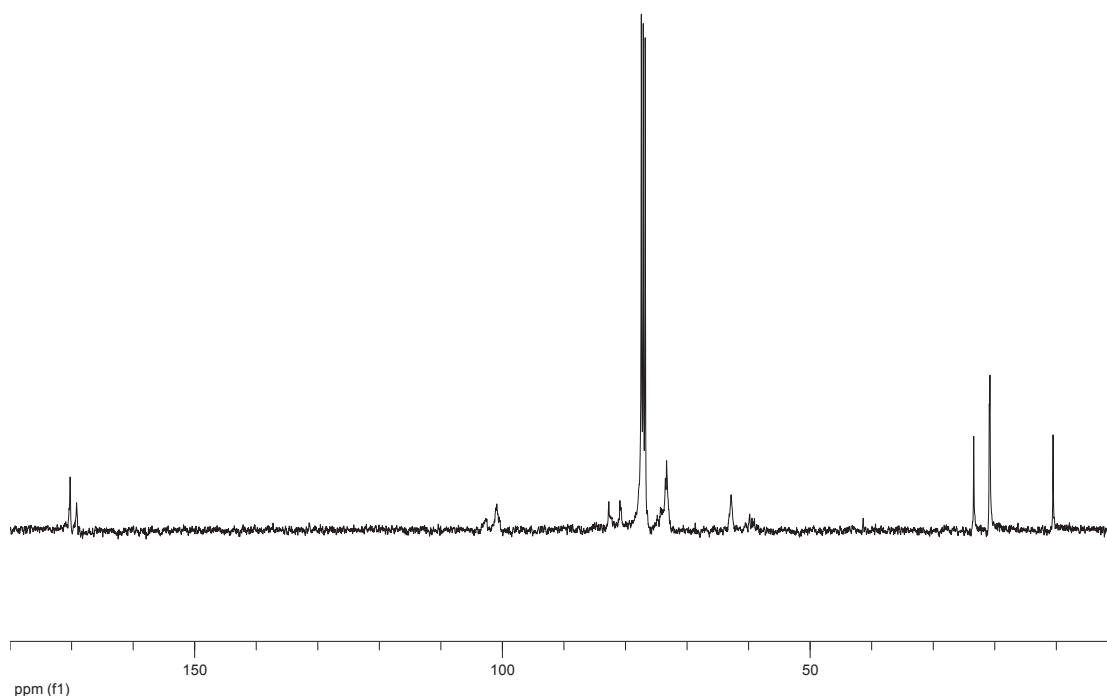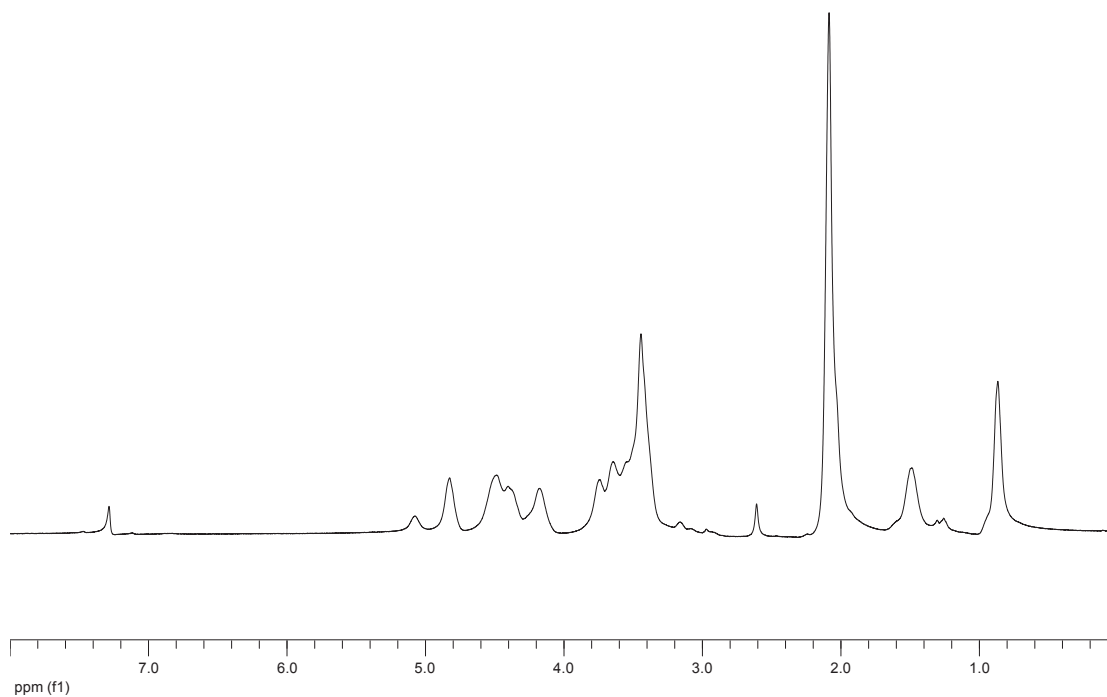
8) ^{1}H and ^{13}C NMR spectra of 2,6-di-*O*-acetyl-3-mono-*O*-ethyl/propyl cellulose with DS$_{Et}$/DS$_{Pr}$=0.27/0.19, synthesized via peralkylation in presence of *n*-BuLi **5a'**
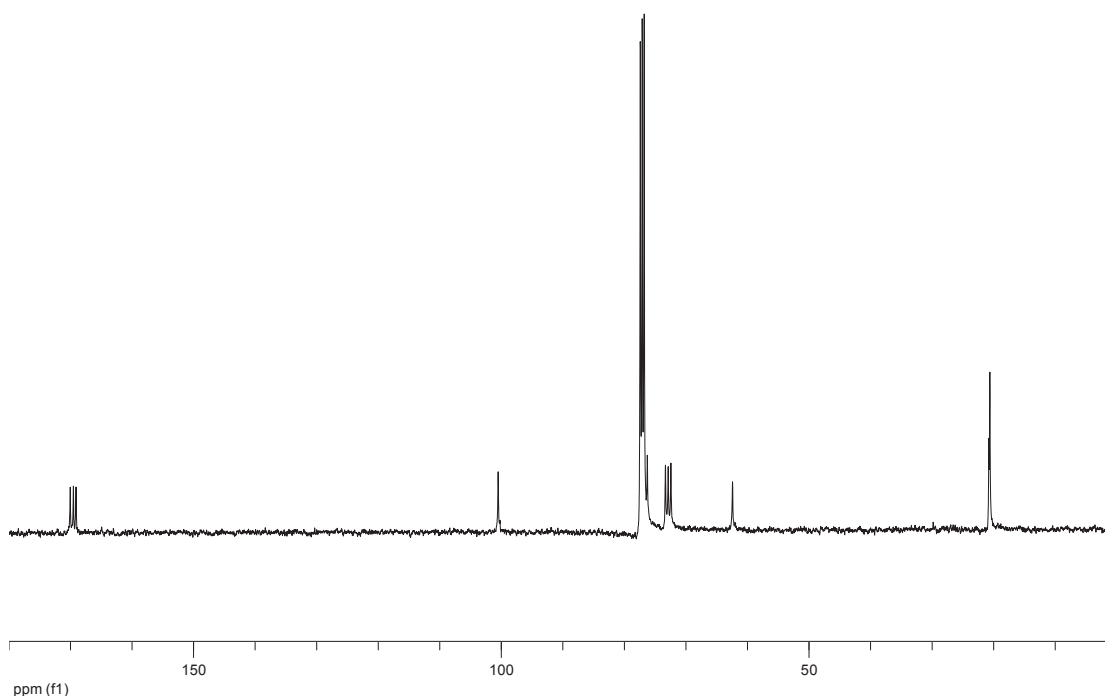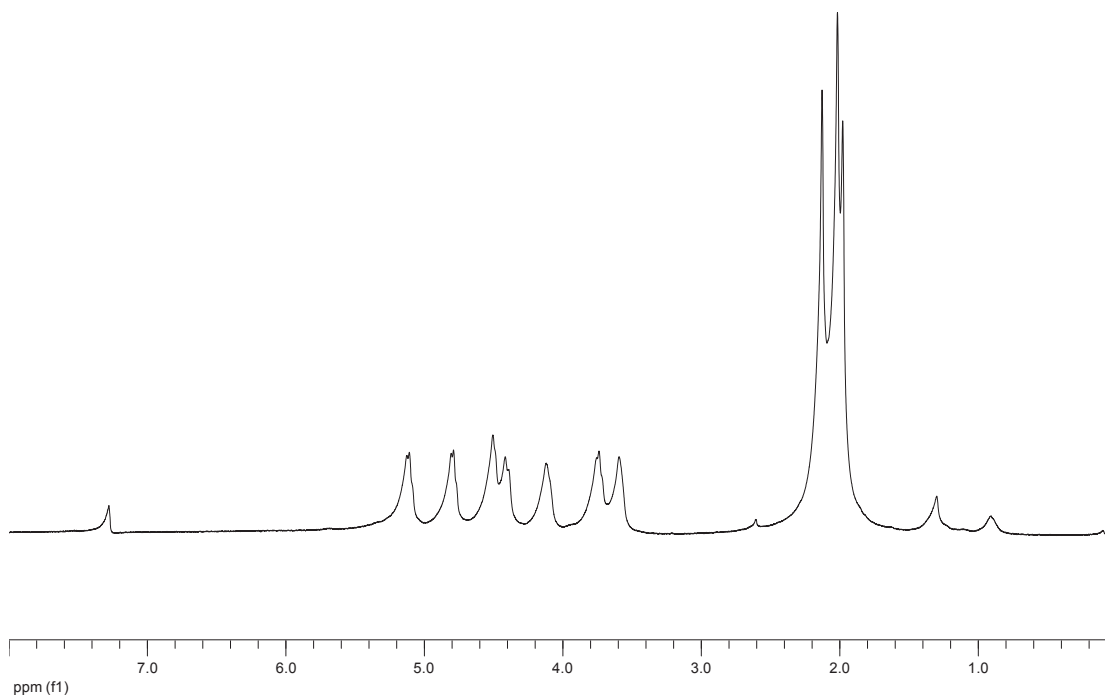
9) ^1H and ^{13}C NMR in DMSO-d6 of 3-mono-*O*-acetyl cellulose synthesized by tris(4-bromophenyl)aminium hexachloroantimonate (TBPA$^+$• SbCl$_6^-$) **7a**
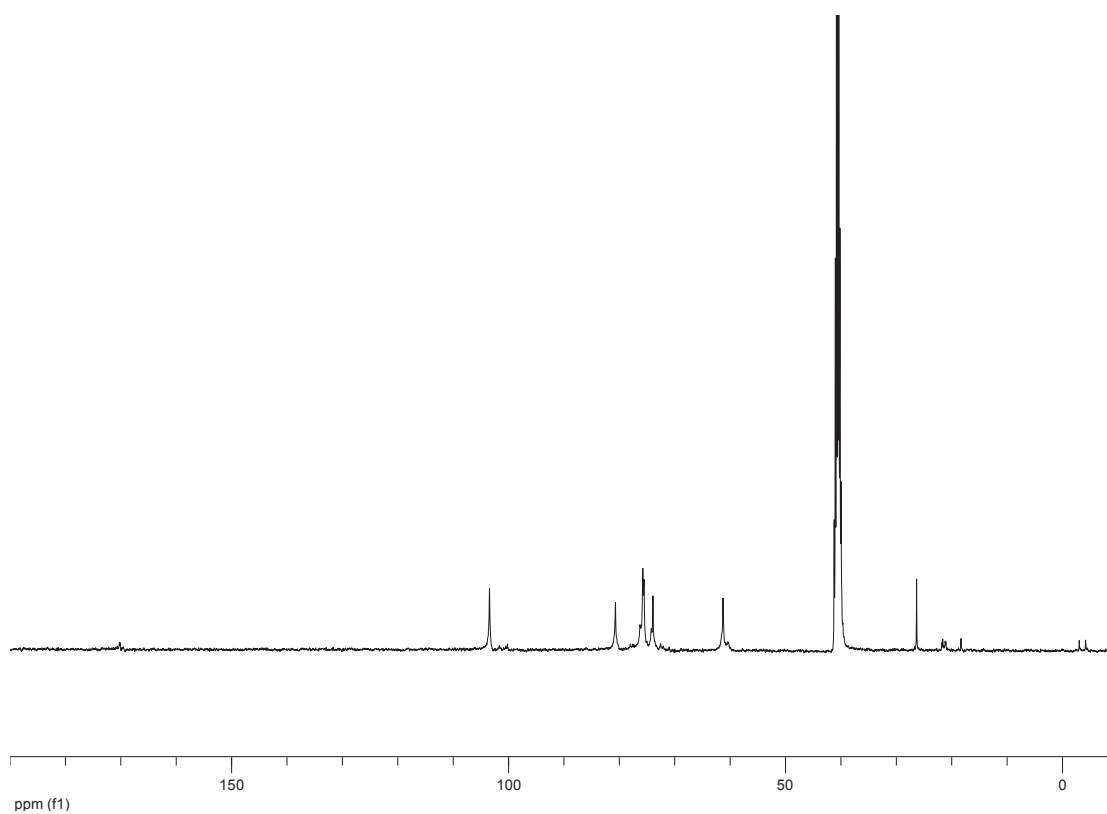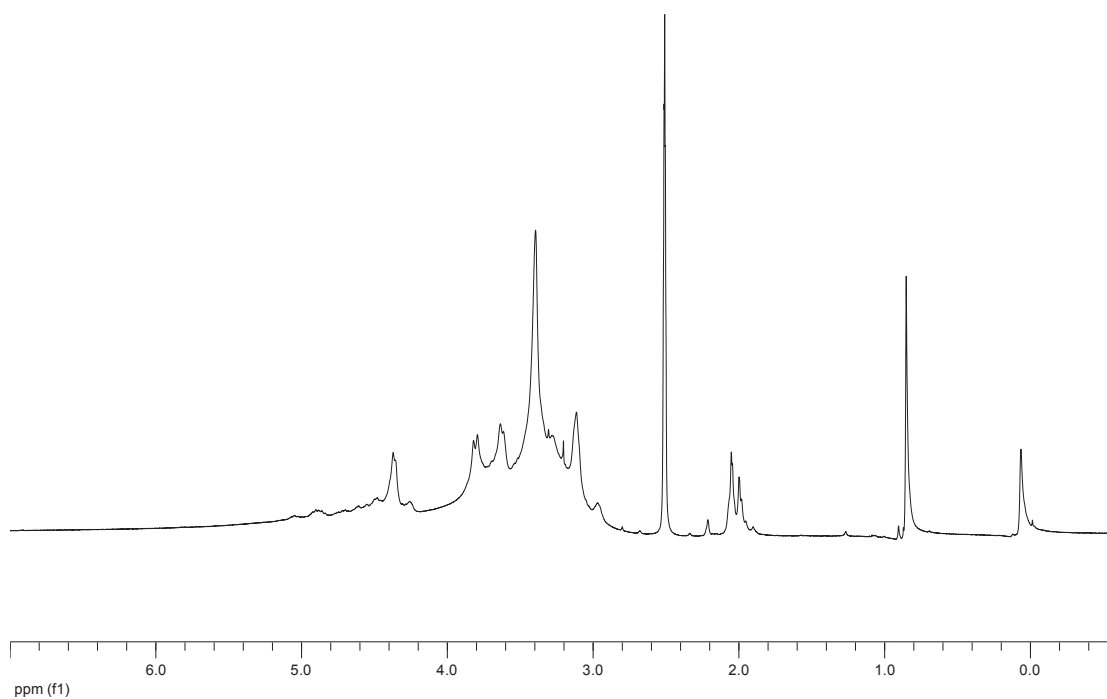
10) ^{1}H and ^{13}C NMR in CDCl$_3$ of perpropanoylated products of desilylation with CsF in DMSO at 50 °C **8d**

ppm (f1)

ppm (f1)
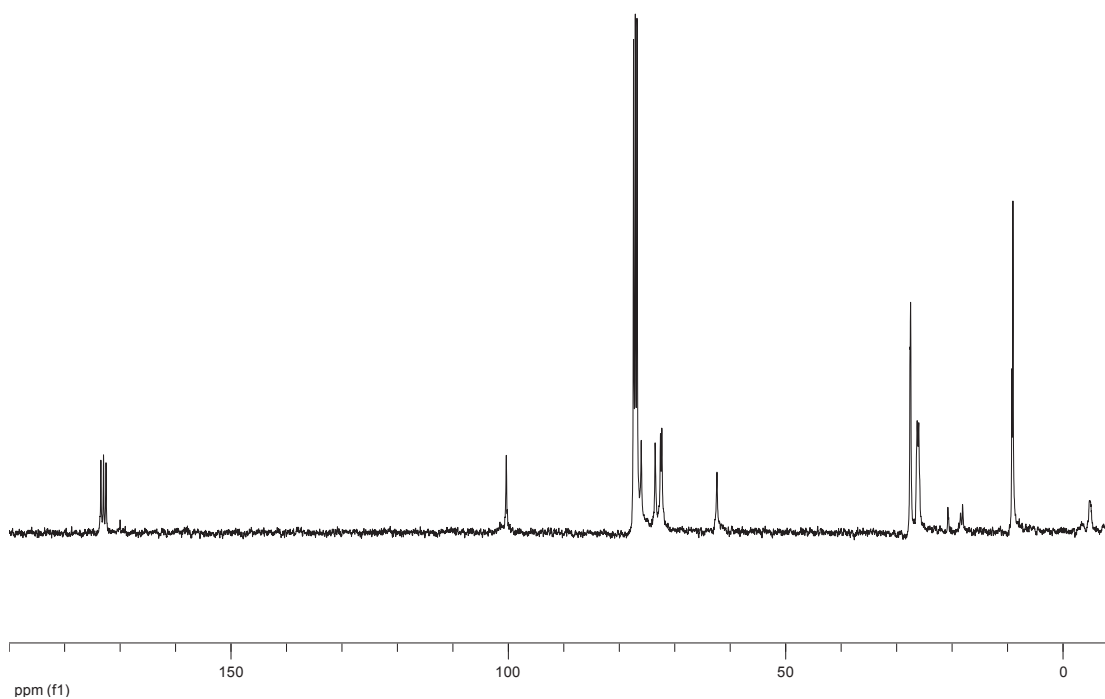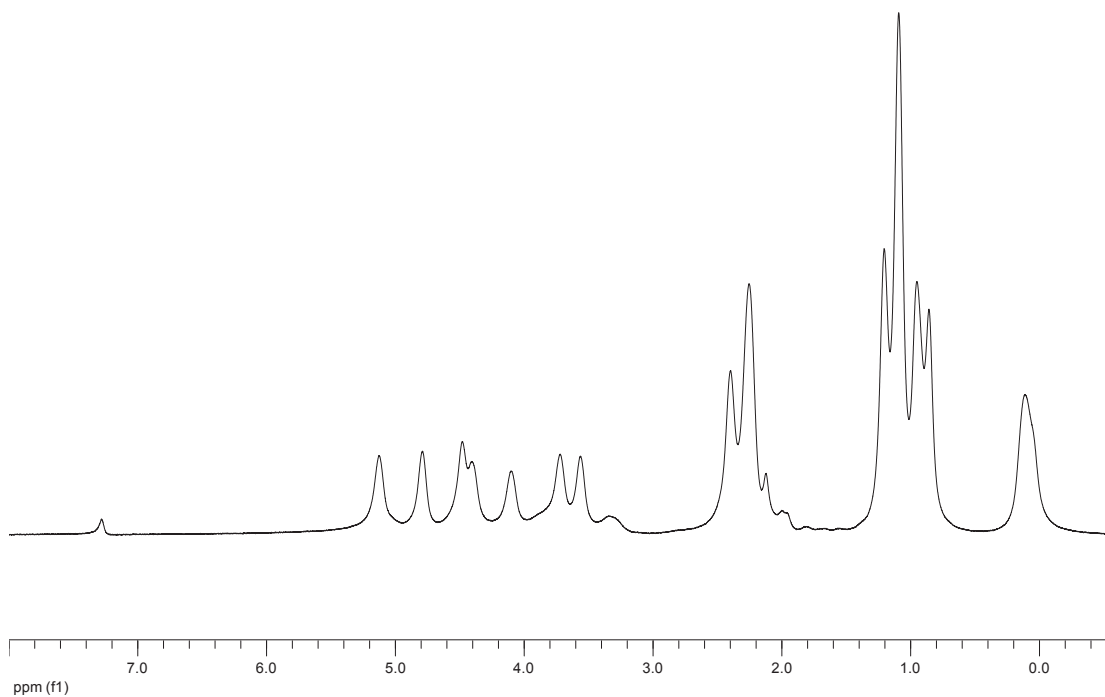
Appendix II: Fourier Transform infra red (FT-IR) spectra

1) FT-IR spectrum of 2,6-di-*O*-thexyldimethylsilyl(TDMS)-3-mono-*O*-ethyl cellulose **3j**
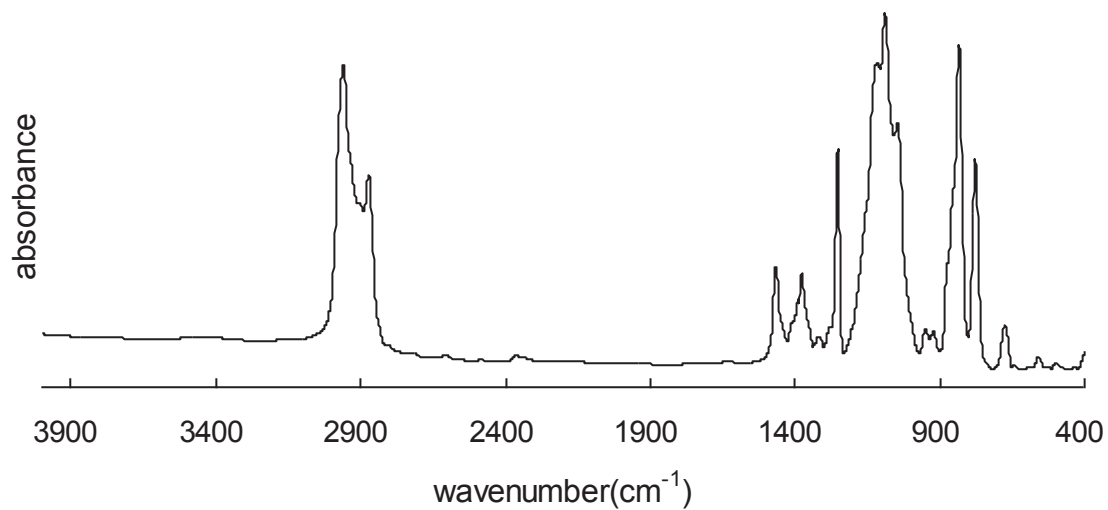
2) FT-IR spectrum of 2,6-di-*O*-TDMS-3-mono-*O*-methyl cellulose synthesized via peralkylation at 50 °C without any catalyst **3i**
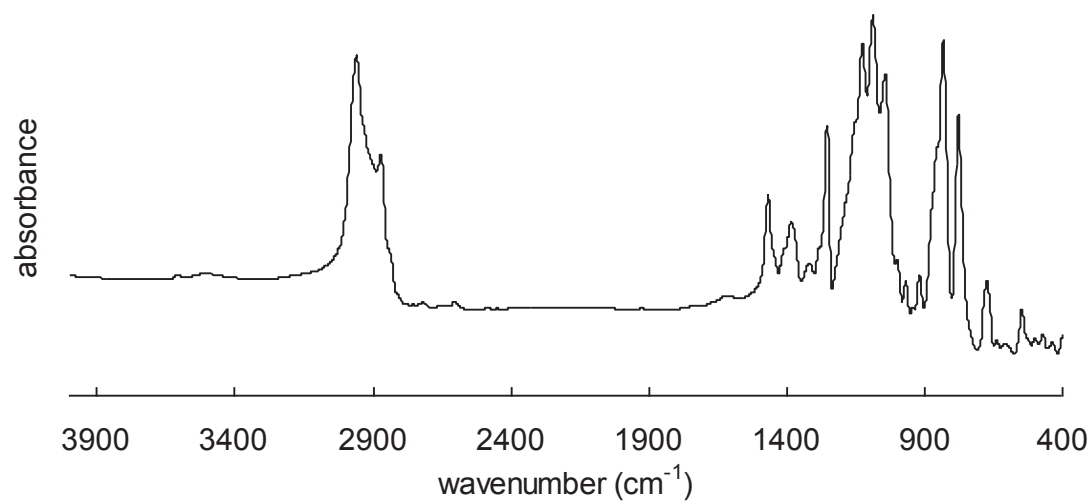
3) FT-IR spectrum of 2,6-di-*O*-TDMS-3-mono-*O*-methyl cellulose synthesized via peralkylation at room temperature with tetrabutylammonium iodide (TBAI) as phase transfer catalyst **3i'**
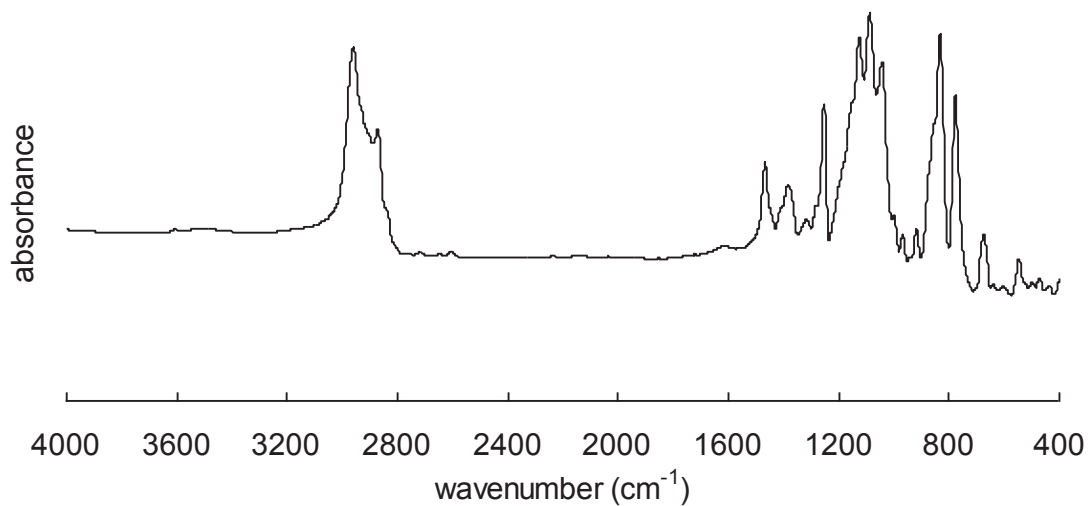
4) FT-IR spectrum of 2,6-di-*O*-TDMS-3-mono-*O*-acetyl cellulose **6**
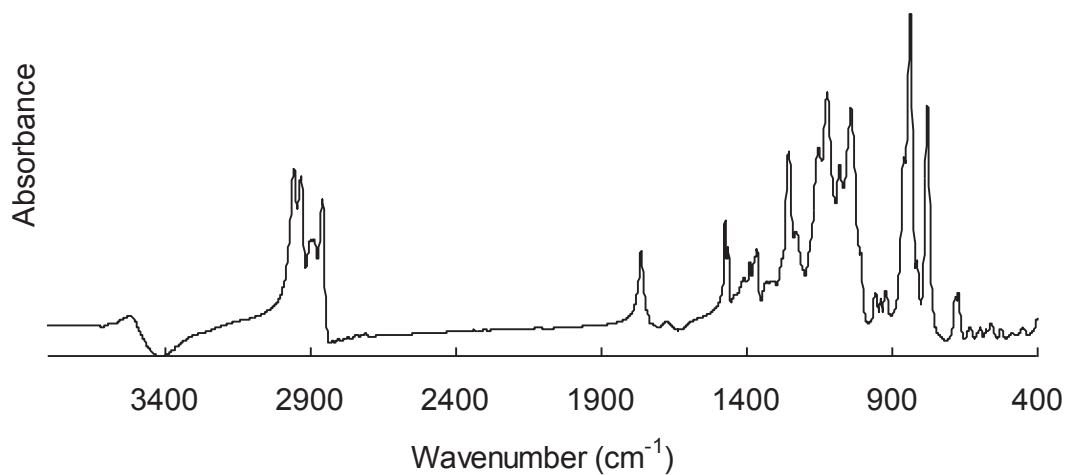
5) FT-IR spectrum of 3-*O*-acetyl cellulose synthesized by tris(4-bromophenyl)aminium hexachloroantimonate (TBPA$^+$• SbCl$_6^-$) **7a**

Publication list

➢ Th. Heinze, Y. Wang, A. Koschella, A. Sullo, T. J. Foster, *Novel mixed 3-mono-O-alkyl cellulose: Synthesis, structure characterization and thermal properties*, *Carbonhydrate Polymer*, **2012**, *90*, 380-386

➢ Y. Wang, A. Koschella, Th. Heinze, *Recent Developments in Structure Design of 3-O-Ethers of Cellulose, Lenzinger Berichte* **2012**, *90*, 93-102

➢ A. Sullo, Y. Wang, J. R. Mitchell, A. Koschella, Th. Heinze, T. J. Foster, *New regioselective substitued cellulose ethers: thermo-rheological study*, *Special Publication-Royal Society of Chemistry*, 2012, 335 (Gums and Stabilisers for the Food Industry 16), 45-57

Curriculum vitae

Family name: WANG   **Name:** Yunhui

Gender: Male

Birthday: July 11th, 1982

Birth place: Shashi, Hubei province, China

Marital Status: Married

Adresse : Wude Lu 1, B21, 434001, Shashi, Jingzhou,

Hubei province, P. R. China

E-mail : waynebuddy@gmail.com

Educational background

2000.9-2004.6	Wuhan University, Wuhan, China	Bachelor's degree in Applied Chemistry
2004.9-2005.6	CUEEP(language centre of University Lille 1), Lille, France	Certificat of French Level B1
2005.9 -2008.10	University Louis Pasteur, Strasbourg, France	Master 2 in Green Chemistry
2009.9 -2012.9	Friedrich Schiller University of Jena, Germany	PhD within Marie-Curie project

Professional experience

2009.3-2009.6   Teaching Assistant of Organic Chemistry Experiment (for 1st year students of

Biological Technology), Beijing Normal University, Zhuhai Campus

Selbständigkeitserklärung

Ich erkläre, dass ich die vorliegende Arbeit selbständig und unter Verwendung der angegebenen Hilfsmittel, persönlichen Mitteilungen und Quellen angefertigt habe.

Jena, den   --
                                                Unterschrift